POLYTECHNIQUE MONTRÉAL

affiliée à l'Université de Montréal

Planning and Integrated Design of Urban Heat-Sharing Networks

SAMUEL LETELLIER-DUCHESNE

Département de génie mécanique

Thèse présentée en vue de l'obtention du diplôme de *Philosophiæ Doctor*

Génie mécanique

Décembre 2019

POLYTECHNIQUE MONTRÉAL

affiliée à l'Université de Montréal

Cette thèse intitulée :

Planning and Integrated Design of Urban Heat-Sharing Networks

présentée par **Samuel LETELLIER-DUCHESNE**

en vue de l'obtention du diplôme de *Philosophiæ Doctor*

a été dûment acceptée par le jury d'examen constitué de :

Martin TRÉPANIER , président
Michaël KUMMERT, membre et directeur
Daniel PEARL, membre et codirecteur
Massimo CIMMINO, membre
Timur DOGAN, membre externe

DEDICATION

"Good artists copy, great artists steal"

− Pablo Picasso

ACKNOWLEDGEMENTS

Readers may find this dissertation's quote quite curious in the context of this thesis: *good artists copy, great artists steal*. The academic world is probably the most ardent defender of intellectual property, and anyone that is aware of its stringent standards should feel uncomfortable in front of strong words such as "copy" and "steal". Apart from Pablo Picasso, other artists such as Igor Stravinsky and William Faulkner were attributed this expression, but its most fervent exponent and defender remains Steve Jobs, founder of Apple. I believe a PhD student not only aspires to become a great artist, but he or she is also mastering the art of "stealing". Of course, some interpretations of this expression are definitely wrong. It undoubtedly does not mean "plagiarize" nor explicitly means "copying". Neither copying nor plagiarizing turns anyone into a good artist, nor a great one. Then, what does it mean? Simply put, to "copy" is more akin to "imitation" while "stealing" is more akin to "inspiration". The distinction is in the intent: imitation is laziness or refusal to accept your influences; inspiration is recognizing the influence and turning it into something new (Nick Douglas, 2017). As Adam J. Kurtz (2016), author of creative inspiration books such as *1 Page at a Time*, puts it:

> "'Great artists steal' is at its root about finding inspiration in the work of others, then using it as a starting point for original creative output. Artists may recontextualize, remix, substitute, or otherwise mashup existing work to create something new. Sometimes it's as simple as calling something art."

It is the role of PhD Students to find inspiration in their peer's work and then to decode, assimilate and make sense of this body of work through the extensive processes such as the literature review or through career affirming academic internships. After understanding and appreciating the rules dictated by their scientific world, they can build and create their work – or as I like to see it, their *art* – and ultimately present it to the world.

The idea of comparing a thesis to art resonates with me. A thesis is the product of years of hard work and efforts, planning and surprises, failures and successes, pain and excitement, first attempts and refinements. It is something that makes us stretch and grow as scholars because it is not something we do well… from the beginning; we learn and become better along the way like an artist learns to use his instrument or his tool. Like art, a thesis is a reflection of humanity, although

a very specific and precise one. Like art, a thesis is the expression of human creative skill and imagination.

One of the most difficult part of writing a thesis is acknowledging that you have already what it takes to see it through. One thing is certain, if it were not for a handful of extraordinary people that I had the pleasure of meeting along the way, I would not be sitting down trying to finish this endeavour and actually enjoying it.

To my co-supervisor, Danny Pearl, I would like to offer my sincere thanks for the support and encouragement throughout my PhD. Thank you for the opportunity to be able to apply my ideas outside of the engineering realm. You managed to let the tiny architect in me speak louder and take its rightful place. This, I believe, has only enriched my experience and the work I am presenting here.

Most of all, I owe a deep dept of gratitude to my dissertation chair and supervisor, Michaël Kummert. Meeting him has had a profound impact on my life and professional career since my humble beginnings as a Master Student. He has been fully supportive of my research and professional career and has always been thoughtful, supportive and encouraging. Five years ago, I met you in your office and warned you that I was graduating with a Civil Engineering degree. It remains a miracle that you took me in your research team and began to foster my development. The rest is history. Thank you.

Long gone are the days of dreaded loneliness often imposed on grad students – I truly had no such experience. I remain eternally grateful for the friends I have made at Polytechnique Montréal: Pauline Brischoux, Bruno Marcotte, Corentin Lecomte, David Lessard, Laurent Gagné-Boisvert, Samuel Bouheret, Simon Maltais-Larouche, Kun Zhang, Louis Leroy, Alex Laferrière, Camille Beurcq, Gregor Strugala, Walid Lallam, Yves Brussieux, Behzad Barzegar, Benoit Delcroix, Florent Herbinger, Houaida Saidi, Adam Neal. You made the Bee® Lab my home.

Special thanks to Christoph Reinhart for giving me the opportunity to brush neurones with some of the best. Never would I have ever imaged setting foot at an institution as prestigious as the Massachusetts Institute of Technology. In particular, my experience there has shaped my understanding of academic research in profound ways. I am deeply indebted to the conversations, critiques, and advice I have received from you. Finally, I am eternally grateful for the friends I have made over my short visit in Cambridge: Paul Mayencourt, Alpha Arsano, Shreshth Nagpal,

Irmak Turan, Carlos Cerezo Davila, Nathan Collin Brown, Andrew Brose, Jamie Farrell. Your intellects, humility, and willingness to accept me amongst your ranks have served as both a model and an endless source of motivation.

Only five years ago I was graduating from Civil Engineering and looking at life with no proper plan. I was debating with my friends Olivier Pettersen and Émile Sylvestre whether we should continue on at Polytechnique Montréal with graduate studies—job opportunities were looking bleak following a government breakdown of corruption in the engineering sector. But then again, if not for the two of you, I would probably be working a boring job instead of writing this thesis all day in Montréal. Thank you for pushing me towards my goals.

Lastly, I must thank my family. My parents, Michèle and François, and my brother, Sébastien – you have shaped the person I have become.

RÉSUMÉ

Ces dernières années, les villes ont dû renforcer leurs obligations en matière de réduction de leur impact sur l'environnement. Heureusement, les villes relèvent ce défi et sont déterminées à trouver des solutions. La consommation d'énergie des bâtiments est l'un des principaux obstacles au développement durable. Les villes sont construites pour fournir des espaces confortables et habitables à leurs habitants, ainsi que pour assurer un environnement résistant aux événements météorologiques et climatiques. Cependant, fournir ce confort nécessite de grandes quantités d'énergie, ce qui participe aux changements climatiques.

Les besoins en énergie des bâtiments étant en grande partie le résultat de décisions en matière de conception, les constructeurs des villes de demain ont un contrôle sur les différentes solutions proposées dans le domaine de l'environnement bâti. Des solutions technologiques existent, mais la bonne solution doit être mise en œuvre dans le bon contexte. Cette thèse porte sur une solution technique clé : l'utilisation de réseaux urbains d'énergie pour répartir — ou partager — la chaleur entre les bâtiments et équilibrer les charges de chauffage et de refroidissement restantes avec des sources de chaleur ou des puits hautement efficaces et à faible émission de carbone.

Cette thèse est également motivée par les relations interdisciplinaires complexes entre les concepteurs participant à l'urbanisme, à l'architecture et à l'ingénierie de l'environnement bâti. Elle plaide en faveur d'un processus de conception intégrée piloté par les données et propose des méthodologies et des outils pour informer et activer ce processus de conception.

Un indicateur de performance, *l'indice de diversité thermique*, est proposée pour localiser et évaluer la compatibilité thermique entre des bâtiments présentant différents niveaux de filtrage spatio-temporel. La thèse apporte ensuite des contributions aux différentes étapes nécessaires à la conception et à l'évaluation de réseaux de partage de chaleur, faisant souvent partie de la 5e génération de systèmes de chauffage et de refroidissement urbains : évaluer la demande thermique des bâtiments à l'échelle de la ville en optimisant la topologie des réseaux urbains d'énergie et l'intégration de sources d'énergie efficaces et à faibles émissions de carbone.

Les archétypes, ou représentations typiques des bâtiments sont les fondements de nombreux outils de modélisation énergétique des bâtiments urbains (UBEM). Une méthodologie est proposée pour générer automatiquement des modèles d'archétype adaptés aux méthodes de modélisation contextuelles telles que celle implémentée dans UMI, l'un des principaux outils UBEM.

La thèse aborde ensuite la complexité de la combinaison de sources de données partiellement complètes et parfois contradictoires pour obtenir une carte dynamique de la demande de chaleur pour une ville telle que Montréal. La méthodologie proposée comprend l'utilisation d'empreintes de bâtiment virtuelles basées sur des données ALS (Airborne Laser Scanning) (également appelées données LiDAR) pour estimer les empreintes au sol et les hauteurs de bâtiment. Elle est appliquée pour obtenir une carte dynamique de la demande de chaleur de bâtiments résidentiels, commerciaux et institutionnels pour l'ensemble de la ville de Montréal.

Pour compléter le processus de conception des réseaux de partage de chaleur, cette thèse propose une méthodologie qui étend la capacité des algorithmes d'optimisation de la littérature utilisés pour les réseaux de chauffage et de refroidissement urbains : elle permet des flux de puissance bidirectionnels inhérents au partage de chaleur et optimise la compétitivité à long terme de l'approvisionnement en chaleur en équilibrant les coûts totaux d'exploitation et les coûts totaux d'investissement des différentes unités d'alimentation en chaleur.

L'algorithme proposé, avec les autres contributions de la thèse, ouvre la porte à un cadre d'optimisation visant à peser l'impact des choix de conception inhérents à la sélection de la densité de construction, de la forme du bâtiment et de ses performances. Cette thèse affirme que l'intégration de cette optimisation des réseaux de partage de chaleur dans la phase de planification peut avoir une incidence nouvelle et imprévue sur la performance environnementale des futurs quartiers. Conformément à cet objectif à long terme, les contributions méthodologiques ont été mises en œuvre dans des outils contribuant à l'expansion rapide du corpus de logiciels en code ouvert. Avec les contributions à la littérature et aux pratiques de planification des réseaux urbains d'énergie, ces outils offrent une solution à la planification et à la conception intégrée de réseaux de partage de chaleur en milieu urbain.

ABSTRACT

In recent years, cities have had to step up their obligations to reducing their impact on the environment. Fortunately, cities are rising to this challenge and are determined to find solutions. One piece of the larger sustainability problem is the energy use of buildings. Cities are built to provide comfortable and livable spaces to their inhabitants as well as ensure a resilient environment towards meteorological and climatic events. However, providing this comfort requires large amounts of energy, which exacerbates climate change.

Since the energy requirements of buildings are in large part the result of design decisions, the builders of cities have an innate control over the various solutions in the built environment problem space. Technological solutions exist, but the right solution must be implemented in the right context. This thesis focuses on one key technical solution: the use of district energy systems to distribute—or share—heat between buildings and balance the remaining heating and cooling loads with highly efficient, low-carbon heat sources or sinks.

This thesis is also motivated by the complex interdisciplinary relationships between designers participating in the urban planning, the architecture and the engineering of the built environment. It makes the case for a data-driven Integrated Design process and proposes methodologies and tools to inform and enable this design process.

An urban planning metric, the thermal diversity index, is proposed to locate and assess the thermal compatibility between buildings with various levels of spatial and temporal filtering. The thesis then makes contributions to the different steps required in designing and assessing heat-sharing networks, often part of the 5th generation district heating and cooling (5GDHC): assessing the thermal demand of buildings at the city scale, optimizing the topology of district systems, and integrating efficient and low-carbon energy sources within an overall optimization process.

Archetypes, or typical representations of buildings, are the foundation stones of many Urban Building Energy Modelling (UBEM) tools. A methodology is proposed to automatically generate archetype templates adapted to context-aware modelling methods such as the one implemented in UMI, one of the prominent UBEM tools.

The thesis then addresses the complexity of combining partially complete and sometimes contradictory data sources to obtain a dynamic heat demand map for a city such as Montréal,

Canada. The proposed methodology includes the use of virtual building footprints based on Airborne Laser Scanning (ALS) data (also known as LiDAR data) to estimate building footprint areas and building heights. It is applied to obtain a dynamic heat demand map of residential, commercial and institutional buildings for the whole city of Montréal.

To complete the design process of heat-sharing networks, this dissertation proposes a methodology that expands the capability of state-of-the-art optimization algorithms used for district heating and cooling networks: it allows bidirectional power flows that are inherent to heat-sharing networks and optimizes the long-term competitiveness of heat supply by balancing the total operating costs and the total investment costs of different heat supply units.

The proposed algorithm, with the other contributions of the thesis, opens the door to an optimization framework aiming to weigh in the impact of design choices inherent to the selection of built density, building form and building systems performance. This thesis proclaims that bringing this optimization of heat-sharing networks inside the planning phase can impact the environmental performance of future districts in new and unforeseen ways. In line with this long-term goal, the methodological contributions were implemented in tools contributing to the rapidly expanding body of open source software. Together with the contributions to the literature and the district energy planning practice, these tools offer one solution to the planning and integrated design of urban heat-sharing networks.

TABLE OF CONTENTS

LIST OF TABLES

LIST OF FIGURES

LIST OF SYMBOLS AND ABBREVIATIONS

Abbreviations

ACH	Air changes per hour
ALS	Airborne Laser Scanning
BEM	Building Energy Model
BES	Building Energy Simulation
BIM	Building information modelling
BSM	Building Stock Model
BTAP	Building Typology Assessment Platform
CDH	Cold-Ring District Heating
CHP	Combined heating and power
CityGML	City Geography Markup Language
CNN	Convolutional neural networks
COP	Coefficient of Performance
CTBUH	Council on Tall Buildings and Urban Habitat
DES	District energy systems
DH	District heating
DHW	Domestic Hot Water
DSM	Digital Surface Model
DTM	Digital Terrain Model

ESO	Energy Supply Optimization
EUI	Energy Use Intensity
FAR	Floor-to-Area Ratio
FMI	Functional mock-up interface
GIS	Geographic Information Systems
ICES	Integrated Community Energy Solutions
ID	Integrated Design
IECC	International Energy Conservation Code
IPCC	Intergovernmental Panel on Climate Change
KPI	Key Performance Indicator
LBNL	Lawrence Berkeley National Laboratory
LCA	Life cycle assessment
LDC	Load duration curve
LPD	Lighting power densities
MIDP	Master Innovation and Development Plan
MILP	Mixed Integer Linear Programming
NRBM	National Reference Building Models
NYCHA	NYC Housing Authority
OSM	Open Street Map

PCM   Phase Change Materials

SHGC   Solar Heat Gain Coefficient

SWOT   Strength, Weaknesses, Opportunities and Threats

TDI   Thermal Diversity Index

TEDI   Thermal Energy Demand Intensity

TES   Thermal Energy Storage

TSAM   Time series aggregation module

TSHM   Time Series Heat Map

UBEM   Urban Building Energy Modelling

UMI   Urban Modeling Interface

VBF   Virtual Building Footprint

WtE   Waste-to-energy

WWR   Window-to-Wall Ratio

LIST OF APPENDICES

CHAPTER 1   INTRODUCTION

This chapter introduces the context and the motivation for the study in this dissertation. It then presents the organization of the thesis with respect to the main contributions in each chapter. The integration of district energy in urban energy supply systems has been extensively studied by scientists and engineers, but district energy has rarely been explicitly integrated directly into the urban design process. Moreover, district energy is changing at a quick pace and we have already entered into the so-called *fifth generation*: ambient temperature, heat-pump assisted, heat-sharing networks which promise better environmental performance. The strategy implemented by this dissertation is to break down the planning and integrated design of heat-sharing networks into a framework of data acquisition, optimization and analysis that is compatible with the holistic design process seen in the field of architecture and urban design. This thesis introduces new tools to collect and display urban building energy data, advise on optimal network topology and suggest low-carbon energy supply scenarios.

1.1 Context

Urbanization of the global population is well underway. According to the United Nations, more than 68% of the world population will be urban by 2050 (United Nations Department of Economic and Social Affairs Population Division, 2019). This influx in urban population will put a strain on the existing infrastructure and will force authorities to make adjustments. Without proper policies that favour high density, new urban developments will aggravate the phenomenon of urban sprawl, gradually eating away at valuable agricultural areas and virgin lands. With climate change, more regions will experience an increase in energy use from air conditioning systems as extreme temperature events will become more and more frequent. These trends run counter to sustainability principles which advocate for a reduction in resource consumption and an increase in global welfare. The challenge that presents itself is to do "more and better with less" of this energy.

District energy systems (DES) are a key element in the transition to sustainable energy according to the United Nations Environment Program (UNEP, 2015). They offer a practical way to increase the efficiency of the energy production and energy distribution necessary to heat and cool buildings. Furthermore, they offer the possibility of exploiting synergies between different social activities, such through the recovery of heat rejection. Historically, district energy was developed

around thermal sources in the form of combined heating and power (CHP), waste-to-energy (WtE) or even industrial processes. However, with the latest development in DES technology, renewable energy can have a more important role to reduce global impacts on the environment (Werner, 2017). In reality, DES require a certain built density as well as a combination of various programmatic building usages to reach their full potential. This is especially the case for heat-sharing networks that rely on the heat rejection of some buildings to cover part of the heat demand of others (see chapter 3.2). Evidently, high density cannot simply be the sole reason to build a DES; there is a community aspect that must be addressed in order to design districts that are also *livable*. Liveability is difficult to define, although many design paradigms point to the quality of physical amenities such as parks, green spaces or even the number of good bakeries within a short walk distance; the health of the local economy and the diversity of culture offerings are also good indicators of a liveable community (Ling, Hamilton, & Thomas, 2006). Liveability links with sustainability and infrastructure issues—e.g., the competitiveness of district energy—in its alternative urban development model that goes against sprawling suburbs with low densities (both population and services) that demand infrastructures that put pressure on ecological, economic and social systems (see for example the US Department of Transportation's Liveability Initiative [Fischer, 2000]). While high density can drive down costs linked to district energy, it must not hinder liveability. Therefore, a more thoughtful urban planning process is necessary to achieve the highest *liveable* density to enable both a high energy efficiency promised by DES and a livable community. There is a need for planning tools that will place scientific data and models at the forefront of design practices.

The methodology presented in this thesis focuses on the interface between urban planning, architecture and the development of DES by providing a balanced workflow that enables planning teams to collaborate effectively. Whether it is by providing relevant urban energy diagnosis tools such as the Thermal Diversity Index (TDI) or by integrating with tools already used by practitioners, this methodology aims to bridge the gap between architecture and engineering through a more effective collaboration.

Effective collaboration is the key to ensuring the best designs are built. This is why the foundation of this thesis relies on principles of Integrated Design (ID): mutual understanding of the objectives and a combination of linear and iterative processes. The need for an integrated design approach is not a new reflection and its term is already quite known. However, ID has operated mostly within

the confines of the micro-scale architecture-engineering-construction space. Could urban planning be integrated upstream from those spaces with a focus on data-driven decisions at macro-scales?

To continue with this foundational analogy, the *pillars* of this thesis represent four complementary methods that support the planning and integrated design of heat-sharing networks: (1) The diagnosis of heat-sharing opportunities, (2) the efficient analysis of building energy through the creation of building archetype templates (3) the quantification and visualization of the city's energy demand, and (4) the optimization of heat-sharing network topologies for early design proposals.

ID links these methods through their explicit motivation to interface easily with an iterative design process: fast input data preparation, quick result generation, effective summarization and reproducibility. As we will see, applying these principles to building stock energy prediction, district network planning and energy supply planning, faces challenges of data availability and acquisition as well as model oversimplification. Yet, there is evidence that these issues can be contained by applying various methods of model complexity reduction and combination of multiple data sources.

As discussed in the upcoming chapters, an integrated design approach to the design of energy supply systems offers a way forward to curb greenhouse gas emissions while favouring a high density, a critical challenge we must face. This challenge is escalated by the unique environmental conditions of each city around the world, which require a unique set of solutions. Globally, we know that the average temperature has risen by 0.85 °C between 1880 and 2012 (IPCC, 2014). In Canada, the situation is far worse. The country experiences warming on average twice as fast as the rest of the world. Northern Canada is warming almost three times faster than the world average, according to a 2019 government report (Gillet et al., 2019, p. 125). On the other hand, in Quebec, the home province of the author, mean temperatures have increased at a lower rate than the rest of Canada. Combined with the high penetration of hydroelectricity (61%) in the Quebec building sector and the most competitive energy prices in North America, there is a resistance in the industry to reducing the share of natural gas (19%) by replacing aging systems by other forms of heat production units (Whitmore & Pineau, 2018). Politically, the transportation industry is an easier target that could provide quicker and more apparent results with a "transportation electrification".

1.2 Motivation

This engineering thesis aims at producing science-based tools while paying attention to the needs of the ID process. While it can be situated between architecture, urban design, and mechanical engineering, it presents new techniques and measures for informing good design practices through the lens of urban building energy modelling and energy supply planning. This dissertation proposes to bridge the gap between the *practical* and the *theoretical*—that is, elements that offer 1) a useful toolkit for research to help practising planners and architects and 2) a theoretical lens to reconceptualize oversimplifications of district energy systems.

The structural attributes of urban energy flows influence the built environment and the dynamics that manifest in space throughout the city. Where is the energy needed? Where does it come from? Questions that are usually answered with specialized tools that help designers understand the impact of their decisions. This translates as the primary motivation of this thesis, which aspires to improve design concepts of future district energy systems by providing a scientific toolkit that can empower stakeholders with the cost benefits of the energy supply strategy to use at the time when it is necessary to decide on which strategy to use. In simple terms, this dissertation tries to answer the question: "Can the deployment of a heat-sharing network positively influence the final design of architects and urban planners?" Alternatively, this thesis proclaims that bringing the topology optimization of heat-sharing networks inside the planning phase can impact the environmental performance of future districts in new and unforeseen ways.

Evidently, there exists a plethora of tools that provide some answers to this question by focusing on various phases of district energy planning (exploratory study, feasibility, design, etc.), but, as we shall discuss, a gap exists with district heat-sharing networks.

Another area of concern is the issue with reproducibility in research and in practice. The current landscape of tools and methods offers no ideal technique that balances usability, customizability, reproducibility, and scaleability in acquiring, constructing, and analyzing heat demand for the purpose of district energy systems.

The larger goal is to reintroduce engineering earlier into the design process; structural engineers have been able to play ball for quite some time as more modern buildings can enjoy creative and complex shapes thanks to a closer and more productive relationship between architects and

structural engineers (Olsen & Namara, 2014). Today, state of the art building energy simulation software focus on the design impact of energy consumption in buildings. But the industry, comprised of both mechanical systems engineers and architects, has yet to integrate efficiently these tools into their workflows – i.e., most simulation tools are used to get green credits instead of informing design. At the city level, in the realm of urban planning, the role of energy simulation tools is hardly defined; there is a case where engineering-based tools can inform better urban planning practices by deploying building energy simulation and district energy simulation theories. This thesis proposes such a method through the following contributions.

1.3 Organization and Contributions by Chapter

This thesis starts with an introductory and structuring chapter and ends with concluding discussions and remarks covering the 6 central chapters. These 6 chapters unpack the bedrock of Integrated Design, which this work adheres to, position district energy inside the urban design process, present a method for acquiring, analyzing and visualizing heat demand and create a workflow for influencing design decisions in heat supply optimization scenarios.

1 Introduction
Problematic and thesis structure

2 Bridging the Gap Between
Engineering and Architecture
Key concepts of integrated design and
position within district energy planning

3 District Energy Networks in the
Realm of Urban Planning
District energy network theory and
applied design quantitative measures

4 Archetypes in Urban Building
Energy Modelling
Urban building energy models and a
proposed method to accelerate their
creation

5 Acquiring, Analyzing and
Visualizing Heat Demand
Creation of a dynamic energy map of
Montréal, Qc. Serves data for chapters 3
and 6.

6 Heat-Sharing Network Topology
Optimization
An optimization model for heat-sharing
network design

7 Open Source Software
Implementation
Details on software implementation of
methodological contributions

8 Conclusions and
Recommendations
Summary of contributions and potential
trajectories for future research

Figure 1.1 Overall dissertation structure.

1.3.1 Chapter 1: Introduction

This chapter has so far presented the motivation and context of the study presented in this thesis. The remainder of this chapter summarizes the organization and contribution of each of the following chapters of this thesis.

1.3.2 Chapter 2: Bridging the Gap Between Engineering and Architecture

Unlike the other substantive chapters of this thesis, this chapter makes neither an empirical nor a methodological contribution. However, it offers a theoretical contribution to the engineering literature by describing the fundamental concepts of integrated design theory. It provides illustrative examples of these concepts, as well as a general description of the tools for researchers and professionals who are not familiar with the science of multidisciplinary building design and neighbourhood energy design. In doing so, it addresses the transition from focusing on the dynamics of single buildings to consider large-scale urban planning along with energy supply planning and suggests a bridge between the two.

1.3.3 Chapter 3: District Energy Networks in the Realm of Urban Design

Building on the concepts of Integrated Design detailed in chapter 2, chapter 3 lays down the theoretical framework of district energy and, more particularly, heat-sharing networks which is the primary focus of the thesis in the subsequent chapters. District energy systems have evolved throughout the years and scholars have attempted to characterize them with distinct generations. In an attempt to reduce thermal losses and to interface more easily with renewable energy sources, the operating temperature of district energy networks has been steadily decreasing. With these lower temperatures, new generations are appearing, which carry with them a morass of ambiguous terminology. An updated characterization of the nomenclature is welcomed.

Furthermore, this chapter moves on with concepts of rapid prototyping of district energy networks using mathematical models that have appeared in the district energy literature over the past 10 years. They focus on more traditional district energy systems, and less on heat-sharing networks, leaving an opportunity to fill this gap in the literature. Linked to the realm of urban planning, concepts of *complexity* are then addressed. More specifically, the concept of thermal diversity, documented in the literature, is presented and the chapter delves into its significance in the field of

district energy. The chapter then presents two contributions: the use of a *temporal filter* to represent the effect of thermal storage on thermal diversity and a *spatial filter* to represent the spatial extent of a heat-sharing network. Both filters work together to map thermal diversity in any given geographical context. Together, contributions of this chapter form the basis of the subsequent chapters. In particular, measures of building energy usage and energy supply optimization are operationalized in the next 4 chapters.

1.3.4 Chapter 4: Archetypes in Urban Building Energy Modelling

Chapter 4 answers the data needs evoked in chapter 3 concerning the estimation of the energy demand at the district or city scale. A review of methods of building energy prediction culminates with notions of urban building energy modeling. These principles have been applied to the study of building design, energy retrofit strategies and policy making. However, the lack of consistent and reliable data and methodologies have rendered the task arduous. This is particularly true when trying to estimate future energy demands, since uncertainty in planned building usages, occupant behaviour and even climatic trends dominate the inherent differences and errors between simulations and reality.

Building archetypes are the centrepiece of the physical representation of a large building stock through a finite number of generalized candidates. Their use has become the norm in Urban Building Energy Models (UBEM), and they have contributed to the development of large-scale studies providing a detailed representation of the energy consumption attributed to buildings in cities. However, archetypes are location-specific and, where there is a lack of existing databases, they tend to necessitate tedious and labour-intensive work to create. This chapter delves into the UBEM data requirements and suggests an answer to accelerate the creation of UBEMs: the automatic generation of archetype templates.

The methodology of the algorithm is explained, and assumptions are laid out. Finally, the methodology, which is embedded in a Python-based tool called *archetypal*, is used to carry a proof of concept for the creation of more than 15 000 building archetype templates applicable to a wide range of building uses and construction years for both Canadian and American cities is presented. This concept shows promising fallouts for the creation of UBEMs throughout Canada and the United States. Together, the foundation of building stock energy prediction with the archetype template development prepare the methodological heat demand landscape detailed in chapter 5.

1.3.5   Chapter 5: Acquiring, Analyzing and Visualizing Heat demand

Coupled with the UBEM methods described in the previous chapter, this chapter investigates the connections between these various fields of study and proposes a workflow adapted to the data availability of the City of Montréal. The particularity of these heat maps is that they include the dynamics (hourly load profile) of the energy demand and not only the annual energy consumption, as would typical heat maps. The method combines LiDAR imagery with the property assessment roll, two publicly available datasets, to segment buildings into groups sharing similar properties. The process is discussed, and difficulties are highlighted.

1.3.6   Chapter 6: Heat-Sharing Network Topology Optimization

Following the examination of district energy network theory and building energy demand prediction at the city scale through chapters 3 to 5, chapter 6 tackles the energy supply side of the urban energy flow equation. The energy supply is presented from the angle of the energy distribution with the use of heat-sharing networks. The proposed method focuses on the techno-economic optimization of the network topology—e.g., pipe location and capacity.

Network topology optimization is the process of planning the creation—or the extension—of a district energy network in the most economical way. Since the cost equation is heavily dependent on the length of the network, energy planners must choose wisely which areas of the city to connect with the network and eventually to generate enough revenues. At the planning stage, the network topology optimization not only allows planners to evaluate the cost of the future network, but it can also favour some design choices—e.g., a certain building type mix versus another or an envelope performance goal—since they have a corresponding impact on cost, but most importantly on environmental performance. In other words, bringing the topology optimization inside the planning phase can impact the environmental performance of the future district in new and unforeseen ways.

In doing so, this chapter presents the last core contribution of this thesis embed into a tool called *district*: A Mixed Integer Linear Programming (MILP) topology optimization tool for heat-sharing networks. The MILP draws information from all the steps detailed in the last chapters; energy demand profiles, building footprint location, road network topology and energy source location are all necessary data inputs. With them, the MILP is the engine behind the network topology

optimization and informs designers and planners on the techno-economic performance of their design. Together with *archetypal* and *district*, this contribution forms the comprehensive methodology for the planning and integrated design of heat-sharing networks.

1.3.7 Chapter 7: Open Source Software

This chapter presents the methodological contributions of this thesis in the form of open source software. The first is *archetypal*, a python tool developed by the author in which is implemented, amongst other features, the automatic archetype template generation presented in 4.2. While comparable tools usually have to be developed from scratch or rely on expensive commercial software such as MATLAB, developing a tool in Python makes them available to a wider audience. Such tools are open-source, cross-platform and open to further development through community-based programming. More than 50% of the tools listed on the Open energy modeling initiative (openmod) are Python tools (openmod, 2018). *archetypal* contributes 6 significant capabilities for researchers. First, the persistent loading, modification and execution of collections of EnergyPlus models in a programmatic environment; second, the simplified analysis of geometric and non-geometric parameters; third, the query and visualization of EnergyPlus time series result data; fourth, the creation and modification of archetype templates from EnergyPlus models, essentially short-circuiting the manual creation of UMI Template Files[1]; fifth, the conversion of EnergyPlus schedule types to complete Year-Week-Day types. Sixth, a command line interface that can enable the batch processing of complex building archetype manipulations.

This chapter also presents an accompanying contribution named *district*. *district* is also a Python package developed by the author and has the task of interfacing with *archetypal* to acquire, analyze and visualize heat demand. The core elements of *district* used in chapter 5 are: first, the downloading of building footprints and other georeferenced data; second, the estimation of individual building floor area. Additionally, *district* interfaces with the topological optimization

---

[1] UMI is a software tool allowing the simulation of various urban energy flows. A building energy module uses so-called *template files* as data input for an EnergyPlus simulation.

program that is presented in detail in chapter 6. It implements various graph topology analysis methods that are tied to GIS data structures.

1.3.8 Chapter 8: Conclusions and Recommendations

This dissertation concludes with a tour d'horizon of the study, a summary of its key contributions to the literature and to the district planning practice and discusses potential trajectories for future research.

CHAPTER 2   BRIDGING THE GAP BETWEEN ENGINEERING AND ARCHITECTURE

This chapter lays the foundation that is at the core of this thesis. Readers will appreciate the demystification of the reflections made across this body of work. It first provides a background of the Integrated Design process and demonstrates its place as the catalyzer of better buildings and urban design. This premise triggered the formation of the Re4 Montréal research group at the beginning of 2017—Re4 stands for *Réseaux urbains d'énergie de 4e generation*, or Fourth Generation District Energy Networks—tasked with exploring the role of DES in the energy transition. The group's goal was to better understand the relationship between sustainable architecture, urban planning and renewable energy supply systems. The director and co-director of this thesis, together with Lisa Bornstein, professor of urban planning at McGill University, joined forces to explore these topics with a team of dedicated master's and PhD students. As it will be explained in detail in this chapter, the fourth generation of district energy networks must conform to a new era of urban development organized around the integration of renewables in smart grid systems and face the challenges presented by more efficient buildings. The chapter then illustrates the role of quantitative sustainability indicators in urban planning and the logic for bridging with Urban Building Energy Modelling (UBEM). This logic is highlighted by a proposed new indicator of building energy compatibility that short-circuits the need to use detailed modelling techniques to identify the best sites for the implementation of heat-sharing networks. It is one of many methods that establishes the diagnosis of a site, all while transitioning from the urban planning to district energy system planning. This chapter then explores another context linked to sustainability in the built environment: collaborative tools in architecture. The findings relate to the other methodological contributions of this thesis in their aim and form: early design supporting tools. Finally, it follows up on limitations and challenges linked to collaborative tools and lays out the objectives for the subsequent chapters.

2.1 Urban Design Process

We live in cities because they improve our quality of life—this goal is the minimum requirement for any built environment. Nonetheless, not all cities are created equal and not all cities control the "energy flows"—transit of goods and people, energy production and distribution as well as waste

disposal—that operate daily in the macrocosm of the city. When it comes to the built environment, the buildings we live and work in and the negative space they create—the public places—are usually the result of an intention to provide comfort to the occupants. It comes as no surprise that the source of that comfort asks for a lot of energy.

In Canada, 61% of the final energy[2] is consumed in urban areas, and more than half of this energy is consumed in the form of heat or cold (QUEST Canada, 2012, p. 1)[3]. Even in a city like Montréal, which benefits from hydroelectric power, buildings accounted in 2015 for almost one third (28%) of greenhouse gas emissions (Ville de Montréal, 2019). The Intergovernmental Panel on Climate Change (IPCC) identifies the building sector as the one with the best potential for economically viable GHG emission reductions (Intergovernmental Panel on Climate Change, 2014). The energy use of buildings is affected mostly by the climatic conditions, for which we have little control, but the efficiency with which this energy is delivered and the end uses it serves are dictated by design, for which we have total control.

Developing concepts for an urban design from a strictly utilitarian point of view is undesirable. The same goes for elaborating a master plan solely on architectural aesthetics. Many failed attempts at creating the perfect utopian city were the expression of our desire to envision what the future of human civilization would look like. Le Corbusier's "La Cité Radieuse" is most likely one of the better-known examples. Regardless of the design philosophy, professionals involved in the urban design process have agreed today to pay more attention to the environmental impact of cities, sometimes arguably at the expense of aesthetics (Davis, 2011; Hosey, 2007; Smith, 2013), which necessarily positions energy performance and energy supply as a central issue.

2.2 An Integrated Design Approach

The high level of complexity associated with creating a global vision of a new urban environment requires an integrated approach to address all the professions, perspectives and consider all the

---

[2] Final energy is the total energy consumed by end users, such as buildings, industrial processes and agriculture. It is the energy that reaches the consumer's meter and excludes energy used by the energy sector itself.

[3] These are estimates by QUEST based on data from the Comprehensive Energy End-Use Database (Natural Resources Canada, 2019).

independent and dependent variables. If we want to build dense neighbourhoods that are also great living spaces, we cannot afford to work independently. Traditionally, the urban design process is divided between silos of occupations: planners in a silo, architects in a second silo and engineers in another. As part of the traditional silos design process, the planner dictates the general rules of the game, then the architect designs the buildings, and finally the engineer equips the spaces with technical systems. These are linear processes in which the urban planner dictates the requirements for density (housing, commercial, industrial). Then, the architect and the client agree on a design concept consisting of volume/geometry, orientation, window/facade relationship, etc. Then, engineers suggest and implement the necessary technical systems to allow the design to work properly, for example, to achieve an acceptable indoor climate or to ensure adequate structural stability of the building. The contractor then calculates the costs and begins construction. "The design of the building in the [design process] is like a cane that is passed from one interested party to another" (Landgren, Skovmand Jakobsen, Wohlenberg, & Jensen, 2019).

To reduce GHG emissions, research shows that the best approach is to focus on the first design decisions. In reality, the initial programming and the budget, which already have a systematic bias, create an even more constrained situation. For this reason, planners usually look at different scales simultaneously: the city/region scale, the district scale, the neighbourhood scale and the block/development scale. This allows the ID team to more holistically capture and understand the context and the complex relations of the built environment as they mine for quantitative and qualitative synergies (Pearl & Oliver, 2015). Consequently, it is recommended to use new and innovative design processes that combine traditional cost, time and quality assurance with environmental protection, user health, carbon reduction and environmental protection (Gough, 2015). One of these methods is the integrated design method (ID). With ID, high performance is achieved through an iterative and holistic process that implicates all members of the design team from the early stages of the design. With ID, the goal is to produce the best outcome for a project while minimizing costs associated with design changes.

ID offers many advantages that integrate well with district energy planning. First, one searches for complementary synergies where energy and mixed-use complementarity can possibly reinforce each other. For example, a DES could share waste heat using a local heat source such that its process energy is compatible in time (hourly or daily demand, with/without storage capacity) and energy demand (magnitude). Second, the ID process can ask questions such as "what *density* is

sufficient to justify a DES infrastructure, without surpassing the *carrying capacity* of the site". For example, "corrected compactness" (Barcelona Urban Ecology Agency, 2012, p. 449, 2018, p. 10) is a planning metric that adjusts density to the "quality" of the space. It can measure the "carrying capacity" of a neighbourhood by directly considering the amount of high-quality public spaces; the higher the quality of public spaces, the more density is acceptable, since high quality public space entails greening of the public realm and socializing spaces in a given area. Greening helps biodiversity and air quality, the site conditions, the culture, the outdoor thermal comfort, the heat island problems, the access to daylight, etc. The amount of green spaces inside the site can determine the maximum acceptable densification without inhibiting the aforementioned benefits (Czechowski, Hauck, & Hausladen, 2014). Third, ID can answer questions that relate to the selection of HVAC systems that can help "future-proof" the requirements for "accepting/receiving" energy but also "rejecting/sharing" this energy. What form is the energy in? Is the energy considered to be a low-grade energy[4] such as the excess heat from a data centre or is it considered to be a high-grade energy such as the high temperature excess heat from an industrial process? How can the energy be stored without relying on expensive and inefficient batteries? Are the promising Phase Change Materials (PCMs) better than traditional sensible heat storage using water or other mediums? Should the investments instead favour high thermal mass of buildings? Fourth, ID can also look at synergies that may exist amongst various infrastructures. For example, can a municipal water reservoir be doubled as a daily or seasonal energy storage? Can compost/biomethanization provide low-grade energy while capturing methane (Antizar-Ladislao, Irvine, & Lamont, 2010)?

All of these questions can positively influence the designer's actions on an urban development project. As explained in the introduction of this thesis, the larger aim of this work is to provide designers with tools that can positively influence their actions. While a plethora of tools may be conducive to this larger goal, this thesis focuses first on the key elements of the energy diagnosis

---

[4] The "quality" of an energy source (e.g., electric, thermal, etc.) refers to its ability to be converted into another form. For thermal energy sources, low-temperature thermal energy, which is considered to be a "low-grade" energy, does not offer the possibility of being converted to as much end-uses than high-temperature thermal energy, which is considered to be a "high-grade" energy. Electric energy is also considered a "high-grade" energy source since it can be converted to almost any other forms of energy such as thermal energy (by use of an electrical heater for example).

of a site and later on the responses triggered by design choices on the energy performance of new urban development projects. As it will be discussed later, the diagnosis of a site allows designers to adapt the design interventions to the specificity of the site. Understanding *what* can be done to improve the design is as important as *how* it can be done. These questions of methods and techniques are best answered at the beginning of a project where the cost of change (e.g., modifying one of its features) is the lowest and designers can have the most influence.

According to Daniel Davis (Davis, 2013, p. 34), Boyd Paulson (1976) was the first to sketch the graph of the designer's influence on an architecture project. He claimed that the further a design was developed, the harder it was to change. Since change can be linked to cost in terms of time and money, the sketch was later reinterpreted by Patrick MacLeamy, former CEO of the architecture firm HOK, as the "ability to impact [a project's] cost and functional capabilities at the start of the project." This is the origin of the *MacLeamy Curve* (MacLeamy, 2004), as illustrated in figure 2.1, which is often used in many project management presentations to reaffirm the need for holistic design practices.
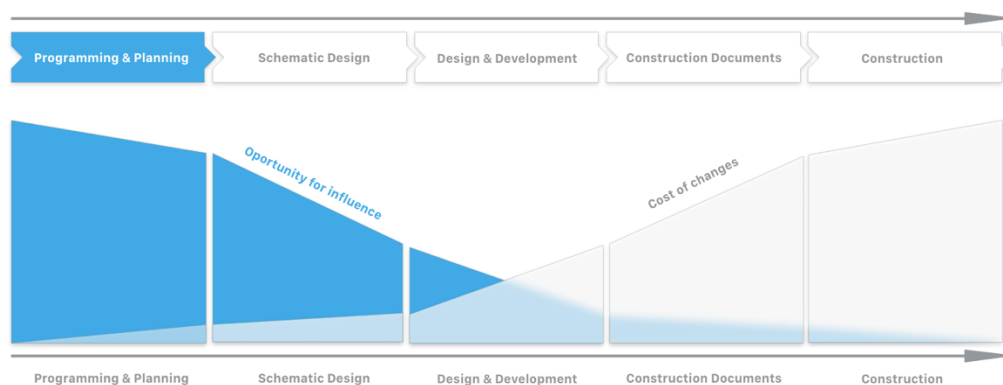
Figure 2.1 MacLeamy Curve, visualizing that project impact capacity is greater in early design phases and that the cost of modifications is highest during the later design phases. This highlights the importance of integrating technical knowledge early in the design process. The grey curve indicates the cost of design changes. The blue curve indicates the possibility of influencing the project.

This notion of cost of change and the intrinsic relationship between urban design, architecture and energy systems design has led this research to take a path towards "front-loading" as much as possible the analysis of district energy systems. While ID can provide the structure for a more holistic design approach, the main challenge is to align the intrinsic potential of mixed use, complex and dynamic urban fabrics with dynamic and balanced energy profiles—ultimately guaranteeing a

high quality public space that is sufficiently diverse, compact and carbon neutral without becoming overly compact and unhealthy.

This challenge, as daunting as it may, can be met with the help of methods and tools that provide objective/quantitative and qualitative evidence to support design decisions. All actors of an urban design have different approaches and methodologies that must be taken into account as to provide the same grounds for optimal collaboration (Vraa Nielsen, 2012, p. 40). Evidently, this poses quite a challenge; some authors argue that ID can actually be less effective because of challenges linked to tool complexity and accuracy, missing information, notions of embodied energy, poor environmental design decisions and decision-making based on green certification credits (Leoto & Lizarralde, 2019, pp. 43–45). This is why a focus on tools that bring empirical and data-driven evidence to district energy planning in an interdisciplinary context forms the premise of this thesis.

2.3 An Interdisciplinary Team as a Test Bed

The work presented in this dissertation was strengthened by the research group Re4 Montréal. This group brings together three universities in Montréal, Québec and three closely related disciplines: (1) The Mechanical Engineering Department of Polytechnique Montréal, (2) The University of Montréal School of Architecture, and (3) the McGill University School of Urban Planning. This interdisciplinary group was created with the goal of developing methodologies and tools to enable the implementation of district energy networks in Montréal by jointly addressing technological, socio-professional, political and legislative barriers. The research team aims to improve urban energy performance to reduce dependence on fossil fuels and alleviate power grid constraints, while maintaining affordable housing and energy service, and contributing to energy efficiency and neighbourhood resilience (energy, social, and economic resilience).

The long-term goal is to tap into the potential that district heating networks in Montréal have to contribute to urban redevelopment and create mixed, compact, diverse, efficient and resilient neighbourhoods—i.e., sustainable. The group also aims to train highly qualified students in the integrated and ecosystemic design process. Through this group, a workshop was organized with community stakeholders of different neighbourhoods in Montréal. We discuss here the findings from this workshop that relate to the objectives of this thesis.

2.3.1   Triggering the "Talk"

On September 14, 2018, at l'Université de Montréal, the first edition of the *For Sustainable Neighbourhood Symposium* was organized by the multidisciplinary Re4 Montréal research group and funded by the Trottier Energy Institute. The aim of the symposium was to identify the barriers and opportunities for sustainable neighbourhoods and to outline the guidelines for a multifaceted framework for the fourth generation of district energy networks (refer to section 3.1 for a description of district energy generations). This framework included the legislative framework, the subsidy strategies and financing opportunities, the missed synergistic timing opportunities and the identification of common divergent scale issues. The event brought together stakeholders from different decision-making levels across the province, the city of Montréal and Rosemont-La-Petite-Patrie, the geographic context of the study. In all, about 50 participants contributed to the workshops and brainstorming activities. Many engineers, urban planners, architects, members of the community or professionals from industry were able to share their ideas and creativity throughout the day. The mayor of the Rosemont-La-Petite-Patrie borough, Mr. François William Croteau, took part in the activities and issued a call to action against climate change during his presentation. Participants were also able to discuss opportunities for professional collaboration, aimed at shaping a future with better energy management.

Through the brainstorming sessions, the participants highlighted a major requirement for sustainability: citizen participation. By raising awareness and empowering citizens, they can become active stakeholders in their neighbourhoods. It is important to involve them in future projects. The central role of the citizen is highlighted by the complex interconnections between the different citizen groups and other exoteric supporting groups (see also figure 2.2). Moreover, without the citizen taking a proactive position in the development of the neighbourhood, a risk arises from the two beguiling visions of sustainable development and livable communities. Both visions have their own value conflicts, with sustainable development balancing ecology, equity and economy and livable communities balancing land use design aspects (Godschalk, 2004). Without the citizen at the centre of these values, creating sustainable and livable communities will be challenging.
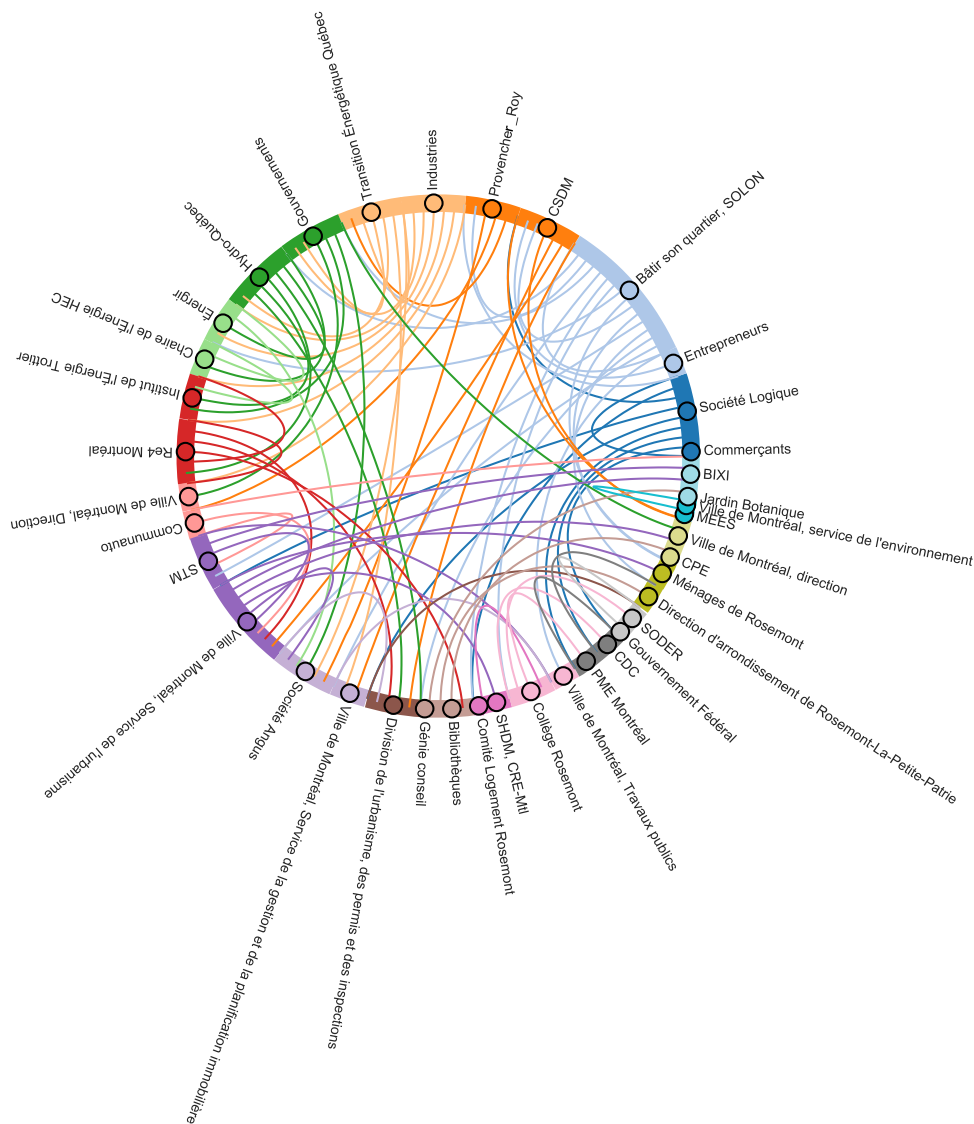
Figure 2.2 Connectogram of the stakeholders and citizen groups in the Rosemont-La-Petite-Patrie borough.

Citizens have a direct link with energy consumption through their role as users of energy. Research shows that when users are not made aware of the energy they consume, which is often the case when energy metering is centralized in district energy systems, they use more energy because they do not feel compelled to pay attention to their behaviour (Brounen, Kok, & Quigley, 2013; Delmas, Fischlein, & Asensio, 2013; Gustafsson & Gyllenswärd, 2005). On a more philosophical note, this raises the question whether or not building energy efficiency should be accounted for in terms of kilowatt hours per occupant instead of kilowatt hours per square metres as it is usually the norm.

Moreover, participants highlighted the necessity of ensuring that community participation is not only deep but early enough to have an impact on decision-making by enriching the co-learning and co-production activities. Co-learning and co-production activities are management methods where the citizens are not only consulted, but are part of the conception and design of public services (Bason, 2010).

Another finding is that there is a growing need for Montréal to enable and encourage public spaces and multifunctional buildings. Cities would benefit from weaving more workplaces (office and industrial) inside or closer to residential areas through mixed-use development. This would also benefit heat-sharing networks by pooling heat resources closer to one another. On the other hand, mixed-use developments can create their fair share of conflicts (Godschalk, 2004; Gough, 2015). To design effective/sustainable mixed-use communities, we must pool opportunities from different areas and move away from the traditional siloed design process in order to see the interconnectivity and synergies between projects; We must decompartmentalize the decision-making and regulatory powers and promote flexibility in the interactions between the various stakeholders. Here, multidisciplinary and diversity of expertise and perspectives are essential.

In addition, another key message from the event is that we should determine the actions that should be done in the short term and those that can be implemented in the long term. For example, democratization and open data access are immediate priorities, as they are prerequisites for developing multifunctional and synergistic projects in the future (see also section 5.2.1 for more on the importance of data access). In fact, the open data movement has only started to reach the different levels of government (Montréal changed its open data policy in 2015, for example). More and more datasets are taken out of closed rooms and uploaded for the public and researchers to use. The category of data sources that can still present some privacy issues such as the energy consumption of buildings or the disclosure of excess heat have yet to become public in Montréal. In this era of information and computation, the best diagnosis of the city will be achieved through transparency and accessibility of data. This is already the case for the cities of Toronto and Vancouver which are far ahead with strict enforcement of data transparency for energy and water use (Ontario Regulation, 2019; Union of BC Municipalities, 2014, para. B94). In the meantime, there exists some techniques that can help us "estimate" some features of the urban environment, and more specifically in terms of energy in buildings. On this particular subject, such a technique models the building stock of a city is presented in chapter 4 and applied in chapter 5.

On the longer term, participants suggested that the development of new neighbourhoods anticipate infrastructure work so that investments are phased while still being future-proofed. Organizing district energy expansion in sync with other urban infrastructure works such that investment costs can be shared presents itself as the main challenge. There are also public health opportunities like the reduction of excess heat which aggravate heat islands in urban canyons and the removal of hazardous water towers which have been linked to Legionella epidemics. These various advantages of district energy networks are addressed in chapter 3.

2.4 Data-Driven Design in the Era of Information and Computation

Discussing data-driven design—often called "knowledge-driven design"—through quantitative measures poses two questions. First, what kind of information are we looking for? And second, how can this information be produced? This section will discuss both questions through the lens of sustainability diagnosis and through tools and methods that enable such a diagnosis.

2.4.1 The Diagnosis of the City

In the world of urban planning and architecture, before a masterplan is issued and accepted, designers will try to conduct a site analysis to identify potentials and eventual barriers (Oliver, 2018), thereby more favourably answering the urban problems in question. To carry out a diagnosis of sustainability, the urban analysis method takes place in three stages: the reading of the site, the establishment of indicators of sustainability and finally the formulation of the diagnosis. Thus, a complete "portrait" of the neighbourhood is achieved through the analysis of multi-scale performance indicators. Finally, on the basis of sustainability principles, a complete diagnosis identifies the sites with a high potential and defines what is necessary for the construction of a sustainable district.

Through their work at Re4 Montréal, architecture students studied and applied the indicators of the Urban Ecology Agency of Barcelona (AEUB). The AEUB developed an urban sustainability diagnosis tool which looked at a series of indicators that go well beyond the usual suspects: compactness, complexity, efficiency and stability. By use of quantitative indicators, the diagnosis proposed by the AEUB is unbiased and allows designers to objectively compare different sites. The agency published methodologies for fifty or so indicators organized under the aforementioned categories (refer to figure 2.3 which summarizes the different indicators under the four principles).

The agency developed this methodology with the aim of "quantifying sustainability levels of a neighbourhood and to issue a score" (Oliver, 2018, p. 295). Based on maps, tables and diagrams, this tool communicates the various sustainability variables in a visual way.

Figure 2.3 Urban Sustainability Indicators of the Urban Ecology Agency of Barcelona (AEUB). Adapted from: AEUB.

The *Metabolism* and *Density & Morphology* indicators relate to this research since they provide an understanding of the main drivers of energy consumption. While these indicators can help DES planners identify high-density areas that can justify district energy networks, no indicator of the AEUB looks specifically at heating or cooling uses. Moreover, none of the indicators is conducive to clearly and visually understanding the on-site synergies between buildings; a desire to identify an indicator of energy *compatibility* between buildings arose as a consequence. The solution the author proposes is a spatial indicator that belongs to the *efficiency* principle. This new spatial and quantitative indicator is called the Thermal Diversity Index and it is the first step in joining urban planning with district energy planning. It is discussed in length in section 3.5.

Since it is not the role of this thesis to describe the AEUB diagnosis tool in detail, readers are referred to the document *Pour des quartiers durables: Les réseaux urbains d'énergie au cœur d'une stratégie holistique pour Montréal* (2019) which was prepared in French by the Re4 Montréal research group. It presents the AEUB methodology along with different architectural case studies of neighbourhoods in Montréal. Another excellent reference in English is the thesis work of Amy Oliver (2018) which not only presents a critical view of the AEUB diagnosis tool but also analyzes other frameworks.

2.5 Collaboration in Architecture and Engineering

The second question posed by data-driven design, which was introduced in section 2.4, concerns how we can sample the data space of the urban fabric to generate the data points necessary for design. The following section will discuss the current landscape of collaboration through the lens of collaborative tools in architecture and district energy planning.

2.5.1 Tools in Architecture

The energy simulation of buildings, which has long been the responsibility of engineers at the end of the design process, is being utilized more and more as a design-decision tool instead of a green-credit validation tool. There exists today a market for digital tools which unlock an untapped energy efficiency opportunity by allowing architects to understand the impacts of design on building energy efficiency. This market is currently occupied by a handful of companies seeking to valorize their techniques. Table 2-1 provides a summary of the most influential commercial products at the time of writing. In addition to this new service offer, there is an emergence of architectural firms that are restructuring to integrating in-house engineering services in an effort to bridge the gap between engineering and architecture (Mairs, 2017; Novitski, 2009). With robust urban building energy models just around the corner, architecture firms are also seeking to bring this conversation into the realm of master planning.

Many of the existing tools are built around known shape-modelling platforms and calculation engines. They are then integrated into company processes and into their operations through BIM (building information modelling). By using existing tools known to users, it is easier for them to adopt the solution quickly (Olsen & Namara, 2014). Thus, Sefaira and OpenStudio both have interfaces to SketchUp. Ladybug + Honeybee uses Rhino, a 3D shape modelling platform. Insight 360 and Green Building Studio are extensions of Autodesk Revit, a leader in BIM.

The rapid growth of these tools is explained by the democratization of building energy simulation engines such as EnergyPlus which have seen their development accelerate in recent years. It is now possible to make plausible assumptions and obtain a relatively accurate idea of the performance of buildings in a very short time. Studies at the city scale are now accessible to all thanks to the timely execution of thousands of simulations on relatively affordable cloud computing platforms.

Automation techniques with regards to the preparation of models further elevate modelling on the urban scale (see chapter 4 for more details on Urban Building Energy Modelling).

Table 2-1 Modern tools for energy simulation of buildings in Integrated Design

	Name	Company/Source	Compatible with	Engine	Cost
1	Sefaira	Trimble / sefaira.com	SketchUp and Revit	EnergyPlus, Fulcrum, Radiance, DaySIM	Variable depending on the chosen modules
2	OpenStudio	NREL / openstudio.net	SketchUp, EnergyPlus and files such as gbXML	EnergyPlus and Radiance	Free
3	BEopt	NREL / beopt.nrel.gov	n/a	EnergyPlus	Free
4	gEnergy	GreenspaceLive / greenspacelive.com	n/a	EnergyPlus	800 $/users-yr
5	Ladybug + Honeybee	Grasshopper3d / grasshopper3d.com	SketchUp, Revit, EnergyPlus and files such as gbXML	EnergyPlus, DaySIM, Radiance, Therm+Window	Free
6	Insight 360	Autodesk / insight360.autodesk.com	Revit and FormIt 360	EnergyPlus	Included in the subscription of Revit or Formit 360 Pro
7	IES VE	Integrated Environmental Solutions Limited/ iesve.com	SketchUp, Revit	ApacheSim	Variable depending on the chosen modules
8	TRNSYS	Thermal Energy System Specialists, LLC / trnsys.com	Sketchup	TRNBuild (Type56)	5060$ (single-user license)
9	DesignBuilder	DesignBuilder Software Ltd / designbuilder.co.uk	Revit, Microstation, ArchiCAD and SketchUp using gbXML	EnergyPlus, Radiance	Variable depending on the chosen modules
10	DIVA/ Archsim	Solemma LLC	Rhino	EnergyPlus, Radiance	950 $ (single-user license)
11	Green Building Studio	Autodesk / gbs.autodesk.com	Revit and files such as gbXML	DOE-2	Included in the subscription to Autodesk

Source: Aggregated data from (Overbey, 2016; Roberts, 2013) and this author.

Many tools presented so far focus on the impact of the design with respect to the orientation of the building, its shape, the performance of the envelope, the amount of glazing, the equipment and lighting loads, etc. While this does provide some insight into which design choice can have the biggest positive impact on energy consumption, these tools usually do not focus on the HVAC systems themselves and certainly don't look at the context of district energy systems. The design of thermal systems within the building cannot occur if it ignores the design of a larger district energy system. In fact, if building systems are not designed to receive energy in the form that is

supplied by a DES, then half the equation is missing. For example, low temperature district energy systems supply temperature that is not high enough to be used in regular vertical radiator units. Systems such as radiant floors are needed. In the case of heat-sharing networks, heat pumps are necessary for both the heating demand and domestic hot water preparation. This may seem trivial with respect to system design, but the designers must understand that the design of thermal systems within buildings will determine how easily a building can receive or reject thermal energy.

2.5.2 Tools in District Energy Planning

The scale and the impact that district energy networks have on the built environment carry their share of technical and economic obstacles. Only good planning in conjunction with economic incentives can render the technology competitive against local heat sources such as gas boilers and electrical heating (Aronsson & Hellmer, 2011). To assess or to ensure this competitiveness, many tools have been created to support district energy system planning across all the stages of planning.

Many quantitative models with various goals, outcomes, and targeted users offer insights into various stages of the lifecycle of a district energy project: hydraulic models, energy system models, control and operational models, financial models, decision-making models, urban planning models, etc. A study by Bradford et al. (2015) published a thorough literature review of modelling approaches for urban energy and district energy. They analyzed commercially available tools from the perspective of their main characteristics and complexity and whether or not they were proprietary or open source models. Most notably, this research—funded by the International Energy Agency District Heating and Cooling program (IEA-DHC)—proposed its own simplified methodology as an Excel workbook: Plan4DE (Sustainability Solutions Group, 2016). In the author's paper *Balancing demand and supply: Linking neighborhood-level building load calculations with detailed district energy network analysis models* (Letellier-Duchesne, Nagpal, Kummert, & Reinhart, 2018), a summary of various tools is presented in a figure that highlights their aim and time of use before and after the construction of a district energy system (figure 2.4).
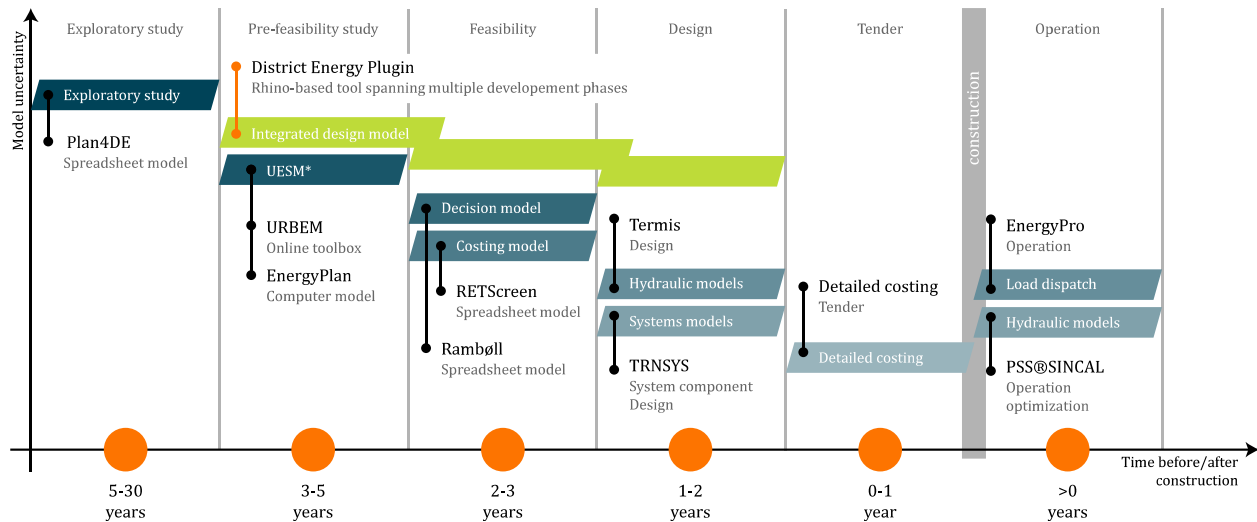
Figure 2.4 A typical district energy project development timeline and examples of tools used during each phase. *UESM stands for urban energy systems model. Source: (Letellier-Duchesne et al., 2018)

2.5.3 Challenges and Limitations

One of the major obstacles to using specialized simulation tools in preliminary design stages is their complexity and the significant time they require to set up an analysis. This is why engineers often develop tools and techniques that are approximations, rules of thumb. It is therefore necessary to design tools that bridge the gap between speed and accuracy. In *Selection criteria for building performance simulation tools: contrasting architects' and engineers' needs* (Attia, Hensen, Beltrán, & De Herde, 2012), the authors encourage interdisciplinary research in the field of energy simulation to address the criteria of architects and engineers in the development of energy simulation tools for buildings as well as the design process.

The challenge is to have a tool that is not overly restrictive or oversimplified. The outputs must reflect reality and be useful at the same time. Tools must also provide rapid information turnaround and enable quick decision-making. This is highlighted by design cognition research that demonstrated a stark divide between a designer's action and the computer's reaction, where high latency could create "change blindness," effectively preventing designers to evaluate model changes (Erhan, Woodbury, & Salmasi, 2009, p. 820). For instance, it was shown that the time between when a user taps the "simulate" button and the time the results appear on the screen, will impact the user's ability to associate the design change to its impact on energy performance.

Other authors argue that "more and better tools are needed in ID" (Leoto & Lizarralde, 2019, p. 44). Although this is accurate, we cannot fall into self-deception; the ID process's main flaw is

simply that there is too little information at the beginning of the process which eventually renders all tools inaccurate. The question then becomes whether or not this inaccuracy works against the better good of the project. As George E. P. Box (1919–2013) famously said: "Essentially, all models are wrong, but some are useful."

2.6 Discussion

This chapter aimed at presenting this thesis through the lens of collaboration between urban planning, architecture and engineering. First, the role of integrated design as a means to improve energy efficiency in the built environment was discussed. Then, the importance of creating the requirements for a holistic design space to create sustainable and livable districts was outlined. The multidisciplinary workshop discussed in section 2.3.1 highlighted the importance of establishing a diagnosis of a district and the need for open access to data, while positioning the citizens at the centre of the effort. The various tools discussed in section 2.5 draw attention to the needs of users in interdisciplinary teams, such as fast model setup and the seamless integration with existing popular shape modelling tools.

These observations present many challenges that could be solved from many different angles. This thesis focuses on bringing knowledge-based evidence to interdisciplinary teams. One key outcome of this objective is the thermal diversity index which fills a gap in quantitative indicators used in the ID process. This indicator is formally presented in the next chapter.

CHAPTER 3   DISTRICT ENERGY NETWORKS IN THE REALM OF URBAN DESIGN

This chapter investigates methods and processes involved in the development of district energy networks during urban planning and design. First, we lay the foundations for understanding district energy systems and present the concept of heat-sharing networks. Next, we propose methodologies for DES planning, introducing a spatial and temporal adaptation of the *thermal diversity index*, a key contribution of this thesis. This chapter concludes with the identification of three fields of work—1) building energy demand prediction, 2) energy supply generation and 3) distribution—where compatible methodology with the Integrated Design Process is lacking. They form the base of the three subsequent chapters.

3.1 Evolution of District Heating and Cooling Systems

District energy systems are, like all technologies, evolving rapidly. Since their advent at the end of the 19th century, different generations of district heating (DH) systems have continued to evolve. The birth of modern district heating is attributed to Birdsill Holly, Jr. (1822–1894), an American hydraulics engineer who pioneered the technology. At the time, pressurized steam was used as the main carrier fluid with temperatures greater than 200 °C. Steam power plant efficiency was increased by making double use of the heat produced from steam boilers used in electricity production. Around the 1930s, the second generation of DH emerged with pressurized water ($T_{supply} > 100°C$), replacing the dangerous and inefficient steam (Frederiksen & Werner, 2013). Subsequently, increased building efficiency allowed further reduction of the carrier fluid temperature in the third generation (to between 70 °C and 100 °C). Furthermore, thanks to the reduced operating pressure, the introduction of pre-insulated plastic jacket pipes combined with prefabricated substations (customer stations) "democratized" DH around the world. Today, the majority of district energy systems around the world are of the 2nd and 3rd generations (Werner, 2017, p. 622).

Like district heating, district cooling (DC) can be categorized into generations, and authors often tie them to district heating generations. Early generations primarily served small systems in the food supply chain (e.g., grocery stores) and practical applications appeared as early as 1889 with the Colorado Automatic Refrigerator Company. At the time, ammonia and salt water was used to

produce ice (Fernald, 1891), even before the invention of the modern centrifugal chiller by Willis Carrier in 1921. Large-scale commercial systems appeared in the 1930s (Phetteplace, 2013). At the time, centralized condensers served decentralized evaporators for each customer using refrigerant as the carrier fluid.[5] Today, modern district cooling systems distribute thermal energy in the form of chilled water (approx. 3 °C to 6 °C) from a centralized production plant. The first large cooling systems served *private institutions* as early as the 1930s in the United States. This market paved the way for *commercial district cooling systems* with chilled water as a commodity for air conditioning around the 1960s in the United States, Europe and Japan. Although most systems were developed in the United States, there has been a notable increase in activity in the Middle East and in Europe after 1990 motivated by the eminent phasing out of CFCs (chlorofluorocarbons), the principal refrigerant used in cooling systems for buildings (Frederiksen & Werner, 2013).

3.1.1 Fourth Generation DHC (4GDHC)

As mentioned in the introduction, many attempts have been made to define the future of district energy systems. Most notably, Henrik Lund and Sven Werner, two important authors in the field, coined the term *4th Generation district Heating* in their most cited work (H. Lund et al., 2014). Researchers agree that future district energy networks should aim to better meet the challenge of more energy efficient buildings as well as integrate holistically with smart energy systems (i.e., smart grids). According to the definitions detailed in their paper, a significant drop in the temperature of the carrier fluid is the main characteristic differentiating generations. Correspondingly, the 1st generation is identified as having a carrier fluid operating at more than 200 °C, the second generation higher than 100 °C, the 3rd generation lower than 100 °C and the 4th generation lower than 70 °C. The consistent reduction of operating temperatures have introduced some challenges—e.g., the difficulty to produce domestic hot water while minimizing risks of

---

[5] A more modern concept of this method has been proposed by Weber and Favrat (Weber & Favrat, 2010) and then further refined (Henchoz, Chatelan, Maréchal, & Favrat, 2016; Henchoz, Weber, Maréchal, & Favrat, 2015). This concept uses a network of evaporators and condensers (just like the 1st generation DC) circulating CO_2 as the carrier fluid. A concept for the city of Geneva shows that this technology could supply the city's heating and cooling demand with only 16% of the energy the city currently uses.

Legionella bacteria or the necessity to match the demand between the source energy and the load energy—which various research projects around the world are currently tackling (e.g., Schmidt, Kallert, Orozaliev, et al., 2017). Surprisingly, Lund et al. (2014) does not mention district energy networks operating at even lower temperatures. As we will see later, district energy networks operating at ambient temperatures between 15 °C and 25 °C have been proposed in certain energy supply schemes and have been, in some cases, in operation even at the time of Lund's publication. These DES are part of what a few authors are now calling the *Fifth Generation* of district heating in a few recent publications (Buffa, Cozzini, D'Antoni, Baratieri, & Fedrizzi, 2019; Pattijn & Baumans, 2017; von Rhein, Henze, Long, & Fu, 2019).

3.2 Fifth Generation District Heating & Cooling (5GDHC)

The fifth generation follows the trend of temperature drops and efficiency gains described by the previous generation schemes, using carrier fluid temperatures in the range of 15 °C to 25 °C. However, this very low temperature range is only permissible by using decentralized heat pumps that elevate (in heating) or lower (in cooling) the supply temperature at each building. Renewable energy sources such as solar thermal energy and geothermal energy can connect to 5GDHC networks to help balance the network (see figure 3.1).
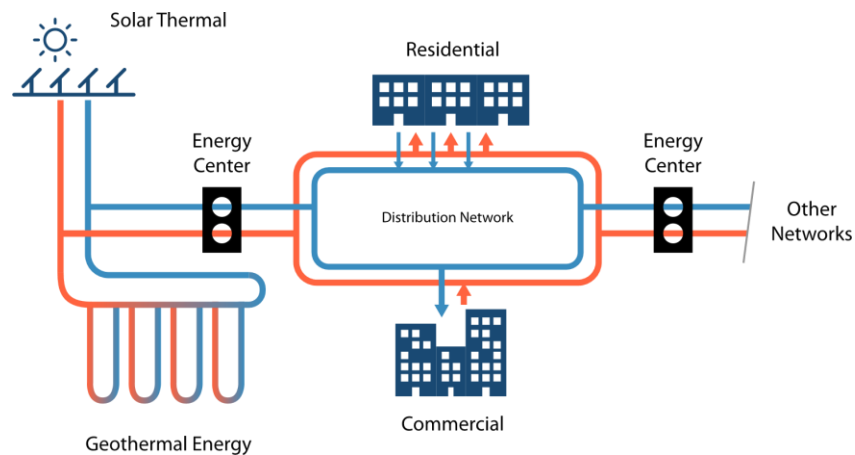
Figure 3.1 Illustration of the structure of a 5GDHC network. Residential and commercial prosumers can work together with power stations and renewable energy sources to balance the network. A 5GDHC network is scalable and can connect to other networks.

There is little consensus amongst researchers as to how to characterize and identify the district energy technologies currently tagged as 5GDHC. This is highlighted by Buffa et al. (2019) in the

first review of district energy systems of this kind. The study, financed by the FLEXYNETS European program (European Commission, 2015), uncovered a wide range of nomenclature and terms for technologies. Some examples include cold district heating (or "cold ring"), low temperature district heating and cooling, low temperature networks and even "anergy grids."[6] One of the first implementations in Canada is described as an "Ambient Temperature Loop" (Hart & Lindquist, n.d.; Perry & Ren, 2013). A summary of the nomenclature of district energy is presented in Table 3-1 along with references to the key literary work.

Table 3-1 Summary of various district heating nomenclature and key references on the subject.

Gen.	Name	Acronym	Supply temp.	Return temp.	Refs
3rd	District Heating	DH	~85 °C	~45 °C	10
	District Cooling	DC	~6 °C	~16 °C	10
4th	Low-temperature District Heating	LTDH	55 °C to 75 °C	25 °C to 40 °C	1
	Ultra-Low Temperature District Heating	ULTDH	35 °C to 50 °C	20 °C to 35 °C	4
	Fourth Generation District Heating	4GDH	30 °C to 70 °C	20 °C to 40 °C	5
	Two-way District Heating	-			7
5th	Fifth Generation District Heating & Cooling	5GDHC	15 °C to 25 °C	-3 °C to 15 °C	2
	Cold District Heating ("cold ring")	CDH			3
	Low Temperature District Heating & Cooling	LTDHC			
	Low Temperature Networks	LTN			6
	Anergy Grid				9
	Ambient Temperature Loop				8
	District Energy Sharing System	DESS			11

Refs
1   *(Averfalk & Werner, 2018; Ommen, Thorsen, Markussen, & Elmegaard, 2017; Schmidt, Kallert, Blesl, et al., 2017)*
2   (Buffa et al., 2019; Bünning, Wetter, Fuchs, & Müller, 2018; Pattijn & Baumans, 2017; von Rhein et al., 2019)
3   *(Pellegrini & Bianchini, 2018)*
4   *(R. Lund, Østergaard, Yang, & Mathiesen, 2017; Ommen et al., 2017)*
5   *(Cirule, Pakere, & Blumberga, 2016; H. Lund et al., 2014)*
6   *(Pellegrini & Bianchini, 2018; Schluck, Kräuchi, & Sulzer, 2015; Vetterli & Sulzer, 2015)*
7   *(Brange, Englund, & Lauenburg, 2016; Pöyry Management Consulting Oy, 2016)*
8   *(Hart & Lindquist, n.d.; Perry & Ren, 2013; Schluck et al., 2015; Zarin Pass, Wetter, & Piette, 2018)*
9   *(ETH Zurich, 2012; Köppl & Schleicher, 2018)*
10 *(Frederiksen & Werner, 2013)*
11 (Patent No. WO2010145040-A1, 2010)

---

[6] *Anergy* refers to "low-grade" energy (heat) which is difficult to convert into other forms of energy.

In trying to keep the same temperature drop analogy suggested by Lund et al., the authors of the review suggested that the term *fifth generation district heating and cooling* or 5GDHC be reaffirmed following its introduction at the genesis of the FLEXYNETS program (2015). While the concept of generations is common in the circle of district energy specialists, it can be quite uninformative to non-experts. On the other hand, the concept of energy *sharing* between buildings, which is at the core of the newest iteration, is arguably more self-evident. Then again, heat-sharing applies not only to fifth-generation networks but also to some of the fourth-generation networks that include *two-way* district heating and cooling where customers can both use and sell heat. The *heat-sharing* terminology encompasses systems (both 4th and 5th gen) that offer the possibility of using waste heat and is therefore a less restrictive term. This plurality explains why the term *heat-sharing* networks was chosen for the title of this thesis as opposed to the arcane *5GDHC* name. Nevertheless, this thesis embraces the fifth-generation terminology and leverages on its applications in the respective contributions.

Figure 3.2 proposes a graphical representation of the evolution of district energy systems towards heat sharing in the 4th and 5th generations. It illustrates the decreasing temperature trends of district heating generations, but most importantly it reveals how heating and cooling supply temperatures are converging towards ambient temperature fluid in the fifth generation.

The figure integrates some of the elements of the illustration suggested by Lund et al. (2014) but makes some adjustments to better represent the larger context of district energy systems. For instance, district cooling is represented in the third and fourth generation. There is no evidence in the literature as to whether or not supply temperatures increased between the third and the fourth generation of district cooling system, but it is possible to defend such an argument. Unfortunately, there is a lack of worldwide statistical information for district cooling, as stated by Sven Werner (2017).

The figure also lists many of the energy sources that serve district energy systems. In particular, the notion of *prosumer* is included for commercial and residential buildings for the fifth generation.

1st Generation
1880–1930

2nd Generation
1930–1980

3rd Generation
1980–2020

4th Generation
2020–2050

5th Generation
In development

1G STEAM

2G IN SITU

3G PRE-FABRICATED

4G SMART ENERGY

5G HEAT SHARING

Steam system, steam pipes in concrete ducts

Pressurized hot-water system

Heavy equipment

Large "build on site" stations

Pre-insulated pipes

Industrialized compact substations (also with insulation)

Metering and monitoring

Low energy demands

Smart energy (optimal interaction of energy sources, distribution and consumption)

Two-way district heating

Decoupled District Cooling

Decentralized Heat Pumps

Low-grade energy sources

Concurrent energy demands

Smart Urban Planning (mixity)

Energy Source

Steam storage

Coal, waste thermal plant

Energy Source

Heat storage

CHP coal
CHP oil

Coal, waste thermal plant

Energy Source

Large-scale Solar

Biomass
CHP biomass

Industry surplus

Heat Storage

CHP waste
CHP coal
CHP oil

Gas, waster, oil, coal thermal plant

Energy Source

Low-energy buildings

Industry Surplus

CHP waste inceneration

Future energy source

Heat storage

PV, Wave, Wind surplus electricity

Geothermal Energy

Large-scale solar

Seasonal heat storage

Biomas conversion

Two way district heating

CHP biomas

Centralized district cooling pump

Centralized heat pump

Cold storage

Future energy source

Renewable Energy Source

Industrial Surplus

PV, Wave, Wind surplus electricty

Seasonal heat storage

Biomas conversion

Large-scale Solar

Geothermal Energy

Commercial prosumers

Heat/Cold storage

Residential Prosumers

Free Cooling

Decentralized Heat Pumps

HEAT SHARING NETWORK

TEMPERATURE LEVEL

>200°C

>100°C

<100°C

<50-60°C

> 6°C

15-25°C (AMBIANT)

LOCAL DISTRICT HEATING

DISTRICT HEATING

DISTRICT HEATING

DISTRICT COOLING

DISTRICT HEATING
DISTRICT COOLING

DISTRICT HEATING & COOLING
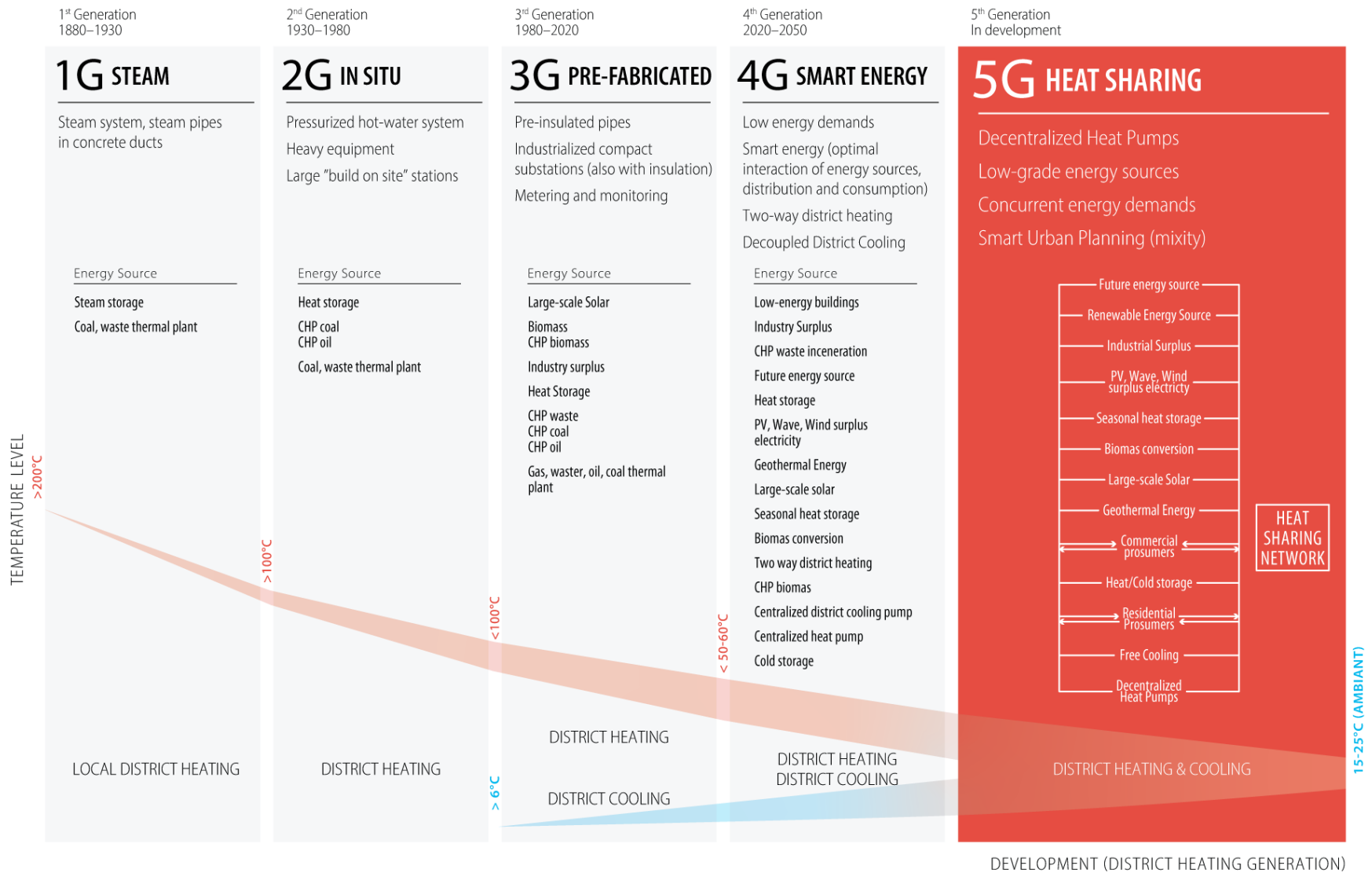
DEVELOPMENT (DISTRICT HEATING GENERATION)

Figure 3.2 The five generations of district heating & cooling. The fifth generation marks a departure in both the carrier fluid temperature level and the energy sources (electric and thermal) as well as the inherent sharing of endogenous excess heat.

3.3 Advantages and Drawbacks of Heat-Sharing Technology

A thorough SWOT (Strength, Weaknesses, Opportunities and Threats) analysis is presented by Buffa et al. in their review paper of 5GDHC systems in Europe (Buffa et al., 2019). The authors state that the most important benefit of 5GDHC is its ability to reduce the primary energy needed to meet the building heating and cooling demands by enabling the recovery of all types of excess heat that would otherwise have been lost to the environment. Equally important is the fact that this excess heat can come from a low-exergy source, meaning that the temperature level of the excess heat can be lower than the one imposed by the demands. This low-grade excess heat can be recovered directly in the network without the use of heat pumps, which is typically required in traditional district energy networks. In addition, because urban excess heat generally occurs close to the heat demand, there is no need to build transmission pipelines outside the city area.

Amongst other benefits, 5GDHC can supply both air conditioning and heating year-round as the networks are bidirectional in terms of thermal power (they can deliver "heat" and "cold"). It also provides modularity, flexibility and resilience to changing boundary conditions, such as increases in building performance in the future[7] or sudden load changes from service area expansions. Modularity is achieved by connecting independent clusters supplied by their own micro-grid (Buffa et al., 2019). Flexibly is achieved by offsetting the time of energy production and the time of energy consumption thanks to the use of either decentralized thermal energy storage (TES) systems at the network level or through decentralized TES at the user substation level (this notion of TES is heat-sharing network is discussed along with the concept of thermal diversity in sections 3.4 and 3.5). Furthermore, due to the low temperature of the network, pipes do not need to be insulated; they can also be made from polymer (high-density polyethylene [HDPE] pipes) rather than steel as it is often the case in the water supply industry. This translates directly into lower installation costs.

As weaknesses, the 5th generation requires larger investments in substations (connections to each building) as not only a heat exchanger but also a heat pump is necessary to increase or reduce the

---

[7] As society increasingly invests into improving the energy efficiency of buildings, existing district energy networks, which rely on a certain heat demand to operate, are faced with the challenge of lower demand which can disrupt their long-term viability. This possibility of obsolescence has been highlighted by Lund et al. as one of the challenges for the 4th generation of district energy networks (H. Lund et al., 2014).

supply temperature. The installation of a tank for domestic hot water is also necessary. Furthermore, the low temperature difference between the supply pipe and the return pipe requires larger pipe diameters so that carrier fluid is transported at an appropriate velocity, resulting in a higher pumping energy.

Since heat pumps use an electricity source to operate, one might argue that the overall carbon balance of a 5th generation district heating system can be less desirable than other generations. Indeed, the advantages of 5GDHC systems are dependent on the environmental footprint of the energy source that runs the heat pumps. This is analogue to the potentially negative impact of electric car use in areas where electricity is produced by coal plants or other fossil fuel-based power plants (Van Vliet, Brouwer, Kuramochi, Van Den Broek, & Faaij, 2011). Fortunately, in Quebec, this factor is negligible given the low carbon content of electricity which amounts to a low ~2 gCO_2eq/kWh. As a comparison, electricity generated with natural gas generates ~600 gCO_2eq/kWh, which is 300 times more (Transition Énergétique Québec, 2019).

Another relevant topic that was not reviewed by Buffa et al. is the resilience offered by 5GDHC. The resilience of a system is not only characterized by its ability to sustain external and internal disruptions to its service but also by the speed at which the system can recover its functions when a disruption occurs (Hosseini, Barker, & Ramirez-Marquez, 2016). The resilience of heat-sharing networks is arguably less ideal than a third or fourth generation district energy system. In fact, a 5th generation system will be impacted more importantly by a disruption of the electrical grid because the decentralized heat pumps rely on the grid to operate and to produce heat and cold in each building. In the case of 3rd and 4th generation district energy, it makes economic sense to install generators to operate the centralized system in anticipation of electrical grid faults. This is why, for example, when hurricane Sandy damaged the electricity grid of New York City, communities connected to a district energy system were the quickest to recover both their heat and electricity. Furthermore, district energy networks (which comprise all technologies including 5GDHC) have an inherent "mass" which can provide some thermal storage. For example, the Copenhagen cooling network has an autonomy of 3 hours[8] simply from the energy contained in the volume of water circulating through the network. It is also easier to include other forms of thermal

---

[8] The 3 hours autonomy was disclosed to the author by the thermal grid operator Hofor A/S (2017).

storage strategies and advanced control strategies for peak shaving, allowing building operators, for instance, to answer demand-response calls from grid operators in an effort to reduce the strain on the grid.

Although resilience seems to be a qualitative attribute, it is possible to measure with a few key metrics. For instance, the resilience of a network can be measured by the *maximum betweenness centrality* and the *average node connectivity*. Betweenness centrality is defined as the "The importance of a node in terms of how many shortest paths use that node" (Boeing, 2017a, p. 77). For example, district energy networks with a high maximum betweenness centrality are more prone to failures or disruptions should a single choke point fail. This vulnerability explains why district networks tend to have a "ring" topology instead of a simple tree structure as it lowers the betweenness centrality (Vesterlund, Toffolo, & Dahl, 2016).

3.4 Measures of Complexity in District Energy

The competitiveness of heat-sharing networks is linked with the notion of "complexity," a notion rooted in urban design that we shall discuss here. As Salat et al. put it: "Complexity is one of the more essential aspects of the sustainable city" (Salat, Bourdic, & Nowacki, 2010). What they imply here is that the complexity of the urban fabric maximizes points of contact, exchange and interface which ultimately will increase the energy efficiency of the city. One could then argue that more complexity results in more efficient district energy networks. In fact, as we will see in this section, diversity of building usages—say for example the proportions of office buildings, restaurants, homes and schools—offers a better *exergy* efficiency, indicating that diversity is linked to better system performance.

Other well-known measures of complexity in the area of district energy are the *linear heat density* and the *effective width*. Linear heat density is defined as the annual heat delivered per unit length of the distribution network (Frederiksen & Werner, 2013). It is an indicator of the viability of a network. This viability is reduced to two components: (i) the competitiveness of centralized heat supply versus decentralized heat supply and (ii) the cost of heat distribution (Urban Persson & Werner, 2011). Unfortunately, estimating linear heat density before a network is established in a city or neighbourhood is particularly difficult since the length of the network is unknown. Without empirical evidence, it becomes very difficult to justify district energy solutions in (re)development

projects. Effective width is a parameter that replaces the need to calculate the linear heat density and is perfectly adapted for district heating systems. On the other hand, it is also tied to specific district heating markets. Nonetheless, the density of the heat demand is not the only criterion for successful heat-sharing systems, as the *complementarity* between thermal rejection profiles and thermal load profiles is also important. This complementarity can be quantified with the thermal diversity index, discussed in section 3.4.2.

3.4.1 System Cost & Linear Density

As mentioned earlier, the cost function of a district heating network can be defined in terms of generation cost and capital distribution cost. The heat generation cost is discussed in the second part of chapter 6. The second component, dealing with the cost of distributing heat in a DES, is explored here to understand how the competitiveness of district networks can be assessed in an urban planning context.

The *capital distribution cost* of a network is expressed as the ratio of the annuity-adjusted total network investment cost ($a \cdot I$, \$) and the heat annually sold (Q_s, GJ/y).

$$C_d = \frac{a \cdot I}{Q_s} \tag{3.1}$$

The network investment cost I can be split into 1) the trench cost, which only depends on the length of the network, and 2) the cost of the pipe, which is a function of the diameter as well as the length. Introducing construction cost coefficients for buried pipes (C_1, \$/m and C_2, \$/m^2) and the average pipe diameter (d_a, m), the network investment cost becomes:

$$I = (C_1 + C_2 d_a) \cdot L \tag{3.2}$$

Substituting in 3.1, the capital distribution cost is:

$$C_d = \frac{a \cdot (C_1 + C_2 \cdot d_a) \cdot L}{Q_s} \tag{3.3}$$

For a known network length, the heat annually sold can be expressed as the *linear heat density* ($\frac{Q_s}{L}$, GJ/m), and the equation above can be reformulated to show this linear heat density:

$$C_d = \frac{a \cdot (C_1 + C_2 \cdot d_a)}{\dfrac{Q_s}{L}} \tag{3.4}$$

Authors have developed price curves based on localized markets and urban densities (Urban Persson & Werner, 2011). A typical heat density threshold in the UK and Scandinavia is 4 MWh/m-year (Heat Network Partnership for Scotland, 2017). In other words, if the linear heat density of a newly planned DES exceeds this threshold, a centralized distribution scheme should be more competitive than a decentralized solution.

As mentioned earlier, the linear heat density is hard to estimate if the length of the network is unknown. As a solution, Persson and Werner (2011) proposed the concept of *effective width* (w), which helps to reduce the required empirical parameters of the cost function to one. Thermal width is defined as the ratio of the land area (A_{land}, m²) to the total length of the district energy network route (L) in this area:

$$w = \frac{A_{land}}{L} \tag{3.5}$$

This is an indicator of the effectiveness of the area coverage by a district energy network with smaller numbers corresponding to more desirable conditions: very densely populated city centres are typically in the range of $50 < w < 60\ m$ (Urban Persson & Werner, 2010).

The land area is related to the building floor area (A_{floor}, m^2) by the Floor to Area Ratio (FAR, also known as the Plot Ratio) of a site:

$$FAR = \frac{A_{floor}}{A_{land}} \tag{3.6}$$

As Persson and Werner (2011) have shown in their effective width study, it is possible to develop an empirical equation from known district energy networks. Data from existing district energy networks in Sweden was collected and analyzed to develop a power function that would apply to this specific district heating market:

$$w = 61.8 \cdot FAR^{-0.15} \tag{3.7}$$

The heat annually sold (Q_s, GJ/y) is related to the heat demand intensity (q, GJ m^{-2} y^{-1}) and to the land area:

$$Q_s = q \cdot A_{floor} = q \cdot A_{land} \cdot FAR \tag{3.8}$$

Substituting Q_s/L in equation 3.4 to introduce w and q gives:

$$C_d = \frac{a \cdot (C_1 + C_2 \cdot d_a)}{FAR \cdot q \cdot w} \tag{3.9}$$

Here the heat demand intensity is expressed in terms of building conditioned area (kWh/m^2), which is a better-known metric in the building industry. The concept of effective width is therefore interesting in traditional district energy planning schemes, but the empirical equation for the effective width is specific to the heat production and construction economy of a given region. Therefore, in other areas where the district energy experience is limited, planners have no choice but to estimate the length of the network to calculate linear heat density and evaluate the benefit of district heating versus decentralized solutions.

Moreover, the effective width has been previously only applied to traditional district energy networks, so no known study of effective width has looked particularly at heat-sharing networks, which have very different economics. Therefore, equation 3.7 cannot be applied directly to this type of network. In contrast, the *thermal diversity index*, a key contribution of this thesis, is adapted to heat-sharing networks and can help estimate the compatibility of customers.

3.4.2 Thermal Diversity Index

Diversity is the most common spatial measure of complexity in the urban design and planning literature (Boeing, 2017a, p. 69). It is used in a myriad of metrics from social diversity to land use diversity. As we have seen so far, the proper balance of the cooling and heating loads in a heat-sharing network is key to ensure its high performance. Not only does a greater imbalance between the cold and heat loads result in higher flow rates in the network (Pellegrini & Bianchini, 2018, p. 10), but the costs of bringing online and running a balancing thermal plant increase. It is thus preferable to design a network that has a more balanced heating load profile from the start. That is

a network that connects buildings with concurrent and compatible loads—i.e., the excess heat of one is the source of another. However, at the planning stage, it is quite difficult to predict the energy balance of the whole project. Could there be a simple index to inform planners on the suitability of certain buildings, building types or groups of buildings to connect to a network and participate positively to its thermal balance?

We can find some inspiration in the field of urban planning and spatial statistics. As mentioned above, an indicator of imbalance, or rather of balance depending on how we look at it, is the *diversity*. The diversity is a quantitative measure that reflects how many different types (or categories) are in a certain domain (e.g., a dataset). Serge Salat (2010) adapted the Simpson Index to reflect diversity in city services. He suggested a diversity index between 0 and 1, where 0 is complete dominance of a singular service and 1 is complete balance. In other words, the closer the indicator is to 1, the closer the distribution is to an even distribution. Salat's diversity index is presented as follows:

$$div = \frac{C}{C-1}\left[1 - \sum_{i=1}^{C} p_i^2\right] \tag{3.10}$$

where *div* is the diversity, *C* is the number of distinct categories and *p* is the frequency of occurrence of each category, *i*. But since optimal diversity implies an equal number of representatives of each category, designing with an "perfect" diversity of office buildings, restaurants, homes and schools would yield a disastrous city with as many schools, homes, restaurants and office buildings. What diversity therefore needs to represent is the scales and shapes of the heat demands in order to reflect the ability to share waste heat. Zarin Pass et al. (2018) adapted this definition to the categories of interest in our case: the building-side thermal loads and the equipment COPs. The authors defined the diversity for 2 service categories *C* (heating and cooling demands imposed on the network). Consequently, equation 3.10 becomes:

$$div = 2\left[1 - \left(\frac{\dot{Q}_{cool}}{\dot{Q}_{cool} + \dot{Q}_{heat}\left(1 - \frac{1}{COP_{heat}}\right)}\right)^2 - \left(\frac{\dot{Q}_{heat}\left(1 - \frac{1}{COP_{heat}}\right)}{\dot{Q}_{cool} + \dot{Q}_{heat}\left(1 - \frac{1}{COP_{heat}}\right)}\right)^2\right] \tag{3.11}$$

where $\dot{Q}_{cool}$ and $\dot{Q}_{heat}$ (always positive) are the *zone* cooling and heating demands at a given time and COP_{heat} is the COP of the heat pump. The use of the COP modifies the zone load into the load "seen" by the network—effectively the energy taken from the district loop. Readers should note that in Zarin Pass's study, the cooling loads are met directly by the network fluid in a free-cooling fashion. The $\dot{Q}_{cool}$ variable is thus not adjusted for a chiller COP in equation 3.13. The complete equation, including a cooling COP is:

$$div = 2\left[1 - \left(\frac{\dot{Q}_{cool}\left(1 + \frac{1}{COP_{cool}}\right)}{\dot{Q}_{cool}\left(1 + \frac{1}{COP_{cool}}\right) + \dot{Q}_{heat}\left(1 - \frac{1}{COP_{heat}}\right)}\right)^2 \right. $$
$$\left. - \left(\frac{\dot{Q}_{heat}\left(1 - \frac{1}{COP_{heat}}\right)}{\dot{Q}_{cool}\left(1 + \frac{1}{COP_{cool}}\right) + \dot{Q}_{heat}\left(1 - \frac{1}{COP_{heat}}\right)}\right)^2\right] \tag{3.12}$$

This equation will be used for the remainder of the following analysis. First, we can observe the effect of the fraction of cooling load and the relationship with the COP of the heat pump. In other words, the diversity and the relative heating and cooling loads can be illustrated with different heat pump performances. Figure 3.4 illustrates this relationship for 5 different heat-sharing network temperatures. COPs are assumed to be 30% of the theoretical COP of a Carnot heat engine for a source temperature ranging from 6 °C to 70 °C and a load temperature of 6 °C in cooling and 70 °C in heating. The selected points are illustrated in figure 3.3 and are used in figure 3.4.

With figure 3.4, it becomes apparent that the asymmetric function of the heating and cooling COPs shifts the diversity such that a perfect diversity occurs when there is slightly more heating demand than cooling demand. This is in fact an advantage of heat-sharing networks in heating-dominated climates like Montréal.
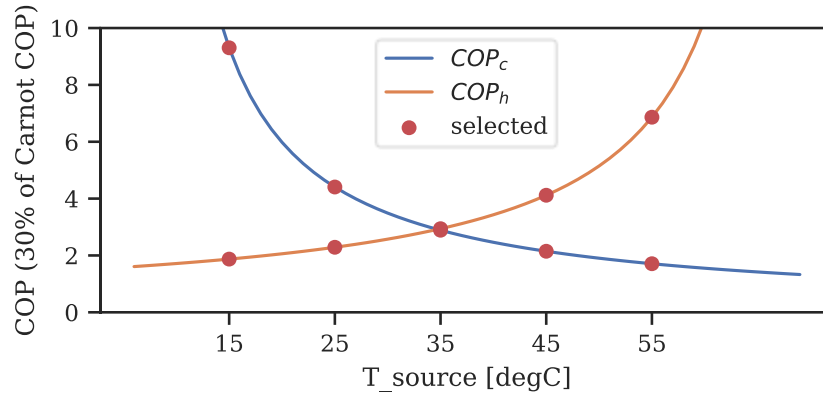
Figure 3.3 Selected operation points for heating (h) and cooling (c) COPs. The target temperature in heating is 70 °C and the target temperature in cooling is 6 °C.
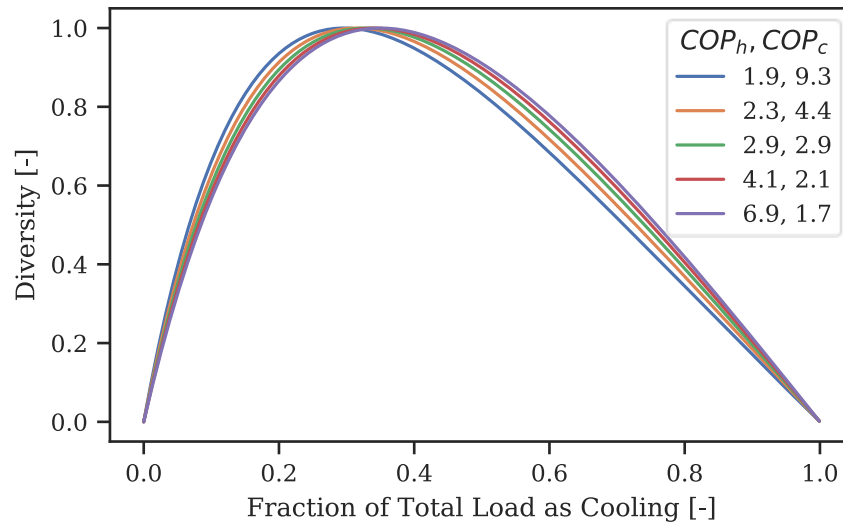
Figure 3.4 The impact of the fraction of total load as cooling and the COP on the diversity. Pairs of COPs are derived from figure 3.3.

The thermal diversity presented so far is applicable to a system state (or an instant). Varying loads and system conditions throughout the year will have an impact on system performance and thus produce varying degrees of diversity. To evaluate an "annual diversity", one could simply return the average value, but that would penalize moments when large heating loads and cooling loads are concurrent compared to similar concurrency with smaller loads. This is why Zarin Pass et al. suggest weighing the average by the amplitude of both loads imposed on the network:

$$div_{annual} = \frac{\sum_{t=0}^{n} div_t \cdot \dot{Q}_{tot,t}}{\sum_{t=0}^{n} \dot{Q}_{tot,t}} \tag{3.13}$$

where div_t is the diversity calculated with equation 3.12 and $\dot{Q}_{tot,t}$ is the sum of both loads (always positive) for a given hour t and n is the duration (e.g., 8 760 hours).

This concludes the literature review of the thermal diversity. Next, we look at how this indicator behaves under various thermal load conditions and we suggest a method to transform the static indicator in a spatial indicator that can more directly answer urban planning requirements.

3.5 Thermal Diversity as an Urban Planning Metric

In the context of urban planning, we ask the question, "what are the chances of success of a heat-sharing network in a given neighbourhood?" According to the definition of thermal diversity, a cluster of buildings which has an overall thermal diversity closer to one, will result in more heat-sharing within the cluster. With respect to the network itself and the energy centre, this can imply two things: 1) the energy centre can store a certain amount of thermal energy, and 2) the network can reach a larger cluster of buildings thereby further improving the performance of the system. The next two sections discuss both variables, starting with the notion of "temporality" for storage and then the notion of "spatiality" for the network's extent. The method is then applied in an area around Downtown Montréal.

3.5.1 Temporal Filter

To understand how the annual diversity responds to different system conditions, we present the following theoretical cases. First, let us imagine a situation that would produce the worst diversity possible, by establishing a sort of boundary in the form of one hour of heating demand during the winter and one hour of cooling demand during the summer. Then, we can imagine different scenarios where the load profile is increasingly favourable to diversity by changing cycling periods between cooling and heating. 6 cases are presented in figure 3.5.
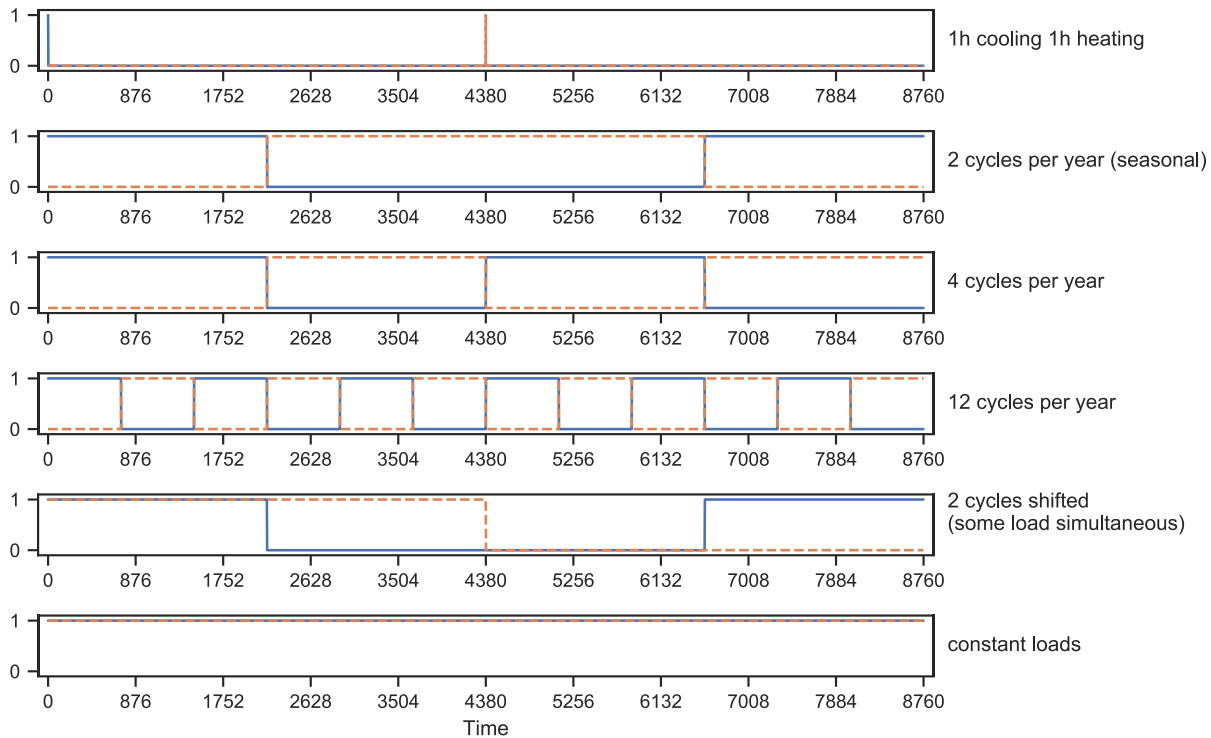
Figure 3.5 Theoretical load cases for analyzing the behaviour of the annual diversity. Heating loads (full lines) and cooling load (dashed lines).

The first four cases have no overlapping heating and cooling demands. Evidently, they all produce an annual diversity of 0. The two last cases show simultaneous heating and cooling loads and therefore show some diversity (0.5 for *2 cycles shifted* and 1 for *constant loads*). But thermal networks sharing heat between buildings could include thermal storage, which would increase the "match" between some cooling and heating loads. To model given levels of thermal storage (expressed in hours of capacity), a moving average function is applied as a *filter* through the different time series. In presence of "infinite" storage, or an average function with a width equal to the duration of the load profile, it is expected that the diversity will be 1 if the total heating and cooling loads are equal. The next figure (figure 3.6) presents the annual diversity as a function of the amount of thermal storage hours (the width in hours of the moving average function).

The two extreme cases ("constant loads" and "1h cooling 1h heating") bound the possible values of diversity as expected. With 2 and 4 cycles of heat and cold demand, perfect diversity is achieved before "infinite" storage is reached at 1460 hours and 4 380 hours respectively. Finally, the case showing some simultaneous loads experiences a non-zero diversity with zero storage (H=0) and gradually increases as storage increases.
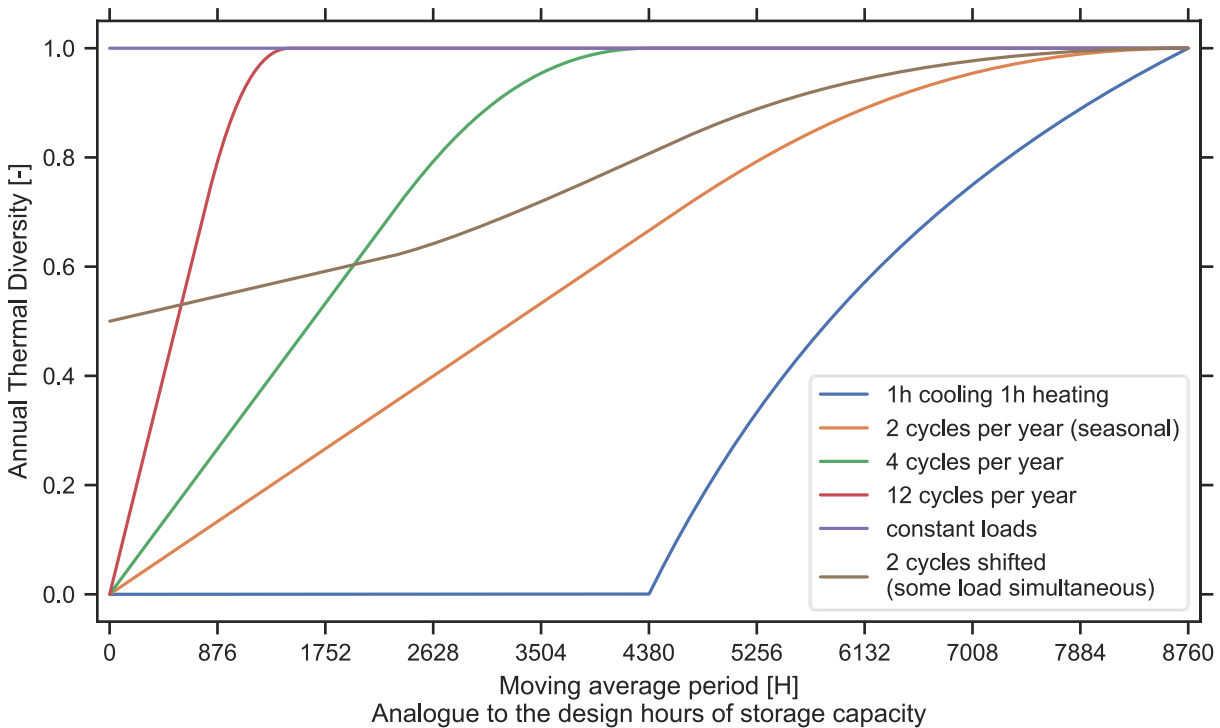
Figure 3.6 Annual Diversity of 6 theoretical load profiles with increasing storage capacity.

A similar behaviour is shown in the next figure for two practical cases (figure 3.7). An additional pair of curves illustrates a typical load profile for an urban development of approximately 10 million square metres of mixed-use space ("typical building loads") simulated in Montréal. The second curve simulates the effect of having a constant external source of heat such provided from a data centre for example ("typical building loads + DC"). Both curves were modelled by normalizing the simulated load profiles and scaling them to a certain annual energy quantity. The ratio of cooling energy demand to total energy demand was adjusted for 3 cases (one fifth, one third and half the total energy demand, represented in figure 3.7).

With a cooling demand representing 20% of the total annual demand (left), the figure shows that the presence of a data centre without any storage provides the same positive effect on the diversity than 3 356 hours of storage without the data centre. (This study is performed using a simple storage model that ignores thermal losses and transfer efficiencies; more detailed storage models may show different magnitudes, but the trends will be largely the same.)

The thermal diversity increases sharply as storage is added until approximately 24 hours of storage capacity is reached. At this point, the capacity is enough to smooth out much of the diurnal energy

demands. As the capacity is increased, the observed rate of change decelerates until it reaches a second "knee" at 700 hours of storage. Beyond this point, the system reaches storage capacities that allow seasonal storage to occur and a gradual increase in thermal diversity is observed. In this range of storage hours, energy stored in the summer can be used in the winter. Interestingly, Duffie and Beckman (2013) describe a similar phenomenon with solar thermal energy storage systems: adding thermal storage rapidly increases the solar fraction of a system until daily cycles can be smoothed out by the storage capacity (i.e., the storage has a capacity of 24 h). Further increasing the thermal storage capacity only increases the solar fraction marginally until much larger capacities are reached that smooth out seasonal phenomena. While the study focused on smaller scale systems, the authors argued that a similar curve would be observed for community-scale systems such as district energy systems.
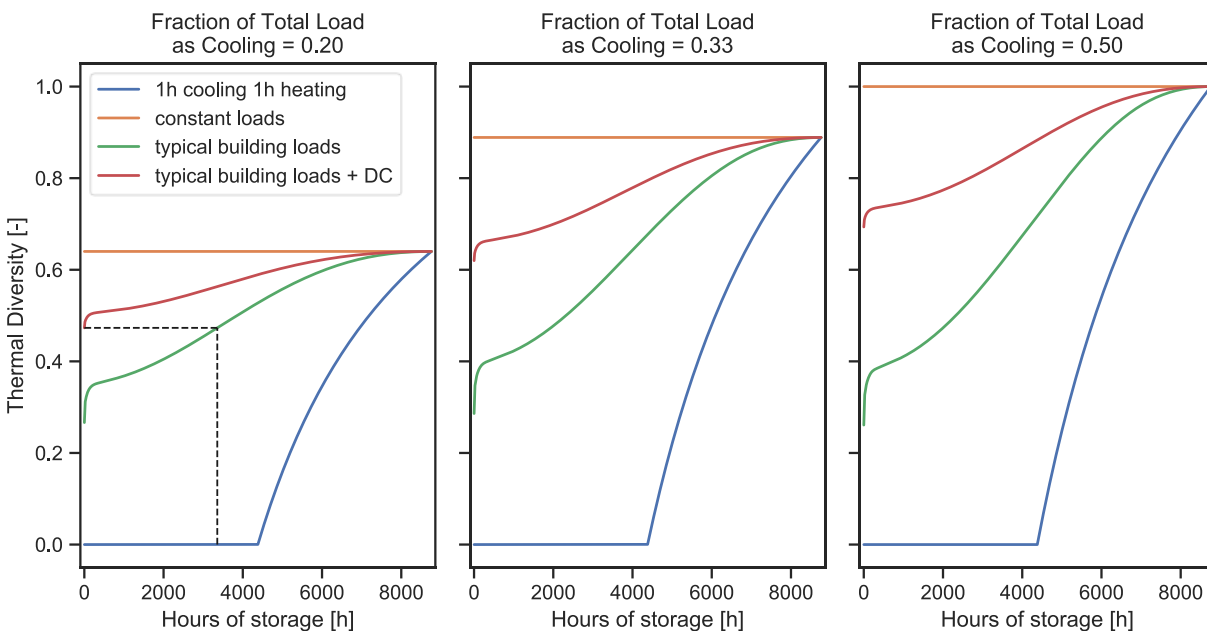
Figure 3.7 Behaviours of thermal diversity with respect to the fraction of the total load as cooling.

3.5.2 Spatial Filter

Applying a thermal diversity equation as a *filter* across an equally spaced grid of points in a given region of interest adds a geographical dimension to the thermal diversity index. A filter, in GIS terminology, "essentially creates output values by a moving, overlapping neighbourhood window that scans through the input raster" (ESRI, 2016). As the filter passes over each input cell, the value

of that cell and its neighbours are used to calculate the output value using an aggregator function—e.g., mean, max, etc. The thermal diversity *spatial* filter works similarly but with two important distinctions:

1. The neighbourhood region is a circular buffer of a certain radius around the cell for which the diversity is calculated. Any building intersecting with this buffer will be part of this neighbour region including the processing cell itself;

2. The aggregator is the annual diversity as defined by equation 3.13, potentially including a time-based filter to represent thermal storage.

Figure 3.8 illustrates this process with a circular neighbourhood of 4 cells (radius). The figure only shows the results of two cell values (on the right), but one must imagine that the moving filter is applied to all cells across all *rows* and *columns* of the cell grid.
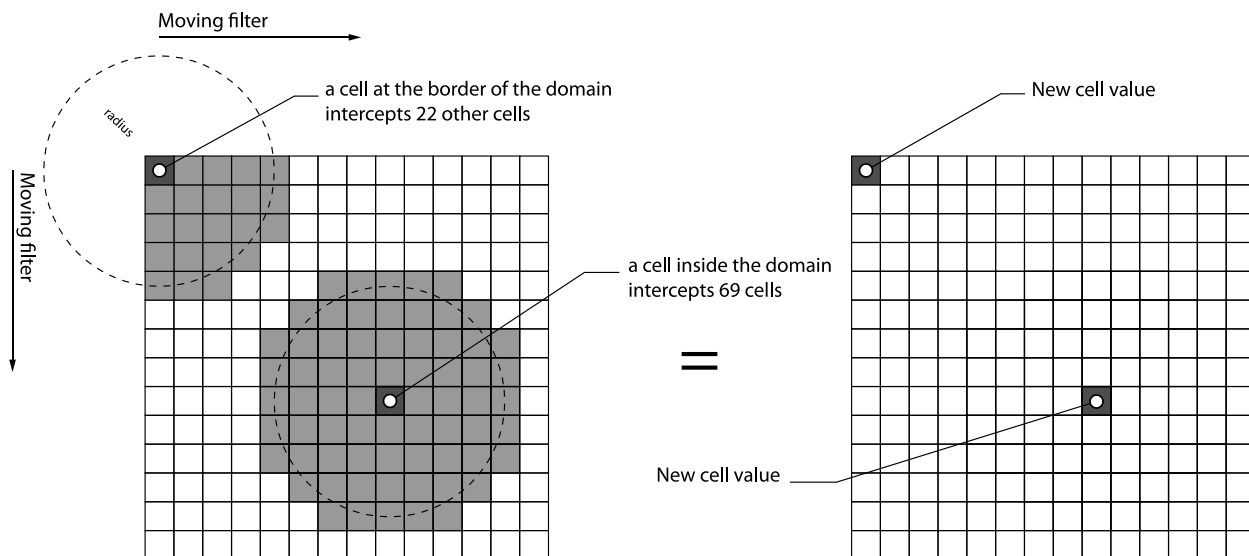
Figure 3.8 Diversity filter with circular neighbourhood example (radius = 4 cells). The thermal diversity index is applied to a grid of cells by use of a filter which is applied to a moving window of a certain radius. In this image, two resulting cells are shown (right) along with the cells (or buildings intersecting with the region) that participated in their calculation (left).

In practice, the thermal diversity index is a 3-step operation. First, a *sum* aggregation filter is applied: the dynamic load profiles of each building that geographically intersect a cell neighbourhood (light gray in figure 3.8) are summed along the time axis, returning the total load profile (one profile for heating and another for cooling). At this stage, thermal storage can be simulated by applying a *temporal filter*; in this study, a simple moving average is used, but more advanced algorithms could be applied. Second, the diversity (equation 3.12) is calculated for the

cell neighbourhood at each time step (8 760 diversities for a full year if hourly load profiles are used). In equation 3.12, the $\dot{Q}_{cool}$ and $\dot{Q}_{heat}$ variables are the previously spatially aggregated time step profiles. Third, the *annual* diversity is calculated for each cell by use of Equation 3.13: the time step diversities are averaged and adjusted to the magnitude of the total load ($\dot{Q}_{tot,t}$). This operation yields a thermal diversity index that is aware of spatiality and thermal storage. Finally, a colour map is applied to visually distinguish the diversity values between 0 and 1 (as shown below in figure 3.9 in the following section).

3.5.3 Application

A practical example is presented here. It was created by this author as part of a study prepared for the *C40 Reinventing Cities* project in Montréal (C40 Reinventing Cities, 2019). In this example, the thermal diversity index was calculated for an area including Downtown Montréal and other neighbourhoods in a radius of 5 km around the city centre. The *spatial filter* cell radius was chosen as 250 metres on grid discretized by 100×100 metre squares.

The underlying data used to create this map originates from the results of the building stock energy model presented in chapter 5 which estimates the hourly load profiles of all buildings on the Island of Montréal using a method of Urban Building Energy Modelling. The heating loads (space heating + domestic hot water) and cooling loads (space cooling demand) were converted to network loads using a constant COP of 3 (in heating and cooling).

Figure 3.9 shows areas of the city where the heating and cooling demands are concurrent (darker red) clearly identifying which areas of the city are best suited for a heat-sharing scheme. The method can therefore offer insight for planning protocols of heat-sharing networks.

It is also worth mentioning that the *cell-radius* can be adjusted to reflect the service area of the planned network. This parameter indicates the *extent* of the network. For example, with a cell radius of 500 m, the computed diversity includes buildings as far as 500 m around the centre of each cell. Combined with the notion of thermal storage, the same area modelled in figure 3.9 is represented for 3 different network extents and 3 thermal storage capacities (see figure 3.10).

Increasing the extent of the network increases the thermal diversity by allowing it to reach buildings with different heat demand/rejection profiles, but only up to a certain degree: in the absence of a large constant heat consumer/heat rejecter, space cooling and refrigeration can match only some

demands for domestic hot water and perhaps a small share of space heating. Adding thermal storage increases the thermal diversity, potentially modifying the relative attractiveness of different areas for heat-sharing networks. If synergies with different forms of storage are present (e.g., large water reservoir, planned geothermal field in conjunction with the network), assessing the spatially and temporally filtered thermal diversity of a neighbourhood would help urban planners to target specific areas to implement bylaws or regulation favouring heat-sharing networks.

While thermal diversity can serve as an urban planning metric for diagnosing an existing neighbourhood or even an entire city, the next section explores how building density and the diversity of building usages influences competitiveness of heat-sharing networks.
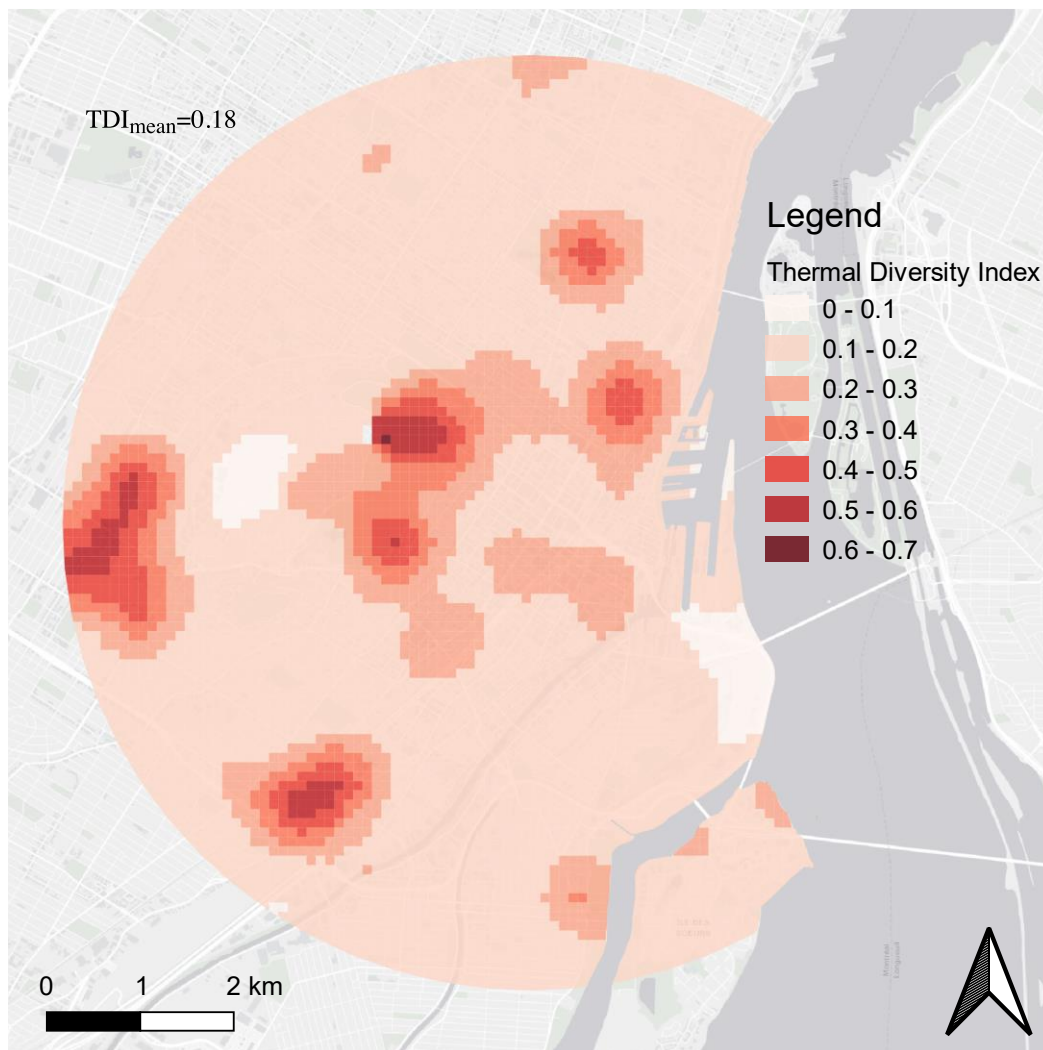
Figure 3.9 Spatial application of the Thermal Diversity Index (250m cell radius) on a 100-meter grid. Darker areas, with a higher thermal diversity, present better synchronicity between heating and cooling loads within the 250 m radius. The map is centred on downtown Montréal, Canada. (Light Gray Canvas Map sources: Esri, DeLorme, HERE, MapmyIndia)
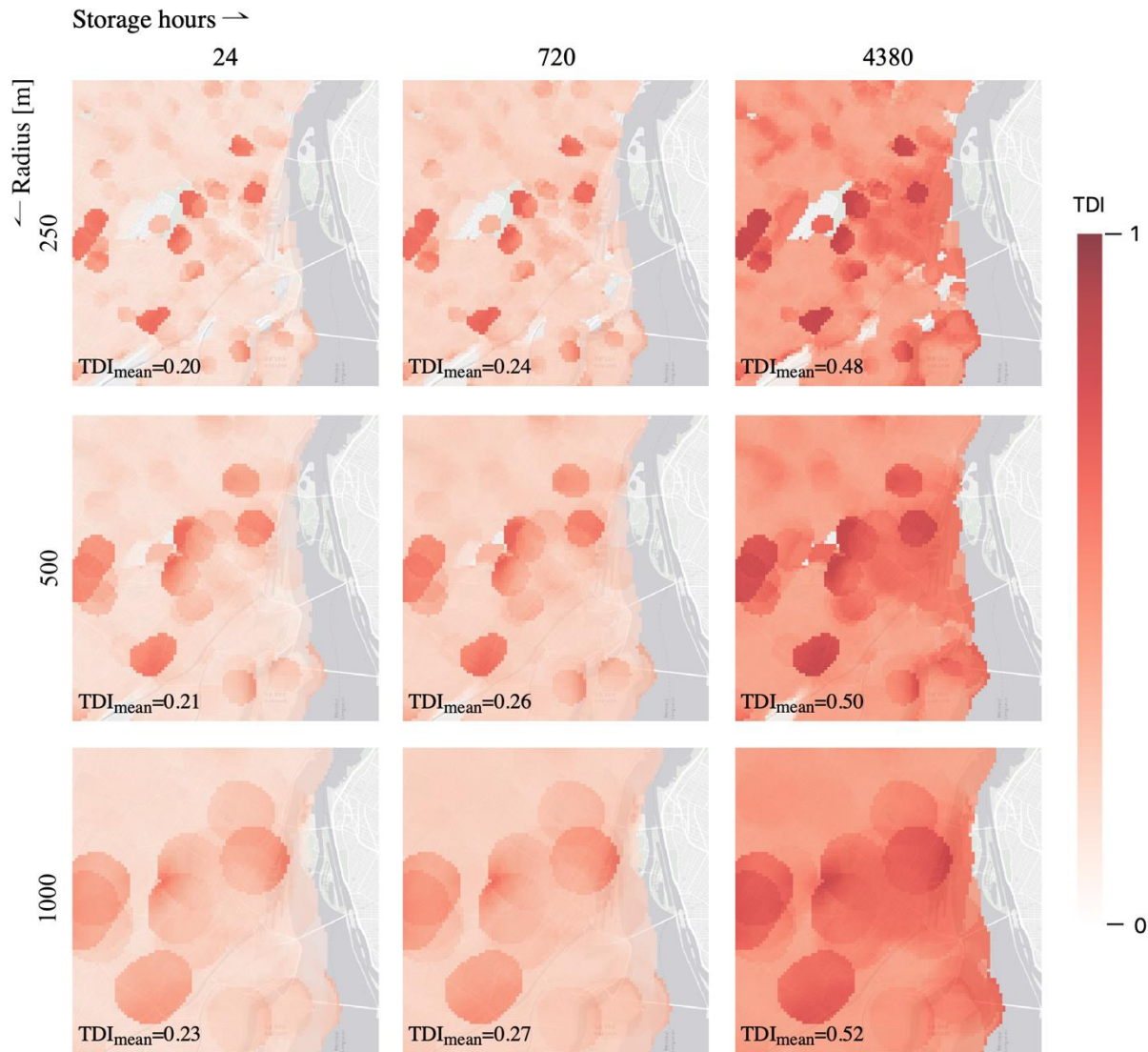
Figure 3.10 Varying *spatial* and *temporal* Thermal Diversity Indices. (Light Gray Canvas Map sources: Esri, DeLorme, HERE, MapmyIndia)

3.6 Impact of Density and "Mixity" on Heat-Sharing Competitiveness

The effective width was presented earlier as a means of estimating the competitiveness of district heating while the thermal diversity index was presented as a way of estimating the compatibility of buildings in a heat-sharing network. Density refers to the amount of built floor space on a given land. It is expressed as the ratio of floor area to land area or simply the Floor-to-Area Ratio (FAR, see figure 3.11). "Mixity," on the other hand, refers to the primary activities (or uses) occurring in multiple buildings. While *diversity* of usage would more properly identify this metric, "mixity"

was chosen as not to be confused with the *thermal diversity*. In the following example, we look at how density and "mixity" influence both metrics.

$$FAR = 3 / 9 = 0.33 \qquad FAR = 9 / 9 = 1$$
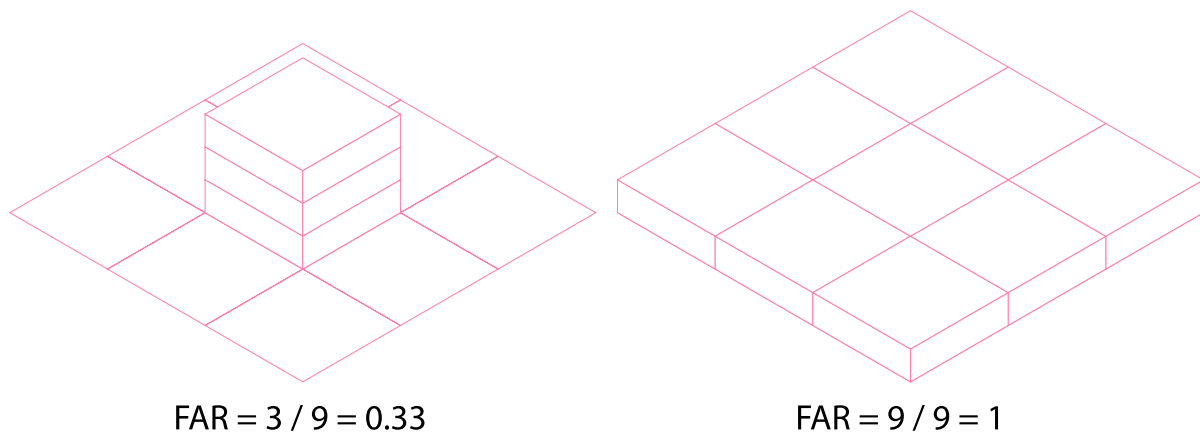
Figure 3.11 Floor-to-Area Ratio (FAR), illustrated

3.6.1 Input data

The example is applied to a fictitious neighbourhood known as a "protoblock" or a prototype of a city block. It measures ~250 metres on each side and holds 15 large buildings. The area of the lot is taken as 64 000 m^2. Three cases of the same protoblock are compared with three densities: low, mid, high (figure 3.12). The density of the protoblock is adjusted by increasing the height of the buildings, effectively adding stories. This is shown in the "mid" and "high" protoblocks which present extra towers (up to 100 m).
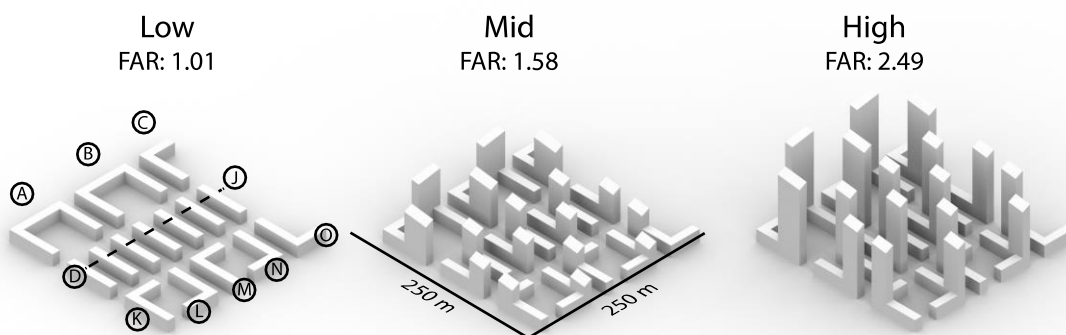
Figure 3.12 Protoblocks showing three different urban densities.

Density: For the density indicator, we rely on the Floor-to-Area Ratio (FAR) as it is a parameter of the distribution cost function detailed above. Another density metric such as the "compactness" could be used.

"Mixity": "Mixity" is expressed as the "share of commercial buildings" in the total floor area. For example, if a quarter of the floor area of the protoblock is reserved for office buildings and the other 75% is reserved for housing, the "mixity" for this neighbourhood is 25%.

Network Length: Since the location of the buildings in the protoblock is known, an approximation of the network length can be calculated by use of an algorithm well known in graph theory: the minimum spanning tree algorithm. The centroid of each building serves as the point where heat is delivered, and the possible routes are represented by all the combinations of connections between all the buildings (a "complete graph" in graph theory). Using the edge length as a weight, the minimum spanning tree is a structure that connects all buildings (identified A through O) with the smallest cost, or in this case, the smallest total length. With this definition, the network has a length of 682 m (figure 3.13).

origin	end	Length (m)
A	E	87
B	C	67
B	H	87
D	E	30
D	K	72
E	F	29
F	G	31
G	H	29
H	I	31
I	J	30
K	L	50
L	M	46
M	N	50
N	O	43
	total	682
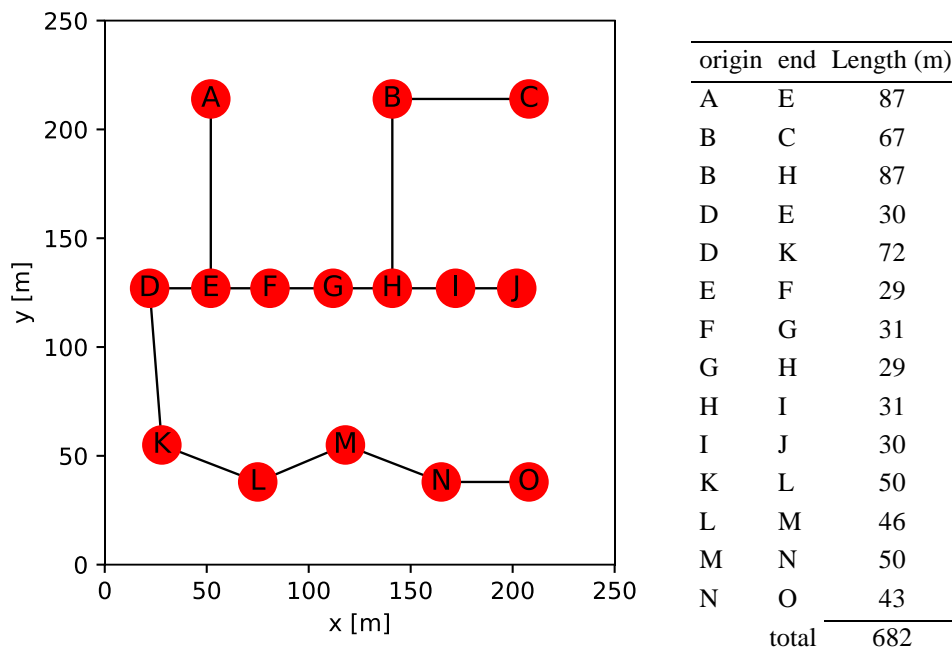
Figure 3.13 Minimum network length of the district energy network in the protoblock.
Refer to Figure 3.12 for the identification of the buildings.

Thermal width: Since both the number of buildings (and their location) and the lot size do not change, the calculated theoretical thermal width is evidently the same for all 3 cases. This highlights one of the limitations of the effective width in which it ignores density that is increased by building vertically as opposed to density which is increased by building on unused land.

Buildings loads: This example uses building archetypes modelled by the U.S. Department of Energy (NREL, 2011). Specifically, the "Midrise Apartment" and the "LargeOffice" archetypes are used and simulated for the Montréal climate. Simulation results are normalized by floor area (kWh/m^2) and multiplied by the assumed floor area for each building type according to the investigated "mixity."

3.6.2 Results

The results presented below (see figure 3.14) show that the thermal diversity index reaches a maximum around 20%. It is also interesting to point out that the maximum occurs with a relatively low fraction of commercial space. At the end of the spectrum, 100% of commercial space shows a low 10% thermal diversity, due to the use of a single office building archetype in this example. In addition, the thermal diversity, interestingly, seems to be blind to the various magnitudes of the heat and cold demand. As shown in Table 3-2, the low, mid and high cases present the same diversity for the same share of commercial space ("mixity"). Because the same profiles are simply scaled to cover more floor area, the thermal diversity does not change.

In reality, we would typically see a larger share of housing space when density is increased by building more stories, which would produce lower thermal diversities. Understanding not only the annual heat density but also the dynamic heat/cold demand profiles is hence very important, which is why this thesis proposes a method to estimate the shape of annual heat and cold demands as discussed in chapter 5.
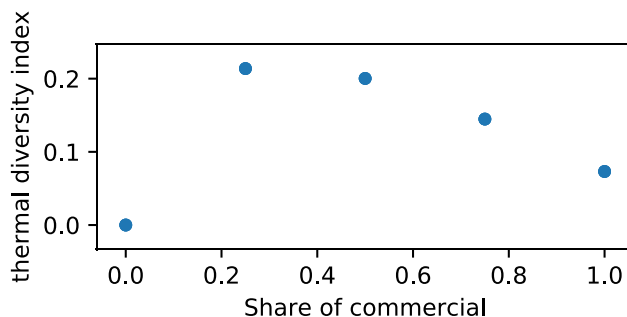
Figure 3.14 Thermal diversity as a function of the share of commercial space ("mixity").

Table 3-2 Thermal Diversity Index Results

"mixity"	Density		
	Low: 1.01	Mid: 1.58	High: 2.49
0%	0.00	0.00	0.00
25%	0.21	0.21	0.21
50%	0.20	0.20	0.20
75%	0.14	0.14	0.14
100%	0.07	0.07	0.07

3.7 Discussion

In this chapter, we explored the evolution of district heating and cooling through their various generations and laid out the rationale for a fifth generation of district heating and cooling (5GDHC). This latest generation follows the trend of decreasing supply temperature and reaches a convergent point where heating and cooling is supplied using the same network. This duality promises increased performance as low-exergy excess heat can be more easily reintroduced in the supply network. On the other hand, the use of heat pumps at each customer (building) requires a clean source of electrical energy; otherwise the efficiency gains will be compromised by a higher environmental impact.

The chapter then presented how DES can be planned in areas where typical district heating metrics such as the linear heat density are harder to obtain. Along with demographic data, the effective width is an indicator which can replace the linear heat density in the cost function of a network. As effective width only changes with respect to the density of the heat demand and not the mixed-use

complementarity of the heat demand, another indicator is necessary to address the particular case of *heat-sharing* networks. This indicator is the thermal diversity index.

The thermal diversity is identified in the literature as a concept that can evaluate the compatibility of buildings within a heat-sharing network. The behaviour of the indicator has been assessed using simple theoretical cases which helped demonstrate how more or less "diverse" heat demands function. Temporal and spatial "filters" were developed to take into account energy storage (a key aspect of successful integration of 5GDHC networks into smart grids) and to obtain an *index* that can integrate with urban planning in the form of a visual indicator. These contributions as an urban planning metric allow planners to identify areas of the city where heat-sharing networks have the best chance of being successful, but also to organize urban planning *for* the heat-sharing capability of buildings.

This chapter then ends with an illustration of the impact of density and "mixity," two urban planning dimensions, on the competitiveness of heat-sharing infrastructures. This analysis concludes that the thermal diversity is not enough to assess the competitiveness of heat-sharing networks and that a more advanced analysis is required such as the one presented in chapter 6.

Such an analysis would require hourly load profiles, but also a way of estimating the shape (or path) of the network. These requirements form the basis for the objectives of the upcoming chapters: the need for a method that quantifies energy demand dynamically is answered in chapter 5, and the need to propose a topological network structure is answered in chapter 6. But first, we must review the foundations of building stock energy prediction and propose a way of accelerating the creation of building stock models in the next chapter.

CHAPTER 4   ARCHETYPES IN URBAN BUILDING ENERGY MODELLING

This chapter addresses the theoretical and practical frameworks of building energy use estimation at macro—*i.e., city block, districts or whole city*—scales, culminating with Urban Building Energy Modelling theory and analysis. Designing and sizing energy supply systems relies heavily on drawing a portrait of energy consumption in buildings. Where measured data is unavailable, scholars and professionals have developed advanced modelling techniques that mimic the thermal behaviour of buildings in to predict their energy consumption. While some techniques have been well suited for single building analysis, a new set of techniques had to be developed to enable city-scale simulations. Recent advances in urban building energy modelling (UBEM) have proposed workflows for creating "bottom-up" models with comfortable computing time, even on a larger scale. This chapter then focuses on one of the main challenges at the core of any bottom-up approach: the creation of building archetypes that require tedious manual work. The availability of National Reference Building Models (NRBMs), such as the Department of Energy's residential and commercial prototype building models (NREL, 2011; US DOE - Building Technology Office, 2018) or Natural Resources Canada's Building Technology Assessment Platform (CanmetENERGY, 2019), based on the EnergyPlus platform (US Department of Energy, 2010), is an opportunity to accelerate the creation of UBEMs. The chapter presents the process of converting multi-zone building *archetypes* to *archetype templates* which form the data structure of the "Shoeboxer" method, a promising UBEM technique based on two-zone distributed models (Dogan & Reinhart, 2017). Finally, we present the methodology for producing more than 15 000 archetype templates covering several cities in Canada and the United States.

4.1 Foundations of Building Stock Energy Prediction

So far, this dissertation has laid out the case for a data-driven district energy planning methodology, but solutions have been shown to rely on understanding dynamic energy flows in buildings. Fortunately, a recent field of research in engineering and building physics studies the development of building stock models that can not only estimate the energy use of buildings but also evaluate their dynamic performance over a typical year. This field of work is part of the larger study of building stock energy modelling.

Building stock energy models are tasked with providing aggregated views of energy consumption of an entire building stock in terms of net energy demand, final energy, environmental impact and energy-saving measure costs. Authors of review papers have consistently separated methods into two large categories: The top-down and the bottom-up approaches (Frayssinet et al., 2018; Kavgic et al., 2010; Lim & Zhai, 2017; Reinhart & Cerezo Davila, 2016; Swan & Ugursal, 2009). These categories are broken down next and a summary is presented in figure 4.1.

While top-down approaches are usually the easiest to set up, they aim to show the links between the energy sector and the overall economic outputs through the relationships between historical energy consumption and socio-economic factors such as demography, fuel prices, climate conditions, and national economics (Lim & Zhai, 2017). They focus on the macroeconomic behaviour of the building stock and are therefore not adapted to the study of heat-sharing networks.

On the other hand, bottom-up methods calculate the individual end-uses of buildings or groups of buildings and apply various weighting techniques to predict energy consumption at various scales (Swan & Ugursal, 2009). Bottom-up methods can be further broken down into *statistical* and *engineering-based* methods on the basis of the type of modelling techniques they use.

Statistical methods use historical data in combination with energy utility billing data and survey data that includes energy retrofitting surveys to recreate the patterns of energy consumption of buildings. Statistical methods use this information to regress the energy consumption as a function of building characteristics. When based on annual data, *statistical* methods cannot estimate higher resolution patterns such as monthly or hourly profiles, but they have the advantage over *engineering-based* methods of being more "robust" since they are based on measured building data and thus can encompass occupant behaviour, a notoriously difficult factor to model analytically (Cerezo Davila, Reinhart, & Bemis, 2016; Swan & Ugursal, 2009). In fact, engineering-based methods typically rely on detailed thermodynamic and heat transfer analysis that must presume a certain occupant behaviour. For this reason, some authors have focused on developing more accurate occupancy patterns in an effort to mitigate errors due to this important modelling factor (Cerezo, Sokol, Reinhart, & Al-mumin, 2015; Dong et al., 2018; Page, Robinson, & Scartezzini, 2007; Rakha, Rose, & Reinhart, 2014; Wilke, Haldi, Scartezzini, & Robinson, 2013).

Engineering-based methods can further be broken down into two other categories: *deterministic* or *stochastic* methods. The first method, referred as the *archetype method*, implies that a sample of

representative buildings, known as building *archetypes*, covers the whole building stock and that individual variations in building properties within a representative subset of similar buildings are ignored. The second method works similarly but goes one step further by suggesting some variability in uncertain model parameters through distribution functions (e.g., uniform probability distributions). When measured data is available for a subset of buildings, Bayesian calibration techniques can achieve more realistic probabilistic distributions (Cerezo et al., 2017). Such a *stochastic* method will tune the shape of the distribution of certain model parameters to the observed data. While this method promises the creation of building stock models that are closer to reality, significant challenges can slow down their development. First, the availability of building properties which offer a high spatial granularity and the availability of measured energy data (especially for residential buildings) poses a challenge for the calibration of parameter distributions. Second, the uncertainty accompanied by occupancy patterns still presents the same challenge as with deterministic methods. Finally, challenges arise from the data availability of measured building energy data for calibrating archetypes. Sokol et al. (2017) assessed the impacts of these challenges by comparing stochastic modelling with deterministic modelling. The authors found that the deterministic archetypes were unable to properly represent the measured Energy Use Intensity (EUI) distribution of the buildings within the study area while probabilistic parameters (e.g., infiltration rate, occupancy density, temperature setpoints, plug loads intensity and domestic hot water demand intensity) led to more accurate distributions of building energy.

Another area of research focuses on the local *context* of buildings within UBEM (Reinhart & Cerezo Davila, 2016). Individual building models that use dynamic thermal simulation engines such as EnergyPlus, DOE2, TRNSYS or IDA-ICE can model solar shading and building adjacency conditions, but this evaluation is usually replicated to the whole building stock when end-use results are simply scaled up; this is usually the case with *deterministic* methods. A *context-aware* urban model is based on the premise that the context of each building, and by extension the solar incidence, has a non-negligible impact on model accuracy. The variations in building geometry (e.g., depth, width, etc.) suggested by a finer 3D modelling context will also give more weight to considerations such as the ratio between core and perimeter thermal zoning. Context awareness also suggests that buildings which have adjacent walls will behave differently than isolated buildings.

An example of a *context-aware* UBEM was developed by Cerezo Davila et al. (2016) to model the City of Boston by creating as many multi-zone building energy models as there are buildings in the city (83 541 modelled buildings) and assigning the thermal properties of 52 different archetypes based on building use and age. The Lawrence Berkeley National Laboratory (LBNL) developed a similar approach called "CityBES" (City Building Energy Saver). This web-based tool offers an automated workflow to combine city GIS datasets which provide the building massing information (building footprint, year built, building type, building height, and number of stories) with a library of EnergyPlus building archetypes that are generated programmatically (Chen, Hong, & Piette, 2017; Hong, Chen, Lee, & Piette, 2016). To circumvent issues of simulation time, CityBES leverages a server farm to parallelize the simulation of each individual building. This evidently comes at a high cost which cities—the target customer of the tool—usually have resources for. Another team developing a similar strategy claim that they achieved "realistic" simulation times by deploying EnergyPlus simulations on a national supercomputer (New et al., 2018). These examples suggest that simulating the urban context of buildings requires a "brute force" simulation strategy. It appears that some solutions may not be a viable avenue for all types of users.

As a result, Dogan (2015) proposed a solution that would reduce the simulation time—and by extension, the simulation cost—of UBEMs while taking the urban context into account. The method was integrated into the UMI tool and later refined (Dogan & Reinhart, 2017; Reinhart, Dogan, Jakubiec, Rakha, & Sang, 2013). The approach is known as the "Shoeboxer" and operates on the principle of distributed two-zone models—that resemble shoeboxes—and for which *archetype templates* are applied. Another method known as the BBEE method (Building Blocks Energy Estimation) assumes that "the energy demand of [the] whole building mass in the district is close to the sum of each part" (Zhu, Yan, Sun, An, & Huang, 2019). A large library of typical building zones (different zones for different zone uses and orientations) is pre-simulated. Then the studied district is divided into multiple standard zones, similar to Lego blocks, and the energy demand by zone is aggregated back to whole buildings. While this technique does account for the orientation of thermal zones, context shading due to surrounding buildings does not seem to be supported.

As stated above, UBEMs rely on building archetypes that are *theoretical* buildings representative of the building stock. We discuss next how archetypes are created and summarize available public sources of archetypes.
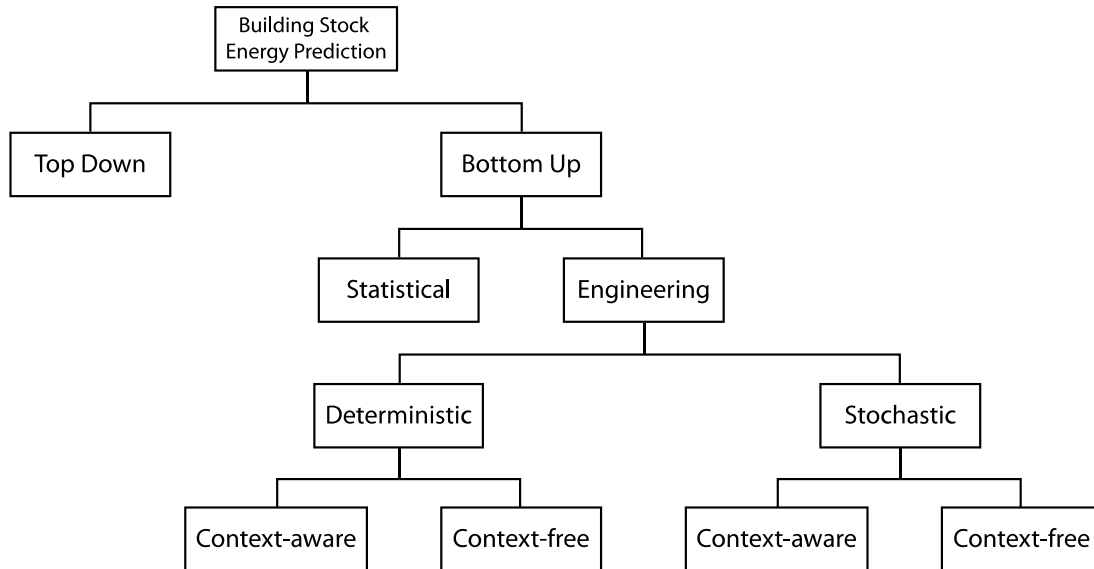
Figure 4.1 Summary of building stock energy prediction methods. UBEM methods are part of the engineering-based subgroup.

4.1.1 Archetypes

Various UBEM methods rely on "building archetypes" that are common representations of buildings with similar properties. Reinhart and Cerezo Davila (2016) identified 17 studies of archetype creation for UBEMs which varied widely in terms of the number of archetypes per study (5 to 3 168) but also the number buildings represented by each archetype (50 to 500 000). By surveying the literature of UBEMs, the authors observed a wide range of methods that do not seem to follow an accepted guideline. Many studies fall back on a deterministic approach where the building stock is *segmented* (sometimes referred as the *classification* step of an UBEM creation) into clusters based on the main building use (e.g., residential, office, etc.). Refinements of the segmentation can occur with respect to other commonly available data points such as the construction year (e.g., average U-value of the building, infiltration rate, etc.) and the heating system (e.g., indoor temperature setpoints, fuel types, etc.).

Characterization of building archetypes occurs with respect to the technical parameters common to each building segment group. These inputs vary largely depending on the type of thermal model (steady state vs. dynamic) and the zoning scheme (single vs. multi-zone models). Most *deterministic* approaches will assign a single value to each parameter which will be used for all buildings. Further improvements can be achieved by "probabilistic estimation" of some parameters such as temperature setpoints, occupancy, lighting power density and plug loads density (Cerezo

et al., 2015). For this kind of analysis, modellers can provide statistical distributions for parameters that present limited or no information. If measured data is available, these distributions can be refined using Bayesian calibration and updated to a "posterior probability distribution" that takes into account the evidence related to the measured data (Sokol et al., 2017).

Many of the UBEM studies that have created building archetypes do not publish the archetypes themselves but rather publish the energy and statistical results. This leaves modellers with the task of developing custom archetypes or to adapt archetypes from a few public repositories. A summary of publicly available building archetype databases is presented in Table 4-1. For North America, the most notable sources of building archetypes are the Commercial Reference Buildings and Commercial Prototype Building Models developed for the US Department of Energy (NREL, 2011; US DOE - Building Technology Office, 2018). 16 base prototypes representing approximately 70% of the US commercial building stock are available for various locations and for different *reference* vintages (e.g., pre-1980, post-1980 and new constructions). In the case of the *prototype* building models, building code assumptions for the ANSI/ASHRAE/IES Standard 90.1 (ASHRAE, 2013) and the International Energy Conservation Code (IECC) are published in their various vintages. A recent adaptation of those archetypes to the Canadian context is in development by CanmetEnergy, an applied research branch of Natural Resources Canada, under the project *Building Typology Assessment Platform* (BTAP) (CanmetENERGY, 2019). For the residential sector, the Pacific Northwest National Laboratory developed two base prototypes (single-family and multi-family) that fit editions of the IECC. Another notable effort in the residential sector is the TABULA project which developed residential archetypes for 17 EU countries (TABULA Project Team, 2012). The archetypes are available through a web tool along with an API that allows the retrieval of archetype parameters for specific building types, countries, etc.

The TABULA archetypes are published in the form of archetype *templates* which are stripped of geometric properties. In fact, once an archetype is defined, the non-geometric properties required for a thermal model can be extracted and stored in an "archetype template." We discuss archetype templates in the next section and suggest a method to accelerate their creation.

Table 4-1 Summary of publicly available building archetype databases in North America and Europe.

Reference	Identification	Building heat-balance modelling	Number of archetypes	Application to geographical region(s)—sector
(CanmetENERGY, 2019)	Building Technology Assessment Platform (BTAP)	EnergyPlus (Open Studio)	10 080 (16 reference building types, across 70 climate locations and 9 different vintage building codes)	CAN-NR, MFD
(NREL, 2011)	Commercial Reference Buildings	EnergyPlus	48 (16 reference building types across 16 climate locations and 3 vintages)	USA-NR, MFD
(US DOE - Building Technology Office, 2018)	Commercial Prototype Building Models	EnergyPlus	2 448 (16 commercial building types in 17 climate locations and 9 vintage building codes)	USA-NR, MFD
(Mendon & Taylor, 2014)	Residential Prototype Building Models	EnergyPlus	11 424 (32 models simulated across 119 climate locations for 3 IECC editions)	USA-R
(TABULA Project Team, 2012)	TABULA	EN ISO 13790	17 countries	EUR-R, NR

R, residential sector; NR, services sector; MFD, Multi-Family Dwellings;

4.1.2 Archetype Templates

Archetype templates differ from regular archetypes in the fact that they are stripped of any geometrical relationship. Therefore, an archetype template can be applied to any building form in an UBEM. In the context of the Integrated Design process and urban modelling applications, knowledge of the building's interior and HVAC systems is generally unknown[9]. In this case, a common modelling approach is to define a large core zone at the center of the building, and one 4.6 m-deep perimeter zone for each façade orientation (this pattern is typically repeated for each floor, optionally grouping identical intermediate floors between the ground floor and the last floor.

---

[9] Although this is generally true, detailed city-scale building data structures that integrate interior zoning are being developed with the aim of mapping accurately buildings across the globe. The most widely accepted data structure is the OGC City Geography Markup Language (CityGML) Encoding Standard, developed by the Open Geospatial Consortium. It aims to "reach a common definition of the basic entities, attributes, and relations of a 3D city model" (Gröger et al., 2012). The last detail tier of CityGML, dubbed LOD4 (Level Of Detail 4), denotes details as small as individual furniture elements. Therefore, it remains in the realm of the possible to imagine a city model that contains accurate and up to date zoned building models for the purpose of large-scale multi-zone building energy simulations.

This practice is for example recommended by ASHRAE Standard 90.1 Appendix G (ASHRAE, 2013).While the separation of the floor plan into core and perimeter zones allows the creation of distinct thermal behaviours, in practice, models often end up having fully conditioned spaces with uniform program distributions and similar temperature setpoints and schedules. This creates situations where the overall temperature difference between two adjacent zones is negligible thus possibly resulting in weak energy flows between them. Dogan (2015) argues that, in those cases, the computational overhead invested in simulating multiple zones is not worth the added accuracy. Therefore, there should be an alternative calculation method that overcomes the computational cost of simulating multiple zones while providing an accurate thermodynamic behaviour. Dogan offers a solution in the form of an algorithm known as the "Shoeboxer."

The shoebox method solves the simulation time constraint by reducing the number of zones needed to model all buildings in the UBEM. The method assumes that the main driver of energy consumption variations between archetypes is the diurnal and seasonal exposure to solar radiation. Therefore, the method clusters façades by orientation and context-dependent solar radiation incidence and assigns a representative "shoebox" with a specific area weight. Different programmatic uses within a building are assigned different shoeboxes, but identical programmatic uses with geometric similarities (e.g., floor/façade, roof/floor, ground/floor, core/perimeter) across the UBEM can share the same shoebox; this further speeds up simulations by a factor as high as 300% when compared to standard multi-zone models zoned according to the ASHRAE 90.1 method (Dogan & Reinhart, 2017).

Because this method yields results that are in line with traditional *context-aware* multi-zone building models while increasing the simulation speed by more than 2 orders of magnitude, the shoebox method is a promising option. However, publicly available archetypes such as the Commercial Prototype Buildings are often developed as full BEMs, and it is a tedious task to summarize them into archetype templates.

4.2 Automated Archetype Template Generation

The shoebox method described in the previous section solves the issue of computing cost, but another challenge remains: the data acquisition and description of parameters needed to define building archetypes used in the model. If a student, a researcher or a consultant wishes to make an

UBEM model, the time spent on defining and converting the archetype parameters to the data format dictated by their tool will be significant. In the author's experience, modellers will often give up on creating adequate archetypes because the time cost is too high, and they would rather fall back on existing archetypes created in earlier projects or shared within their organization even if they do not fit the local context.

These shortcuts have the perverse effect of adding uncertainty to the overall model accuracy through what we identify as "model input blindness." This blindness is the result of accepting too quickly model input assumptions without making the proper "sanity checks". Input blindness is similar to the phenomenon of "change blindness" reported by developers of design-focused software which results in user failing to see changes in models (Davis, 2013, p. 44).

Another factor which throws in more uncertainty with model input blindness is the fact that putting more time and effort in making sure model inputs are correct does not guarantee that simulation results will be closer to reality. Different levels of effort in creating UBEM model inputs were assessed by comparing model results to building measured data in a co-authored study (Leroy, Letellier-Duchesne, & Kummert, 2019). Archetypes developed using more refined parameters did not necessarily deliver better results.

If valid archetype parameters from one format (originally incompatible with the shoebox method) could be translated, it would significantly reduce model input blindness. This chapter's main contribution is an algorithm that aims to solve this issue. It fills a gap between the conversion of multi-zone EnergyPlus models to *archetype templates* used by the UBEM "Shoeboxer" method. In short, the algorithm approximates the non-geometric parameters of a multi-zone BEM by dissecting and combining core zones and perimeter zones. As we will discuss later, this approach introduces a robust method to convert detailed multi-zone models to archetype templates, stripped of geometric properties. Until a standard data structure of thermal model properties is devised (similar to efforts in the field of urban topology characterization such as the CityGML model), such a method will in fact be tailored to specific tools. In this case, the proposed methodology complies with the EnergyPlus and UMI frameworks.

4.2.1 Methods

EnergyPlus models follow an object-oriented structure of zone geometries, surface assemblies, materials, loads, HVAC elements, schedules and more. Together, they form a complex model description that can be read by the EnergyPlus engine. The proposed algorithm essentially converts the EnergyPlus data structure to the UMI *template* data structure. To robustly interpret the Energyplus data structure, the algorithm leverages a scripting language called *eppy* (Philip, Tran, Youngson, & Bull, 2004) that translates the EnergyPlus model definition file (.idf) into a python object-oriented structure (see section 4.2.2). On the other end of the conversion methodology, the Shoeboxer method uses another data structure that organizes model parameters as archetype templates. This data structure was first suggested by Cerezo Davila et al. (Cerezo Davila, Dogan, & Reinhart, 2014) and later integrated into a graphical user interface called the "UMI Template Editor".

The algorithm begins by reading a multi-zone model (see A in figure 4.2) and establishes the list of zones. Using the zone geometry parameters, it computes zone areas and zone adjacencies and stores the information for later use (B). At this stage, the algorithm also establishes the different template data structure elements (listed in figure 4.3) by reading and treating the zone surfaces (constructions), loads, HVAC systems and more. Finally, the algorithm separates core and perimeter zones in two distinct groups (C) and performs a model complexity reduction by "aggregating" elements of each lists into two final perimeter- and core-zone definitions (D).
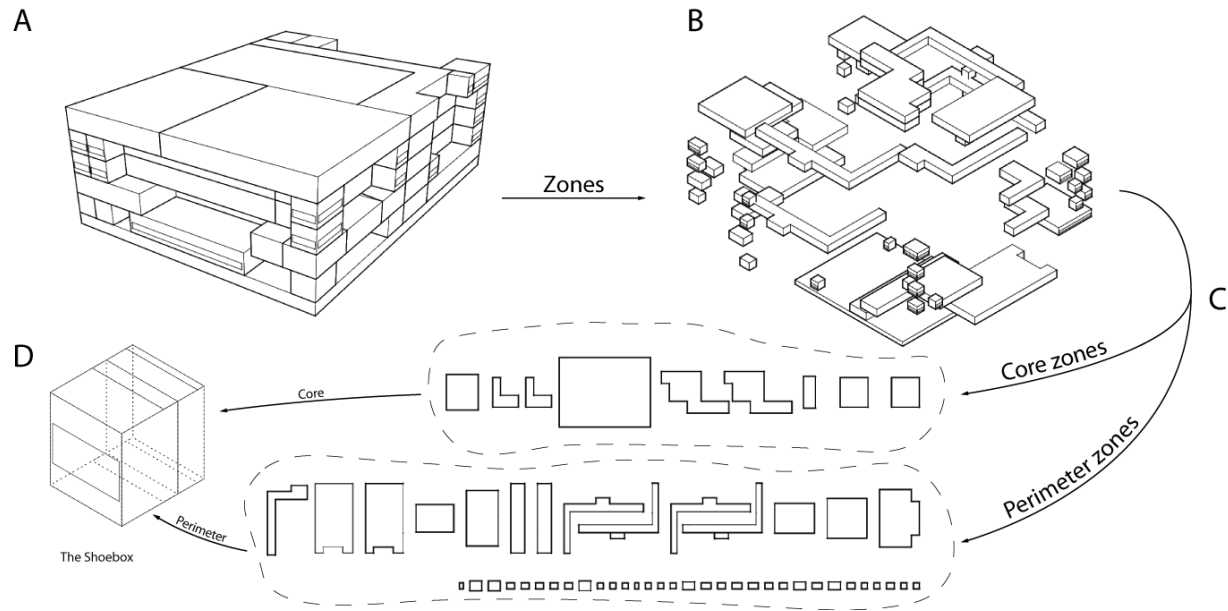
Figure 4.2 Visualizations of the model complexity reduction. Non-geometric properties from core zones and perimeter zones are combined into a shoebox. In this example, the Hospital prototype building is shown.

This aggregation occurs at every level of the model structure. For example, two lighting power densities (LPD) and schedules from two adjacent core zones are combined and weighted by their zone area; the subsequent aggregations will occur with respect to the cumulative area of the combined zones; this occurs until all core-zones (and perimeter zones independently) are covered. For each of the model elements that need to be defined in the final model structure, a series of assumptions are made which can bring their fair share of limitations, as we will discuss in the next section.

4.2.2 Model Structure & Assumptions

For clarity, the following section will present the assumptions related to each step of the algorithm. Each section details the necessary input data, the effective processes and calculations as well as any limitations imposed either by EnergyPlus or the final data structure.

As discussed earlier, the final data structure follows a pattern of zones and zone parameters. Figure 4.3 illustrates the various data elements that are defined for each thermal zone. It is the task of the algorithm to reduce the final number of zones to only two—i.e., one core zone and one perimeter zone. In the various following subsections, we will detail the assumptions that are made

when treating an EnergyPlus model. Right after, we will present examples of this method and demonstrate its validity.
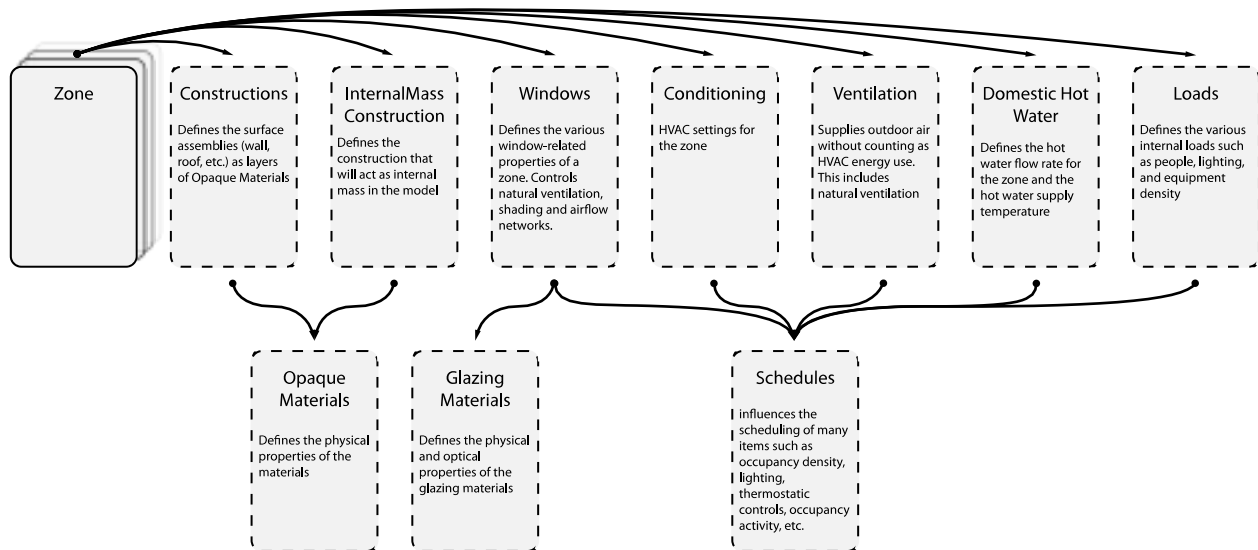
Figure 4.3 Archetype template input data structure. An archetype template zone contains a data structure represented here with their main definition. For a detailed graph dependency structure with all object parameters, readers are referred to the Appendix A.

4.2.2.1 Zone

Zones are defined in EnergyPlus using the `Zone` object. The algorithm uses the zones defined in the model as the starting point for the model complexity reduction. Most importantly, the zone object offers insight into the geometry of the zone (Area, Volume, Height) but also the adjacency of the zone (the elements that are geometrically next to the zone). By identifying the adjacency of zone surfaces (walls, floors, ceiling and windows), the algorithm can use the outside boundary condition of the zone surfaces to determine if a zone is considered a core zone or a perimeter zone.

Core vs. Perimeter: What exactly defines a core zone and a perimeter zone is open to debate. By ASHRAE 90.1 standard, a core zone does not have an adjacency with the outdoors, except for the lower floor core zone and the upper floor core zone. These 2 zones are in contact with the ground and the outdoor conditions respectively. For its simplicity, this is the definition that is assumed in the algorithm: if any of the *wall* surfaces (effectively excluding floors and ceilings) has the field `Outside_Boundary_Condition = "Outside"`, the zone will be marked as a perimeter zone.

Limitations: Some multi-zone energy models contain plenums or attic spaces. These zones are modelled as zone objects that span a whole floor to help model underfloor air distribution (UFDA) systems or to account for thermal losses through the roof. Although these zones participate to the overall thermal behaviour of the model, they pose an accounting issue in the automatic process. This is why, for now, the algorithm will ignore plenums and attic spaces, but future versions of the algorithm could implement a more robust method.

4.2.2.2   Zone Conditioning

Zone Conditioning defines the HVAC settings for a zone: temperature setpoints, mechanical ventilation availability, heat recovery type, heating and cooling capacity and Coefficient of Performance (COP) of the heating and cooling systems. While temperature setpoints are zone-dependent, many of the conditioning parameters are shared between multiple zones since one HVAC loop usually supplies multiple zones. In order to be able to combine zone parameters independently from their assignment to an HVAC loop, it has been decided to apply the overall building HVAC efficiency to all zones. Therefore, the COP of the HVAC loop supplying a core zone is the same as the COP supplying a perimeter zone. Economizer and heat recovery settings are also shared among all zones. A summary of the assumptions for zone conditioning parameters are detailed in Appendix B.

4.2.2.3   Zone Loads

Zone Loads define the various internal zone loads such as the occupancy density, the lighting power density and the equipment density. These metrics are simply weighted by zone area.

4.2.2.4   Zone Ventilation

Zone Ventilation controls various ventilation assumptions such as the supply forced ventilation or natural ventilation. The presence of such settings in any original zone is propagated to the final core and perimeter zones.

Infiltration is also handled in this object. The zone air changes per hour (ACH) are retrieved from the original archetype and weighted by area in the aggregation process.

4.2.2.5 Schedules

Schedules are an intrinsic part of building energy models. They apply temporality to model parameters by adjusting scalars at a particular time step. As shown in Figure 4.4, EnergyPlus defines schedules in many different ways posing a challenge when trying to produce a standard schedule representation. Since UMI defines schedules using the *Year-Week-Day* pattern, a routine was developed to parse virtually any EnergyPlus schedules into a set of `Schedule:Year` `Schedule:Week:Daily` and `Schedule:Day:Hourly` objects. It is worth mentioning that schedules are also aggregated by weighting the zone area, but they are first scaled by the quantity they modify (e.g., a lighting schedule modifying the LPD) and then normalized in order to keep the integrated quantities constant. An example is presented in section 4.2.3.
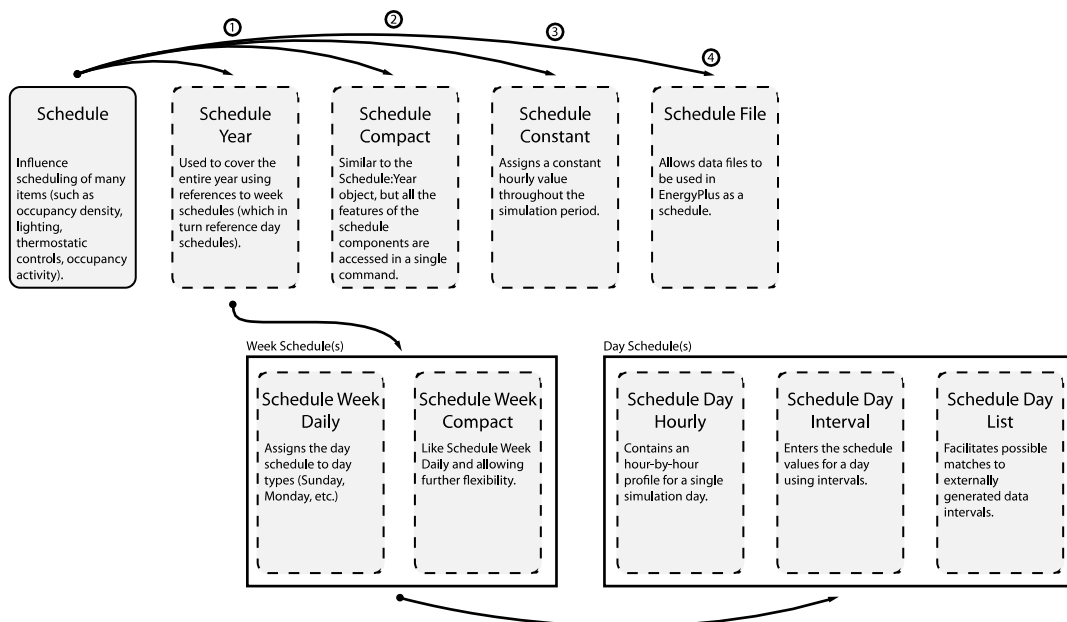
Figure 4.4 Data Structure for EnergyPlus schedules. Schedules are defined using one of four Yearly Schedule objects. The `Schedule:Year` object is in turn constructed through a combination of Week Schedules and Day Schedules.

4.2.2.6 Opaque Constructions

Zone surfaces are defined as Opaque Constructions. The final data structure of the algorithm can only define one opaque construction per surface type and per zone type ([facade, ground, slab, roof and partition] x 2 zones). Therefore, a maximum of only 10 different constructions can define all the surface types for a reduced archetype template. Since it is not uncommon to have more than 10

different surface assemblies in an EnergyPlus model, a simplification must be performed. For example, it is not uncommon to have a certain wall construction for the first floor of a building and then another wall construction for the other stories. Two options are then possible: 1) keep the "dominant" wall construction or 2) create a new wall construction based on the shared thermal properties of the two surfaces. While the first method is quite straightforward, the second method poses a bigger challenge especially when trying to devise a parametrized solution. Should the combined wall have a constant u-factor? Should the final density of the combined wall be weighted in terms of the dominant wall (larger surface area) or should they be taken equal? Plausible results have been achieved in this algorithm by assuming certain assumptions, but as it will be demonstrated, the first option is still recommended.

To demonstrate the second method, the following assumptions are taken:

1. The u-value of the combined wall should be equal to the wall-area weighted average of their respective u-values.

2. The total thickness of the combined wall should be equal to the wall-area weighted average of their respective total thicknesses.

3. The combined wall should be constructed from materials of both constructions. Effectively, the *set* of the list of materials is taken.

In the following example, we demonstrate the simple algorithm and highlight problems that might occur with regards to the thermal property of the combined wall. Let us assume two different façade wall constructions. The first is a 36 cm thick face brick and concrete wall and the second is a 28 cm thick insulated concrete wall as detailed by Tsilingiris (2004). The walls are made from a combination of materials with different thicknesses. Let us also assume that both walls have an area of 1 m^2. Both walls are illustrated in figure 4.5 and materials and thermal properties are listed in Table 4-2.

With the assumptions listed above, the combined wall would have a thickness of 31.9 cm and a U-value of 0.72 W/m^2 K, which is consistent with the conductivity of the original walls. Although these results seem plausible, they omit one important factor: the wall time constant.
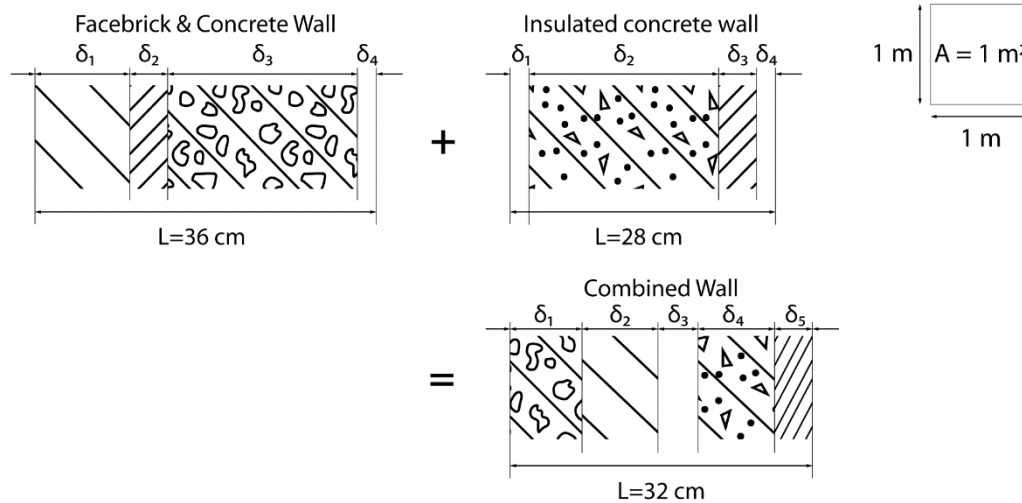
Figure 4.5 Example: Combining two wall constructions of different total thickness, mass, thermal resistance and heat capacity.

Table 4-2 Wall layer thicknesses, thermophysical properties and calculated U and $(\rho \cdot c \cdot \delta)_{eq}$ for two wall assemblies and the combined wall.

Wall assembly	Wall Layer	Material Description	Thickness (cm)	k (W/m K)	ρ (kg/m³)	c (J/kg K)	U (W/m² K)	$(\rho \cdot c \cdot \delta)_{eq}$ (J/K m²)
Face brick & Concrete Wall (36 cm)	δ_1	Face brick	10	1.20	1900	850	0.6740	574 260.0
	δ_2	Thermal Insulation	4	0.041	40	850		
	δ_3	Hollow Concrete Block	20	0.85	2000	920		
	δ_4	Plaster	2	1.39	2000	1085		
Insulated Concrete Wall (28 cm)	δ_1	Plaster	2	1.39	2000	1085	0.7710	511 360.0
	δ_2	Concrete Layer	20	1.70	2300	920		
	δ_3	Thermal Insulation	4	0.041	40	850		
	δ_4	Plaster	2	1.39	2000	1085		
Combined Wall (31.9 cm)	δ_1	Concrete Layer	7.6	1.70	2300	920	0.7169	533 397.7
	δ_2	Plaster	4.4	1.39	2000	1085		
	δ_3	Hollow Concrete Block	7.9	0.85	2000	920		
	δ_4	Face brick	8.0	1.20	1900	850		
	δ_5	Thermal Insulation	4.0	0.041	40	850		

Limitations: When multiple constructions are defined for a single surface type, the selection of the dominant wall construction can create modeling discrepancies. Window constructions pose a similar problem. Windows assemblies and their parameters are detailed in section 4.2.2.8.

4.2.2.7 Internal Mass Constructions

As explained above, the complexity reduction algorithm iterates over the list of core and perimeter zones. When two adjacent zones are combined, the partition wall that separates the two zones is transformed into an internal mass. This is standard practice in BEM modelling where a subdivided floorplan of a unique function (e.g., offices) is estimated as a single zone where partition walls are modelled as an internal mass. By accounting for thermal mass in this way, the algorithm manages to give the reduced model a thermal mass equivalent to the full model.

4.2.2.8 Windows

Window settings define the various window-related properties of a zone. Control of some natural ventilation settings and shading is also defined here (see section 4.2.2.4 for ventilation settings). The algorithm detects the window construction (materials and thicknesses) and common shading devices. Windows that are defined as a `"WindowMaterial:SimpleGlazingSystem"` — a simplified way in EnergyPlus to define a window by specifying the Solar Heat Gain Coefficient (SHGC), the U-factor and the Visible Transmittance — must be converted to a regular window construction made from a glass material, as required by the final data structure. The algorithm performs this step automatically by calling an implementation of the step-by-step method outlined by Arasteh, Kohler, and Griffith (2009) which abstracts the simple window properties to a single glass pane. This procedure is the same used internally by EnergyPlus to process the simple glazing system objects. This procedure could be easily adapted to a more recent method (RP-1588) which creates an equivalent *multilayered* construction (Kruis, Lyons, & Wong, 2017).

Limitations: Combining two window constructions of different optical and thermal properties could be quite helpful but the added complexity may not be worth the trouble. The algorithm therefore keeps the "dominant" window construction, based on the total area, whether it is when choosing a window construction from multiple windows on the same surface or when choosing a window construction from two different zones; only one window construction can be defined for

an archetype template in the final data structure. On the other hand, the WWR of the original model is calculated by façade orientation and is included in the model comments.

4.2.2.9 Domestic Hot Water (DHW)

Domestic hot water (DHW) is referred in EnergyPlus as service water. Loads are defined through `WaterUse:Equipement` objects. The area-weighted flow rate intensity (m^3/h-m^2) is reported by zone along with the corresponding schedule.

Limitations: The current algorithm cannot properly model the water consumption of a hot water plant loop, as it is often the case in larger buildings. Only the zone spot consumption is reported, which could underestimate the actual water consumption.

4.2.3 Results

To demonstrate the capabilities of this algorithm, results of the model complexity reduction are compared with the original EnergyPlus model for an archetype of the Commercial Reference Database (US DOE - Building Technology Office, 2018). The purpose of this section is to demonstrate the methodology using an archetype that features a designer-centric zoning scheme (i.e., as opposed to the ASHRAE 90.1 zoning scheme). The Strip Mall archetype is constructed from 10 adjacent zones (see Figure 4.6) which have various internal load conditions. The resulting archetype template defines a perimeter zone that is duplicated for the core-zone because the original archetype contains only perimeter zones.
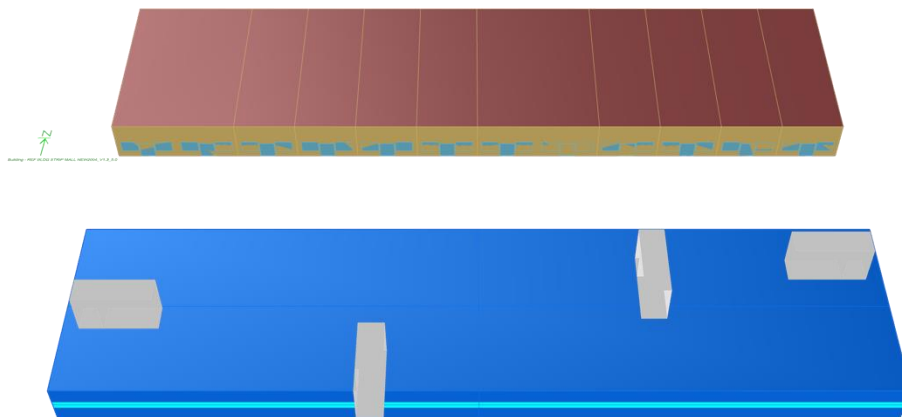

Figure 4.6 Shoebox archetype (foreground) and EnergyPlus archetype (background).
Four shoeboxes are represented over the geometry (screenshot from UMI).

Results of the complexity reduction algorithm show a good agreement with the original archetype. For example, the three different occupancy patterns that define the internal gains due to occupants in the zone are compared with the equivalent template; one typical week is represented in Figure 4.7 (top). The equivalent schedule, as calculated by the complexity reduction algorithm, is shown below. The *combined* schedules, which are constructed such that an integrated quantity is kept constant (see Figure 4.7) produces the expected results. For instance, the original archetype's three occupancy patterns compute a total weekly occupancy of 5 005 person-hours for the 10 zones. This value is the result of the integration of the product of the zone occupancy density (person/m^2) by the zone area (m^2) and scaled by the occupancy schedule (see Table 4-3 below). Similarly, the single *combined* occupancy of the archetype template is multiplied by the shoebox *perimeter* zone occupancy (computed as 0.086 person/m^2) and the *perimeter* zone area (equivalent to the whole building conditioned area; 2090 m^2). The archetype template yields the same 5 005 person-hours for the shoebox approximation.

The current methodology focuses on the creation of data inputs for the shoebox method implemented in UMI. While it would have been of interest to compare simulation results between the original EnergyPlus strip mall archetype and its approximation as a shoebox model simulated in UMI, this would have had the effect of crossing the boundary into the validation of the "shoeboxer" method. The shoebox method was tested on some 10 000 variants and it was shown to be accurate by the authors of the method (Dogan & Reinhart, 2017).

Table 4-3 Details of the occupancy calculation of the strip mall building archetype.

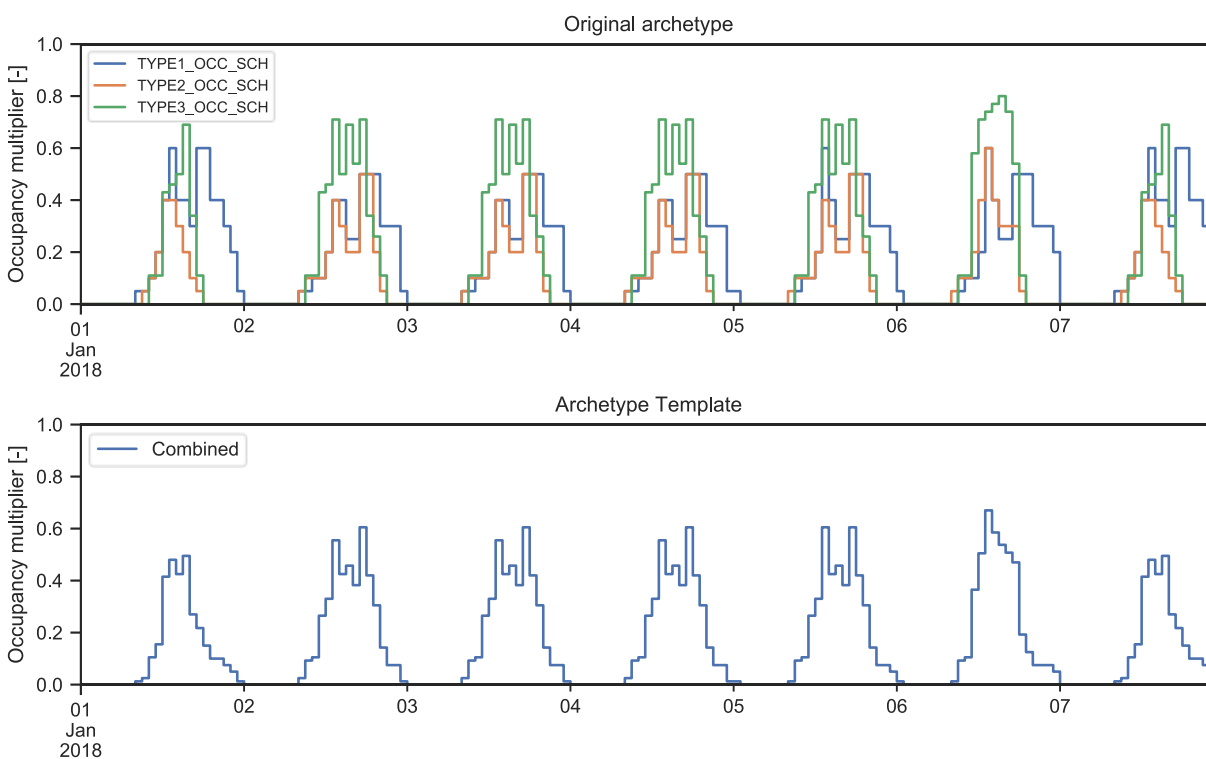| Original archetype					Archetype template				
Zone Name	Area (m²)	Occupancy (person/m²)	Schedule Name	Weekly traffic (person-hours)	Zone Name	Area (m²)	Occupancy (person/m²)	Schedule Name	Weekly traffic (person-hours)
LGstore1	348	0.086	Type1_OCC_SCH	961	Perim	1045	0.086	Combined	2 502.5
LGstore2	348	0.086	Type3_OCC_SCH	918	Core	1045	0.086	Combined	2 502.5
SMstore1	174	0.086	Type1_OCC_SCH	481					
SMstore2	174	0.086	Type2_OCC_SCH	270					
SMstore3	174	0.086	Type2_OCC_SCH	270					
SMstore4	174	0.086	Type2_OCC_SCH	270					
SMstore5	174	0.086	Type3_OCC_SCH	459					
SMstore6	174	0.086	Type3_OCC_SCH	459					
SMstore7	174	0.086	Type3_OCC_SCH	459					
SMstore8	174	0.086	Type3_OCC_SCH	459					
total	2090			5 005		2090			5 005

Figure 4.7 Occupancy pattern of the *strip mall* archetype. The original building archetype has three different occupancy schedules (top, labelled *Type 1, 2* and *3*). These schedules are represented by only one equivalent schedule in the archetype template (bottom, labelled *combined*).

4.3 Towards a National Archetype Template Database.

Public repositories of archetypes such as summarized in Table 4-1 can be used to produce an equivalent archetype template database. EnergyPlus models developed for various climate zones can be converted to archetype templates using the method described in 4.2.

As a proof of concept, a template library of a selection of archetypes from 3 vintages was converted using the Montréal climate file (CWEC). The resulting template library is shown as opened in the UMI Template Editor (Figure 4.8), a graphical user interface designed to manually edit archetype templates for the UMI software.

With more than 15 072 combinations of archetypes, climate zones and vintages, the resulting archetype template database would benefit modellers seeking to create UBEMs of various scales. Moreover, with more than 1042 weather locations in the United States and 71 weather locations in Canada, it would be possible to generate an even more refined database that would be fine-tuned to individual weather files, e.g. adapting the seasonal coefficient of performance of chillers to the detailed simulation results for a particular weather data file. For analyses involving future weather, *morphed* weather files that are adjusted to global climate models could be used to produce a future-set of archetype templates.
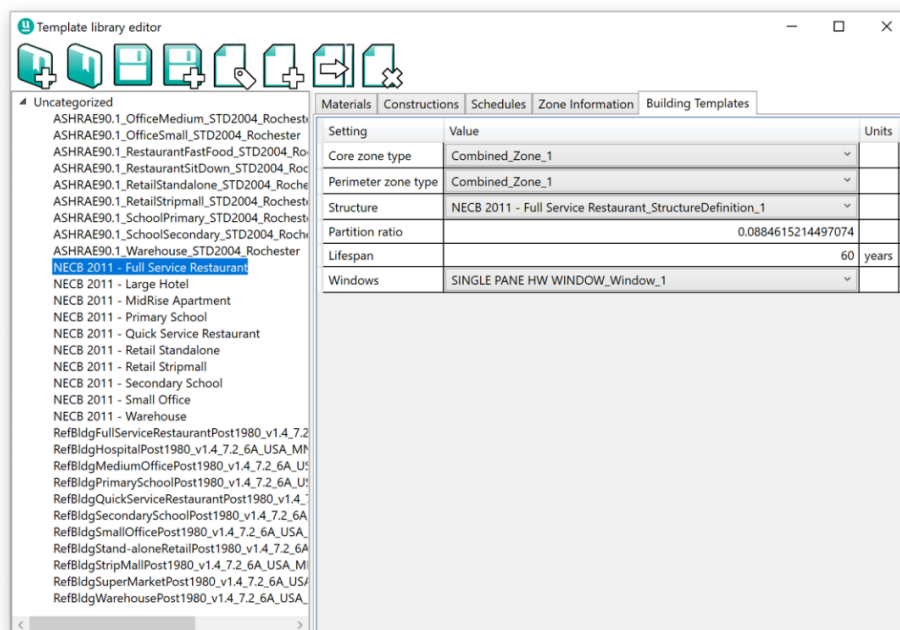
Figure 4.8 The UMI Template Editor. 27 archetype templates created automatically from three sources of building archetypes.

4.4 Discussion

This chapter focused on the building energy use estimation at an urban level. The importance of building archetypes was uncovered thanks to various studies of urban building energy modelling. Two of the biggest challenges of UBEM were found to be the creation of building archetypes and the significant computational demand of large-scale studies. With the advent of a promising solution known as the "shoebox" method centred around building archetypes templates, a methodology for the automatic creation of archetype templates was proposed. This methodology leverages existing public libraries of building archetypes and suggests a way forward to accelerate the creation of UBEMs across the United States and Canada.

This chapter specified all the details of the methodology and highlighted some limitations that could be addressed in future iterations of the method. Yet again, in the larger context of this dissertation, a simplified vision of building energy use at the urban level is sufficient to move forward with other objectives of this dissertation.

The next chapter looks particularly at modelling the building energy use of the City of Montréal with a focus on the difficulties that arose from the unavailability of the necessary datasets that are fundamental to the creation of UBEMs.

CHAPTER 5   ACQUIRING, ANALYZING AND VISUALIZING HEAT DEMAND

On the path towards the planning and integrated design of urban heat-sharing networks, estimating the dynamic building energy profiles of individual buildings is a requirement; this has been demonstrated earlier in chapter 3. Chapter 4 has introduced the theoretical landscape of building stock energy use estimation and presented a methodological contribution to accelerate the creation of urban building energy models; Chapter 5 implements a method that is adapted to the data availability and the context of Montréal, Qc. with the objective of producing a dynamic heat map of space heating, space cooling and domestic hot water demand. Gathering this information is crucial for the next phase of this dissertation's methodology which occurs in chapter 6: the topology optimization of the heat-sharing network.

5.1 Introduction

Analyzing heat demand at the city scale blurs the lines between geography, data science and mechanical engineering. Because of a prevalent spatial context, specialized geographic information systems (GIS) form the underlying data structure necessary to acquire, analyze and visualize heat demand. Additionally, national statistical surveys, municipal property assessment rolls, energy use surveys, open source GIS databases such as OpenStreetMap and other forms of occupant- and building-related data enable the process of archetype *segmentation*, *characterization* and *quantification*.

We can study the effects of design decisions with district energy and urban building energy modelling through various building energy performance visualizations. Different methods have been developed to estimate energy consumption at the building level including the top-down and bottom-up methods detailed in chapter 4. Other innovative methods rely on completely different methodologies. For example, Hay et al. (2011) used thermography equipped drones to map the thermal signature of homes at night from which energy usage was extrapolated. Persson et al. (2014) produced large-scale heat maps of excess heat availability by converting CO_2 emission data

into potential excess heat data. This work spanned European Union nations at the NUTS3 level[10]. Here, the goal was to map areas where excess heat was abundant to help plan the extension of new urban energy systems. Similarly, the same authors mapped the location of potential heat sources for the large-scale implementation of heat pump thermal plants in Denmark (R. Lund & Persson, 2016). This granularity, in the thousands of square kilometres for most regions, is ideal for identifying regions where district energy expansion is feasible at the national level but is not detailed enough for studies at the district scale. The Scotland Heat Map (Scottish Government, 2018) is another example of an effort to map heat demand at the national level.

On the other hand, other works proposed heat maps at the building level. Such examples are the Heat Atlas by Möller and Nielsen (Möller & Nielsen, 2014), the Energy Atlas Berlin (Senatsverwaltung für Wirtschaft Energie und Betriebe, 2019), the French National Heat Map (Cerema, 2014) or the London Heat Map (Centre for Sustainable Energy, 2019). Energy maps are a valuable tool for determining cost-effectiveness of energy efficiency policies and renewable energy programs (Howard et al., 2012). On the other hand, many of the heat maps presented so far are based on top-down methodologies. For example, the France Heat Map can be used to estimate the impact of converting domestic hot water from carbon-intensive fuels to renewable sources such as solar energy, but cannot be used to estimate, for instance, the impact of improving building infiltration levels. Only physics-based models can answer this kind of question.

Furthermore, many of the heat map models detailed so far aggregate indicators to annual metrics. This is fine if the target questions relate to evaluations of Energy Use Intensity (EUI) or Thermal Energy Demand Intensity (TEDI). In the case of district energy simulation, a heat map detailing the annual peak heating demand of each building can be paired with a typical normalized load duration curve (LDC)—an indicator of the variability of the heating demand with respect to the time of the year—and a simulation of the DES can be performed quite simply as demonstrated by Dorfner et al. (2017). As seen in the next chapter, when optimizing the topology—or the shape— of a heat-sharing network, a single load duration curve cannot reproduce the behaviour of all heat loads across the service area, thus requiring a heat map model that retains the hourly energy profiles

---

[10] NUTS, or *Nomenclature of Territorial Units for Statistics*, is a standard referencing system of the subdivision of countries for statistical reasons in the European Union. Regions of increasing granularity are labeled 1 to 3.

of each building. There is a need to optimize the energy performance of a district and not only assess its energy use; thus it is necessary to understand *where* and *when* the energy is used.

Such a dynamic heat map allows different stakeholders to answer different questions. For city officials, they may want to focus on the impact of energy policies on buildings across the city and the benefits in terms on air quality and GHG emissions. For utility companies, the aim is to understand the impact of policy changes and new urban development on grid power demand (peak electricity) and resilience. If heat sharing technology is adopted *en masse*, what will be the impact of the added demand? Will this require infrastructure upgrades? For district energy utilities, heat maps may answer questions linked to service area expansion. What other areas are worth connecting to grow the network? Will the expansion require extra capacity? Where are located the surrounding energy sources? All these questions need to be identified prior to developing the heat map as this will narrow down the necessary data inputs.

In the following section, the heat map that is created tries to answer the following questions:

1. What is the *space heating* use profile of each building?

2. What is the *domestic hot water* use profile of each building?

3. What is the *space cooling* use profile of each building?

5.2 Methodology

The archetype method (see 4.1) aims to produce an hourly heat map of an urban context. In this chapter, the method is applied to the context of the city of Montréal. The following sections present the methodology behind the various data manipulations that are necessary to produce a dynamic heat map of the City of Montréal.

5.2.1 Multiple Data Inputs

Collecting the required data is the most important and time-consuming step in the preparation of a heat map or a building stock model. In *Preparing for a City-Scale Building Energy Upgrade Analysis* (NREL, 2019), the authors identify five categories of data that cities should compile: (1) building type and location, (2) building stock geometry, (3) building stock characteristics, (4) energy consumption and (5) cost.

The first two categories of data refer to the "Building Massing Model," a 3D representation of the city; this massing model is supplemented by data from the "virtual building footprint" analysis that uses LiDAR (3D laser scanning) data provided by the City. The third category focuses on building characteristics such as the year built, the building materials and the type of fuel used for heating and domestic hot water (e.g., electricity, gas or oil); this information is covered by the "Segmentation Using Property Assessment Rolls" dataset. Although this dataset does not include fuel types, the absence of this information does not prevent the estimation of space heating and space cooling energy demand. Finally, the fourth and fifth categories relate to metered building energy consumption and energy costs. In the absence of publicly available data, an archetype-based energy model estimates building energy use. Table 5-1 summarizes the various data sources used in the preparation of this heat map.

Table 5-1 Heat map input data availability describing the building stock of Montréal, Qc.

Data Type	Name / Source	Features
GIS	OpenStreetMap	Road Networks and Building Footprints
Property Assessment Roll	Unités d'évaluation foncière (property assessment roll) http://donnees.ville.montreal.qc.ca/dataset/unites-evaluation-fonciere	Building type, year built, number of floors, number of residential units, number of commercial units, number of industrial units
GIS	Utilisation du sol 2016 — Communauté Métropolitaine de Montréal http://cmm.qc.ca/donnees-et-territoire/observatoire-grand-montreal/produits-cartographiques/donnees-georeferencees/	Number of residential units, number of commercial units, number of floors, year built,

5.2.2 Building Massing Model Using Virtual Building Footprints

Depending on the scope of the study and the scale of the built environment, there are many ways to determine the volume occupied by building structures or the geometric massing model. In studies spanning larger areas such as this one, designers can rely on public data sources often provided by city councils or even open source datasets like OpenStreetMap (OSM). The information such as the building footprints and the number of floors can serve as the basis for a massing model. Extruding a building footprint to the product of the number of stories by some average floor-to-floor height (often taken as 3 metres) produces what is known as a 2.5D model. Such a model represents the general shape of buildings but will not properly represent more complex building shapes such as setbacks often found in higher buildings.

To get building footprints, one typically looks for an existing dataset provided by city geomatic departments or from other sources such as OpenStreetMap. The methodology behind the creation of building footprints can be either manual or automatic; it can be based on aerial/satellite imagery or on Airborne Laser Scanning (ALS) data (also known as LiDAR data). Manual methods imply having a technician draw the contour of a building on top of georeferenced satellite imagery or aerial photography. This method produces the most accurate results and even differentiates adjacent buildings such as rowhouses but has the highest cost. Automatic methods, on the other hand, currently use high-resolution imagery combined with pattern detection and geometry simplification algorithms. The largest known dataset was created by a research team from Microsoft. The team analyzed aerial imagery by using a technique called "Semantic Segmentation" which is based on deep convolutional neural networks (CNNs). This technique effectively produced 11 842 186 building footprints from all Canadian provinces and territories (Microsoft, 2019a) and 125 192 184 building footprints in all 50 US States (Microsoft, 2019b). Unfortunately, all the aforementioned sources of building footprint data lack one essential attribute, the elevation (or the height) of the building's roof, which is needed to extract the number of stories and the building floor area. ALS data, on the other hand, meets this requirement. ALS implies having a plane (or a drone) equipped with some onboard laser scanning apparatus fly over a region and collect 3D point coordinates (*xyz*) of the survey area at a certain resolution. The advantage of ALS over image recognition is that ALS has no adverse effects from tree canopy penetration and insensitivity to some lighting conditions such as shadows that can affect image recognition algorithms (Yan, Shaker, & El-Ashmawy, 2015; Yu, Liu, Wu, Hu, & Zhang, 2010).

LiDAR techniques have been used to produce digital terrain models (DTM) and digital surface models (DSM). The Digital Terrain Model (DTM) is a simplified representation of ground altimetry. In the case of the city of Montréal, the available data is in the form of an irregular triangular mesh (TIN)[11]. It is a surface numerical geographic dataset constructed by triangulating a set of points gathered with LiDAR technology. The vertices of various altitude are connected to a series of segments to form a mesh of triangles of different dimensions. For this study, the TIN model was converted to a regular raster DTM in order to pair easily with another dataset: The

---

[11] http://donnees.ville.montreal.qc.ca/dataset/modele-numerique-de-terrain-mnt

Digital Surface Model (DSM). The DSM is a representation of the terrain relief that includes volumetric buildings present in the landscape.

In this study, the DSM and DTM datasets are georeferenced raster images which have a resolution of 1×1 metre. Each pixel (or cell) value represents the average altitude of the object in place that reflected the pulsing laser (approximately 10 points per square metre). According to the metadata, the dataset has an accuracy of ± 20 cm. The DTM is already processed and cleaned by the city's geomatic department to ignore other human-made structures such as buildings and bridges. Similarly, the DSM is pre-processed to include human-made structures but ignore trees and other smaller irrelevant structures. A derived feature of DTM and DSM is the normalized DSM (nDSM) which can be extracted by subtracting the DSM with the DTM layer (see figure 5.1). Thus, the space contained between the two layers, one being the ground and the other similar to a blanket carefully covering all buildings, represents the volume of the built environment. The subtraction of both layers produces the height of the built environment which is the key piece of information here. As a bonus, the count of non-zero pixel values yields the total area (m^2) of building footprints (the built area) and the sum of non-zero pixel values yields the total volume of all buildings (m^3).
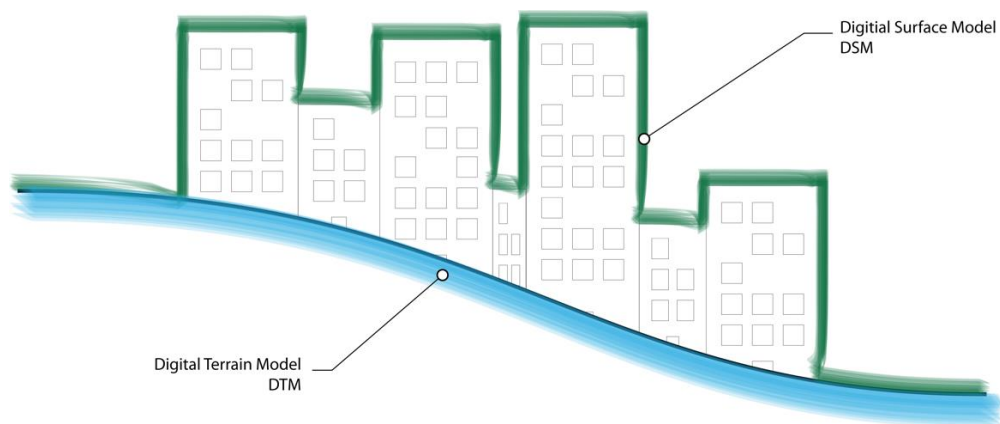
Figure 5.1 Sketch showing both the Digital Surface Model (green) and the Digital Terrain Model (DTM) and their relationship with the built volume between them.

5.2.2.1 How does VBF compare with hand-drawn footprints?

In this study, a dataset containing detailed footprints but covering only a small part of the study area is used as a reference to evaluate the error of the VBF method. A sample of the datasets is presented in Figure 5.2 for a region containing a few residential buildings of different heights. This figure shows that both datasets diverge slightly from the aerial imagery, especially for more

complex structures and landscapes such as the large terraced multi-residential building shown in the center of each image. In this case, the hand-drawn dataset ignores part of the building while the VBF incorrectly interpret part of the land as building area. Finally, recreating the general shape of buildings using VBFs comes with one caveat: the resolution of 1×1 metre creates a jagged perimeter which can overestimate building footprint areas. Although this is undesirable if we were to create 2.5D geometries, this level of detail is more than enough to produce our city-level building energy model which will depend on the height of buildings and their total floor area as the following error analysis shows.

Figure 5.2 Side by side comparison of satellite imagery, hand-drawn building footprints and Virtual Building Footprints. (Satellite Imagery Source: Google Maps)

5.2.2.2 Error Analysis

Looking at the whole dataset, we can compute the relative error introduced by the VBF method. Since the hand-drawn dataset covers a smaller area than the LIDAR data, the following analysis and results will be constrained to the boroughs where more detailed footprints are available. Assuming that the detailed footprints are the "reference" dataset, although it may contain some errors as we have shown in the figure above, the VBF method overestimates the total building footprint area by 30%. This error varies by borough between 13% and 55% (see table A-1 in Appendix A). This variation is illustrated in Figure 5.3 showing the relative error of the total footprint area.

This relatively large error can be explained by two components: first, the VBF can present structures that are not "buildings," such as large storage tanks; these artefacts will be ignored once the building characterization is crossed-referenced with the tax-assessment dataset (see section 5.2.3). Second, the pixels at the periphery of each building extend beyond the actual building limit, thus overestimating the area of the footprint. This is illustrated in Figure 5.4.
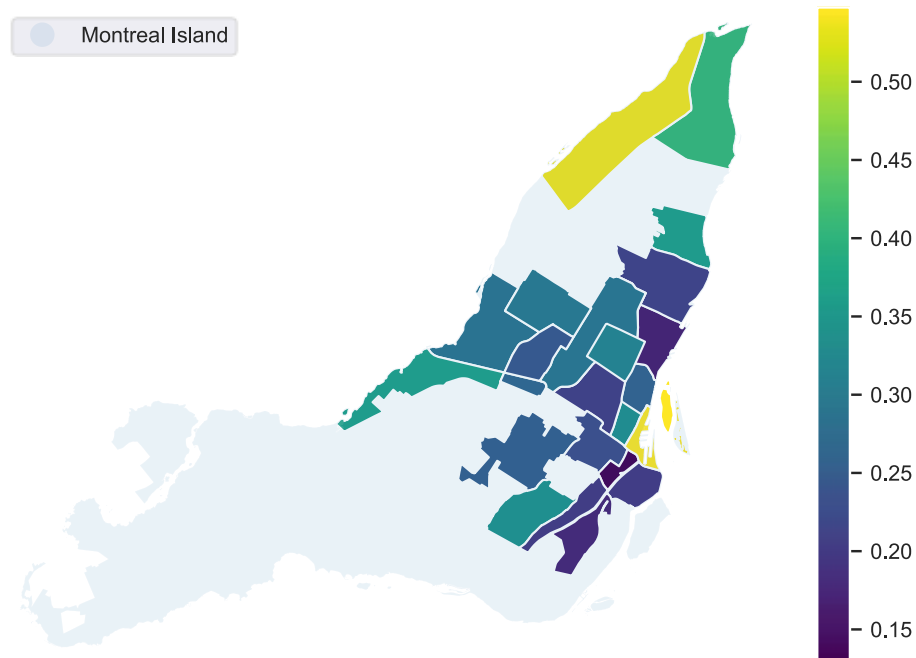

Figure 5.3 Relative difference of the footprint area between the reference BF (where data is available) and the approximation based on LiDAR data (VBF). The island of Montréal, Qc is shown.
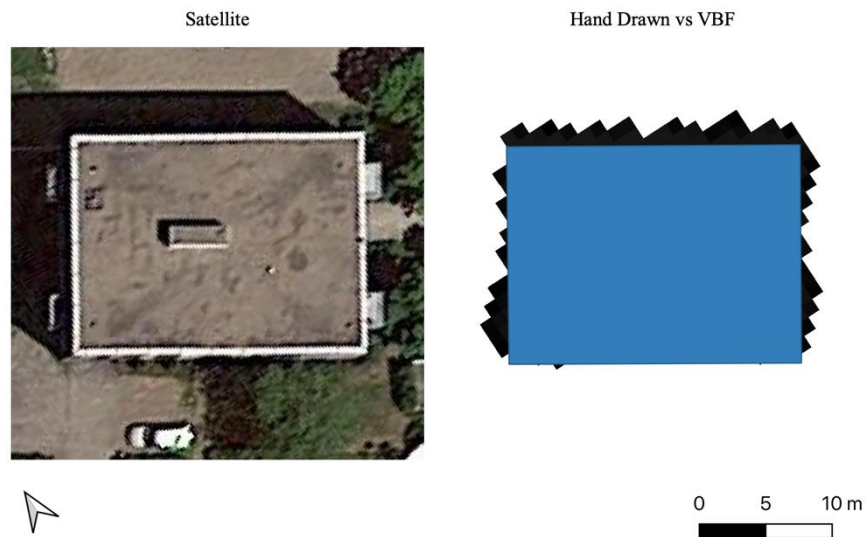
Figure 5.4 Overestimation of building footprints by use of *virtual building footprints*. On the left, the satellite imagery showing a single building. On the right, the hand-drawn building footprint (blue) over the VBF (black).

5.2.2.3 Calculating the floor area

There is no consensus amongst researchers as how to approximate the floor-to-floor height of buildings. It is generally accepted to choose an all-around height of 3 metres, but some authors have suggested to vary the height by building type or by district (Chun & Guldmann, 2012; Dorfner & Hamacher, 2014). For instance, in a study by Yu et al. (2010) in the city of Houston, the authors approximated the floor height by choosing a value for 6 different urban districts, ranging from 3 to 4 metres. In another study, Dorfner (2011) used a height of 3.125 metres. In a study on higher buildings such as skyscrapers, Saroglou et al. (2017) suggested a height of 3.1 metres for residential towers (with a 4.65 metres high ground level) and 3.9 metres for commercial towers. These assumptions were based on the Council on Tall Buildings and Urban Habitat (CTBUH) typical tall building characteristics (CTBUH, 2015a).

In the study presented in this chapter, the building floor height—and consequently the building floor area—was determined for 3 categories of buildings (office, other/mixed-use and residential/hotel) and two categories of building height (regular buildings and tall buildings higher than 23 metres). This creates a set of 6 formulas that are summarized in Table 5-2. The formulas of the tall buildings are based on the CTBUH assumptions mentioned earlier (CTBUH, 2015b).

Table 5-2 Number of floors (*s*) based on building type and building height.

Building Type	Regular Buildings $(h < 23 \text{ m})$	Tall Buildings $(h \geq 23 \text{ m})$
Office	$s(h) = \dfrac{h}{3.9}$	$s(h) = \dfrac{200h}{819} - \dfrac{20}{7}$
Other/Mixed-Use	$s(h) = \dfrac{h}{3.5}$	$s(h) = \dfrac{25}{721} * (8 * h - 77)$
Residential/Hotel	$s(h) = \dfrac{h}{3.1}$	$s(h) = \dfrac{150 * (4 * h - 31)}{1891}$

The building floor area is estimated by multiplying the building footprint area by the number of stories calculated using the formula in Table 5-2. The accuracy of these results can be assessed by comparing our calculations with the building floor area attributes contained in the property assessment roll. The error distribution is summarized in Figure 5.5. As expected, a large portion of the building stock is well represented with some cases where the building floor area is underestimated or overestimated. The smaller variations could be explained by the fact that floor area information provided in the property assessment roll excludes common areas. Larger variations could be explained by disparities between newly constructed or demolished buildings that do not appear in both data sets.
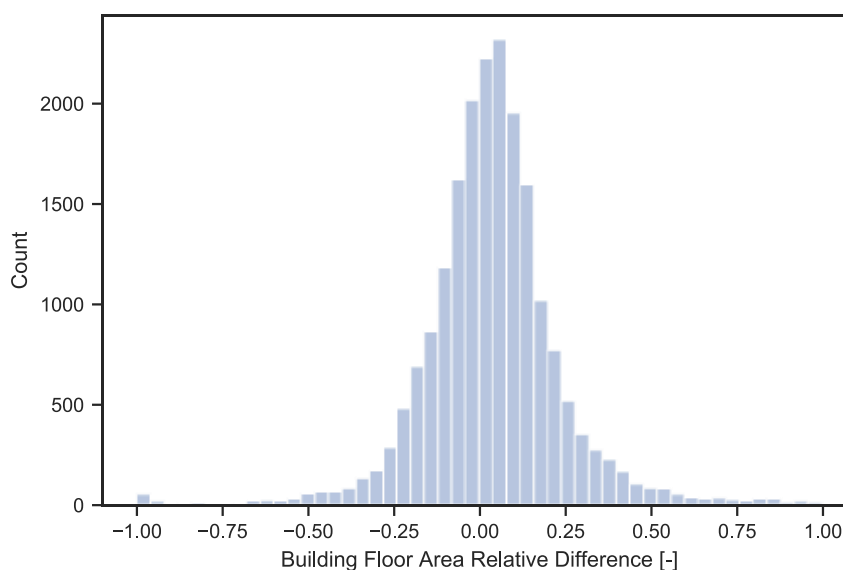

Figure 5.5 Relative error distribution of the estimation of building floor areas.
Only features with a valid "floor area" attribute are shown.

5.2.3 Segmentation Using Property Assessment Rolls

Once the building massing model is created, the segmentation of each building into clusters occurs with respect to the attributes of the property assessment roll. This database is one of the best readily available sources of information which can be used to identify important building characteristics. These records are often part of the public realm and most cities will publish updated GIS data files. The tax rolls in Montréal are updated monthly and offer insight on the main activity occurring in the building. At the time of writing, the dataset contained 513 235 MultiPolygon[12] features with 16 attributes such as the address, the year built, the floor area of the unit and most importantly, in our case, the unit's main utilization.

These polygons are shaped according to the lot, not the building footprint itself. In other words, a single *feature* in the dataset, or a *unit*, represents the boundary of the lot on which it lies. Moreover, the number of features in the dataset does not represent the number of buildings, as condos and interior parking spaces are considered as individual units. Therefore, one lot on which stands a high-rise apartment tower, for example, can have hundreds of overlapping features making up the whole building. Moreover, a unit can span across more than one lot as seen in Figure 5.6. To extract the floor area contained on a lot, a spatial query[13] is performed and units within the same lot are aggregated. Later, this aggregation occurs with respect to the unit's utilization code.

---

[12] Georeferenced datasets take the form of geometric shapes that have coordinates on the earth's surface. Such shapes include `Points`, `LineStrings`, `LinearRings`, `Polygons` as well as collections of those shapes: `MultiPoint`, `MultiLineString` and `MultiPolygon`.

[13] A Spatial Query is a special type of database query in which the geometry of a feature is used to perform a spatial predicate. The most common predicates are Within, Contains, Intersects and Covers.
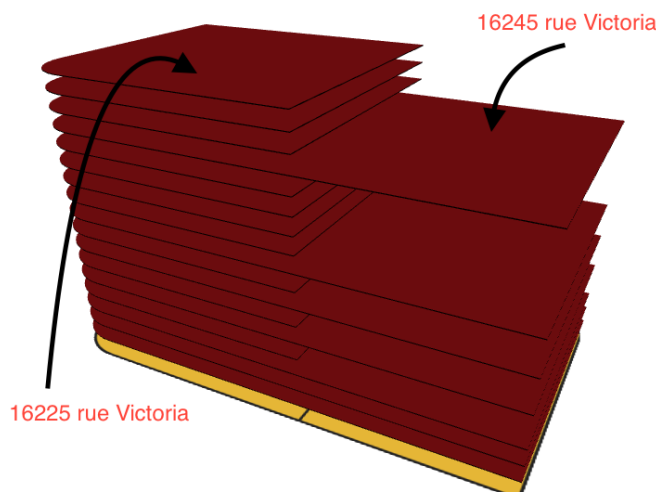
Figure 5.6 Multiple polygon features overlap for distinct
property units. Units may span more than one property lot.

The *utilization code* specifies the main activity occurring in a unit (e.g., school, office building, restaurant, etc.). This attribute plays an important role in the *segmentation* step of the UBEM model creation by helping break down units into typical space type clusters. In the case of the Montréal dataset, the utilization code is based on the provincial "Codes d'utilisation des biens-fonds (CUBF)[14]" or *Property Use Codes*. This codification ensures uniform identification of the different building uses in the province of Québec and consists of a four-digit code (e.g., 1 000 for regular housing). Because the CUBF is a provincial requirement, this methodology should be easily applicable to other cities providing open data access.

The *segmentation* of the building stock was performed with respect to the existence of building archetypes of the commercial reference database (NREL, 2011). These archetypes are defined as a combination of 16 space types (usages) and 3 construction years (pre1980, post1980 and new2004). The building archetypes were matched to CUBF codes manually. These codes include industrial activities, so that industrial building archetypes could be part of a city model in the future. In our approach, these buildings were ignored because such industrial activities are not included in the selected archetypes (NREL, 2011). Finally, the level of granularity offered by the property

---

[14] https://www.mamh.gouv.qc.ca/evaluation-fonciere/manuel-devaluation-fonciere-du-quebec/codes-dutilisation-des-biens-fonds/

assessment roll allowed a segmentation to occur with respect to various usages within a single building. This segmentation also kept the geographical designation of unit clusters in order to be able to map the results.

The *characterization* of the building stock describes each building archetypes with its technical characteristics based on the segmentation process. As mentioned above, these building archetypes come from the Commercial Reference Database and are simulated in EnergyPlus using the Montréal weather file. The space heating, space cooling and domestic hot water annual profiles are extracted and normalized by the floor area.

Finally, the quantification step propagated the energy profiles to all localized unit clusters by scaling them by the total floor area they represent. A summary of this segmentation is provided in Table 5-3 by building type and vintage.

Table 5-3 Summary of the building segmentation, characterization and quantification of the building stock of the Island of Montréal.

Building Type	Vintage	Count	Floor Area [m2]	Building Type	Vintage	Count	Floor Area [m2]
FullServiceRestaurant	All	223	92 431	QuickServiceRestaurant	All	29	14 277
	new2004	32	13 861		new2004	9	5 114
	post1980	73	29 262		post1980	5	4 005
	pre1980	118	49 309		pre1980	15	5 158
Hospital	All	50	2 088 934	RetailStandalone	All	620	1 810 180
	new2004	7	510 117		new2004	121	483 820
	post1980	3	49 091		post1980	221	773 274
	pre1980	40	1 529 726		pre1980	278	553 085
LargeHotel	All	1 136	3 295 658	RetailStripmall	All	256	2 946 342
	new2004	408	916 432		new2004	14	179 696
	post1980	572	885 571		post1980	98	1 056 520
	pre1980	156	1 493 655		pre1980	144	1 710 127
LargeOffice	All	6 022	16 860 175	SecondarySchool	All	160	1 557 370
	new2004	476	1 227 308		new2004	2	30 698
	post1980	1 171	5 501 354		post1980	16	103 759
	pre1980	4 375	10 131 513		pre1980	142	1 422 913
MediumOffice	All	794	2 206 980	SmallHotel	All	77	168 604
	new2004	111	166 029		new2004	1	19 367
	post1980	200	735 942		post1980	3	1 567
	pre1980	483	1 305 009		pre1980	73	147 670
MidriseApartment	All	429 475	106 127 914	SmallOffice	All	121	83 592
	new2004	66 810	11 658 328		new2004	29	23 299
	post1980	98 248	21 373 183		post1980	15	9 872
	pre1980	264 417	73 096 403		pre1980	77	50 422
Outpatient	All	130	145 080	Supermarket	All	131	582 754
	new2004	24	27 397		new2004	27	177 198
	post1980	23	13 946		post1980	39	169 405
	pre1980	83	103 737		pre1980	65	236 151
PrimarySchool	All	387	1 932 415	Warehouse	All	41 580	10 871 423
	new2004	7	35 863		new2004	22 436	1 746 500
	post1980	28	134 752		post1980	14 945	4 183 898
	pre1980	352	1 761 800		pre1980	4 199	4 941 025
All					All	481 191	150 784 130
					new2004	90 514	17 221 026
					post1980	115 660	35 025 403
					pre1980	275 017	98 537 701

5.3 Results

The application of the aforementioned methodology results in a heat map for which the space heating, space cooling and domestic hot water load profiles are known at an individual building resolution.

Although such a large database is best viewed in an interactive environment, visualizing a static heat map can be achieved by assigning the centroid of each building with its annual heat demand (kWh) and applying a spatial kernel density estimation to distribute the demand around each centroid. This results in a visualization where any cell of the map represents the absolute energy demand at that location, which can be divided by the cell area to obtain a heat density. For example, Figure 5.7 shows a colour map on a 100-meter cell grid with a kernel density radius of 1 000 metres. The scale shows kWh per square metres of land area. Each of the three distributions' colour gradient is adjusted to 98% of the dataset to remove outliers.

Integrating the results of these heat maps over the whole island of Montréal shows that, over the period of one typical year, the buildings of Montréal require approximately 21.4 TWh of space heating, 3.5 TWh of space cooling and 6.0 TWh of domestic hot water. According to data from Hydro-Québec, the provincial utility company, the Urban agglomeration of Montréal consumed in 2011 approximately 30 TWh of electricity (Ville de Montréal, 2011). While this metric does not translate easily in terms of space energy demand and domestic hot water demand, it shows that results are in same order of magnitude.

A second figure illustrates the dynamic nature of this heat map by showing one sample data (Figure 5.8). A large mixed-use building is selected and a week of October inside the shoulder season is shown. The dynamic energy profiles present in this heat map offer an additional value compared to the other examples presented earlier. This added value can manifest, for example, through the identification of concurrent energy demands, as shown by moments of simultaneous heating and cooling demands in Figure 5.8. This kind of information could not have been provided by regular heat maps. More importantly, this added value enables the visualization of the thermal diversity index presented in chapter 3.
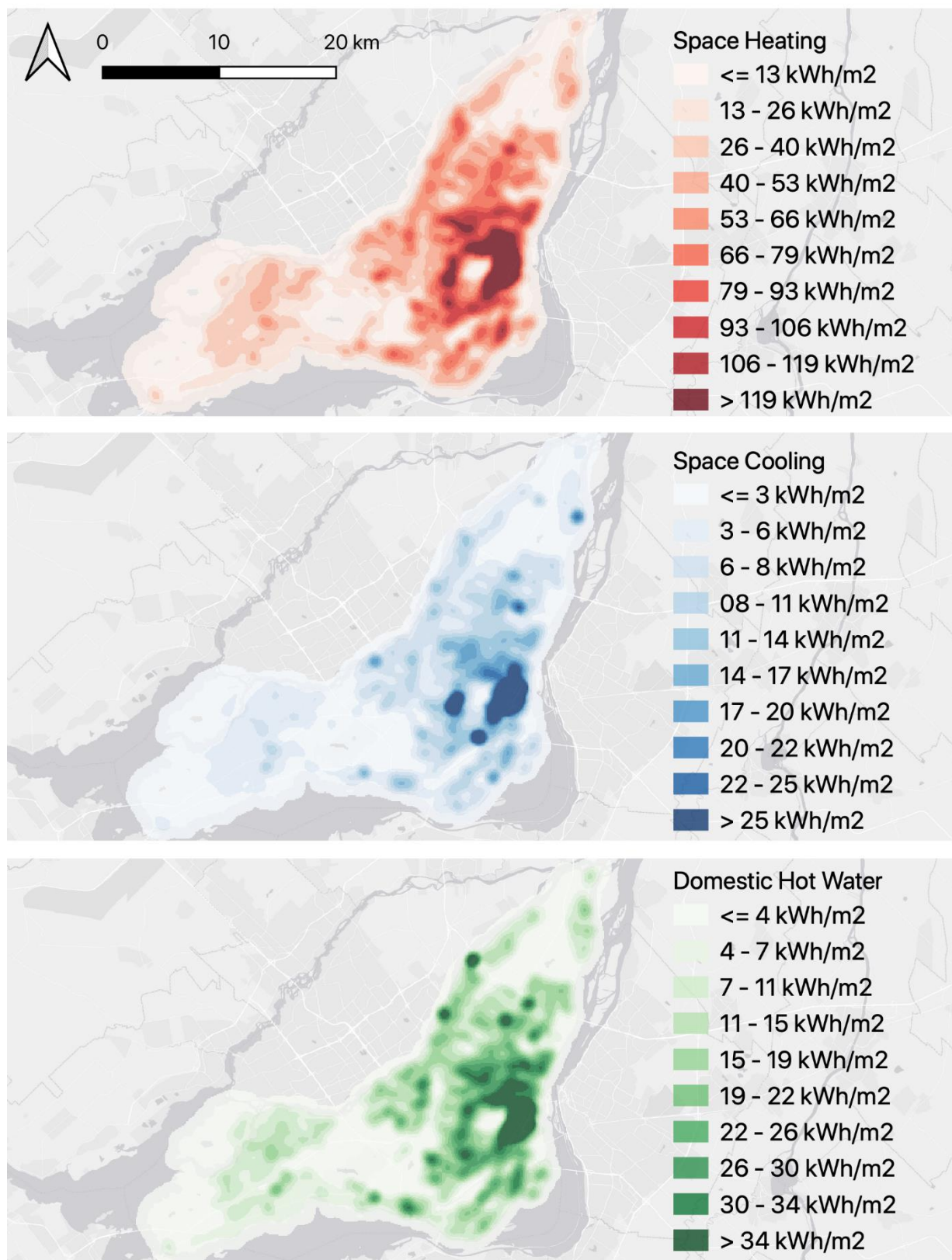
Figure 5.7 Annual energy demand intensity (by land area) of building space heating (top), space cooling (middle) and domestic hot water (bottom). Light Gray Canvas Map sources: Esri, DeLorme, HERE, MapmyIndia
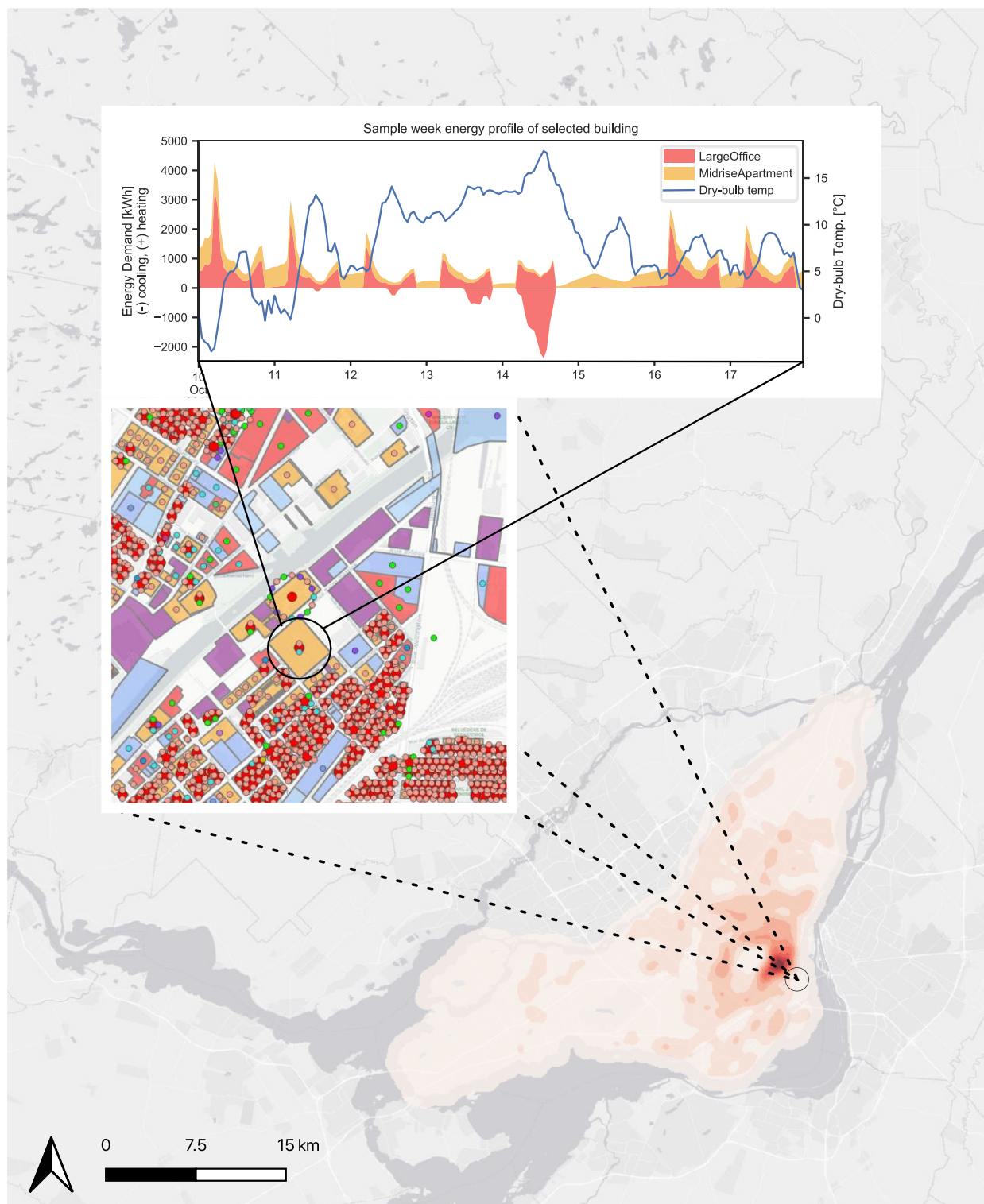
Figure 5.8 Dynamic load profiles of the Montréal heat map. A sample week in October for a selected 140 000 m^2 mixed-use building show space heating and space cooling demands. Light Gray Canvas Map sources: Esri, DeLorme, HERE, MapmyIndia.

5.4 Discussion

This chapter presented the creation of a dynamic heat map of the City of Montréal using available public data sources. The availability of such data sources dictated the level of detail the heat map could portray. In the absence of building footprints covering the whole study area and the presence of inconsistencies in the floor area attributes of the property assessment roll, an indirect estimation of the total floor area, by use of the virtual building footprints, was required. This feature extraction from ALS data, using numerical land models together with numerical surface models, offered an alternative to estimate building footprint areas and building heights.

Compared to other heat maps, the methodology applied in this chapter provides an additional level of insight; various questions related to the dynamic energy demand of buildings can be answered. From the questions relating to heat-sharing networks, a dynamic heat map can provide the necessary inputs to evaluate thermal diversity, for example.

As shown in this chapter, the need to combine partially complete and sometimes contradictory data sources greatly complicates the process to obtain an Urban Building Energy Model (and its results in the form of dynamic heat maps). Some cities are currently deploying efforts to collect, compile, and publish building-focused metrics, which would facilitate the process and make it more robust and accurate. For example, the NYC Housing Authority (NYCHA) publishes energy use data for the building stock they manage in New York City[15]. Heating gas, electricity and water consumption is also published at the meter level, showing a high granularity. The US Department Of Energy has generated unique identification numbers for the buildings of New York City (and others), enabling a better cross-referencing of data sources and helping reduce double counting of energy metrics (Pacific Northwest National Laboratory, 2018). Public access to high-quality energy use data would allow the calibration of models, enhancing the accuracy of heat maps.

Areas of improvements in the science of urban building energy modelling is a vast research subject. One particular element, which has been ignored in this chapter, is the window-to-wall ratio of buildings. Archetypes have a pre-defined WWR for each façade. Yet, in an urban context, buildings

---

[15] https://data.cityofnewyork.us/Housing-Development/Heating-Gas-Consumption-And-Cost-2010-March-2019-/it56-eyq4

have various WWRs even if they share similar properties. Nevertheless, WWRs are rarely a piece of information collected by cities and would thus be hard to characterize at the urban scale. Studies of Remote Façade Surveying (Ramallo-González, Vellei, Brown, & Coley, 2015), could provide an alternative. Perhaps image recognition algorithms could scour Google Maps or Apple Maps street-level imagery for façade windows.

This thesis began by forecasting that better urban design can be achieved through data driven design. The last step in designing city-scale energy systems is to model and optimize the energy sources that serve the heating and cooling requirements of the buildings, and how heat can be distributed within the urban environment. This is discussed in the next chapter of this thesis.

CHAPTER 6 HEAT-SHARING NETWORK TOPOLOGY OPTIMIZATION

Energy supply is both the generation and the distribution of energy. Various energy generation strategies combined with various distribution methods offer endless possibilities. To select the best outcome, this chapter presents decision making through the optimization of energy supply scenarios with a focus on fifth generation district heating and cooling.

6.1 Introduction

Various modeling approaches have been used to analyse district-scale energy systems, with different aims, whether it is district energy, renewable energy and urban microclimate. Tozzi & Jo (2017) reviewed different tools by their scale—multiscale, district-level system, or region-level system—with the intention of helping users and researchers choose the appropriate tool for the task. The authors also make the distinction between simulation (assessing the performance of a given system design) and optimization (selecting system configuration and size based on a set of criteria and constraints).

Another important literature review on urban energy modeling was conducted by Allegrini et al. (2015). The authors presented academic and commercial tools from 4 angles: (1) holistic simulation tools and (2) district energy modeling, (3) renewable energy and (4) urban microclimate. In the first category, the authors analysed the main popular simulation engines (TRNSYS, EnergyPlus, ESP-r) along with more "conceptual tools" such as the Urban Modeling Interface (UMI) (Reinhart et al., 2013) and the Urban Energy Management (MEU) (Rager, Rebeix, Maréchal, Cherix, & Capezzali, 2013). In the second category, the authors listed various network modelling tools that focus on the hydraulics of a district energy network. The balancing of energy supply and demand, which makes use of advanced optimization algorithms, was also discussed.

Studies specifically addressing heat-sharing networks are scarce. A recent study proposed a topology analysis tool to look at the detailed evaluation of heating and cooling supply in a 5GDHC network (von Rhein et al., 2019). The model uses a combination of URBANopt (National Renewable Energy Laboratory, 2019b) and EnergyPlus (National Renewable Energy Laboratory, 2019a) to create reduced order models of buildings as well as Modelica (Modelica Association, 2019) to model a bi-directional hydraulic network. The paper focused on the implementation of a

hydraulic network to model the transient effects occurring in a bi-directional district energy network. The authors concluded that the exhaustive search, where all possible network layouts were considered, created a problem size too large to solve. This problem size issue suggested that an optimization approach would be required to conduct a proper topology optimization.

Two main questions must be addressed to design a district-scale heating and cooling (or heat-sharing) system: how to distribute the heat efficiently from heating/cooling plants to consumers, or between prosumers; and which sources/sinks and conversion devices offer the best performance to supply heat or cold to the network. The design process can be expressed as a mathematical optimization problem, as proposed for example by Dorfner (2016b).

The next section describes in more detail approaches that have been proposed in the literature and their limitations and proposes a method to optimize simultaneously the topology of a 5GDHC network and the choice of thermal plants.

6.2 Proposed Topology Optimization Algorithm

The study of heat-sharing networks in the context of urban planning poses the question: given a certain energy generation capacity, which buildings should connect to a network in order to maximize profits? This question confronts two contradicting elements of the energy supply sector: the cost of reaching one more client as opposed to the revenues this client will bring. Moreover, as seen in Chapter 3, the design choices dictating the share of commercial space together with the design choices dictating building energy performance has an impact on the ability of buildings to share waste heat. Therefore, such an optimization would suggest that design choices can be confronted to their ability to maximize heat compatibility which is also a proxy for the global environmental performance of the network. In other words, design choices can be assessed by computing their impact on the final optimal network topology.

This question can be solved using optimization techniques that balance energy distribution costs, energy generation costs and heat/cold revenues. Such an optimization scheme was suggested by Dorfner (2016b) in the form of a mixed-integer linear program (MILP). This mathematical model focused on traditional district heating networks and district cooling networks and has shown promising applications in existing district energy network markets (Dorfner & Hamacher, 2014; Dorfner et al., 2017).

Although this method offers a simple and promising approach to solve topology optimization problems, it is not adapted to the context of heat-sharing networks. The next section details the areas where improvements can be suggested and where different strategies are needed, after which the mathematical model is detailed and applied.

6.3 Data Preparation

6.3.1 Structural representation: Network graph

Most district energy networks follow paths that are dictated by the terrain and obstacles as well as by a careful attention to reduce costs (or the total length). This usually results in the networks following the street grid. The complexity of a topology optimization mathematical model can be alleviated by using a graph structure, a representation of street edges and intersections in mathematical form.

uesgraphs (Müller et al., 2016) is a good example of an open source effort to describe DES in graph form. This package leverages the *networkx* library and adds methods and analysis tools to represent buildings and energy sources in the graph. A package like *uesgraph* can structure the setup of a DES model, but it does not offer topological cleaning & preparation of the network itself.

On the other hand, *OSMnx* (Boeing, 2017b) focuses on the analysis of street graphs and allows the retrieval of clean street grid topologies based on the Open Street Map (OSM) database. Leveraging this tool speeds up the network grid preparation process. Yet again, this topology cannot be used right away to build the network graph. In fact, a pre-processing step must be performed to return a clean and simplified graph exempt of unnecessary vertices, loops and parallels edges. The methodology presented in this chapter implements this topological cleaning, but, for clarity, this process is presented in section 7.3.3 of the chapter that summarizes the open source implementations of this thesis.

A complex problem like the one that is presented here is best explained using a simple case study. For now, let us assume that the street topology on which the final network will be based is topologically sound and that it has the following structure of edges (streets) and nodes (intersections):
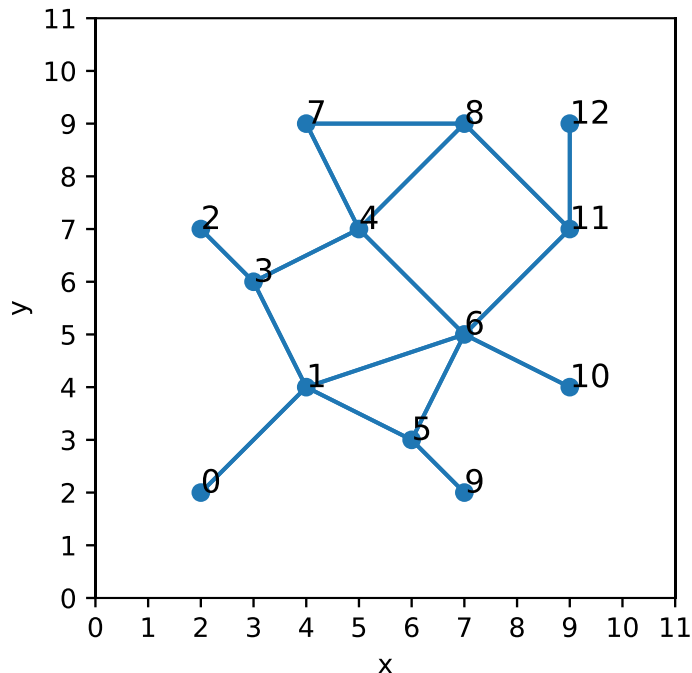
Figure 6.1 A basic topological example forms the underlying
structure of the problem. Nodes and edges are represented in a
basic coordinate system and identified by an integer.

The street topology presented in Figure 6.1 represents all possible branches of a DES—i.e., sections of piping that could be installed. The load (heat added or removed) on a given segment—e.g., between 4 and 6—represents all buildings physically located along that edge (or street), as discussed below. Nodes represent possible intersections between pipes, and possible locations for thermal plants.

6.3.2 Load Duration Curve Clustering

After establishing the structure of the network topology, buildings and their energy demands need to be expressed in a way that can be used by an optimization model. To reduce the problem size, the heat load profile is usually segmented in small number of typical periods that coincide with the different seasons, which can be seen as a discretization of the load duration curve (LDC) in successive "steps". This has been the case in many studies with the goal of reducing the number of variables in the problem by discretizing the time series (Unternährer, Moret, Joost, & Maréchal, 2017). This technique of model complexity reduction has generally delivered good results in

various studies of standard district heating technologies (Dorfner, 2016a; Dorfner & Hamacher, 2014; Dorfner et al., 2017). An example of the discretization of a heating load profile extracted from the heat map of Chapter 6 is shown in Figure 6.2.
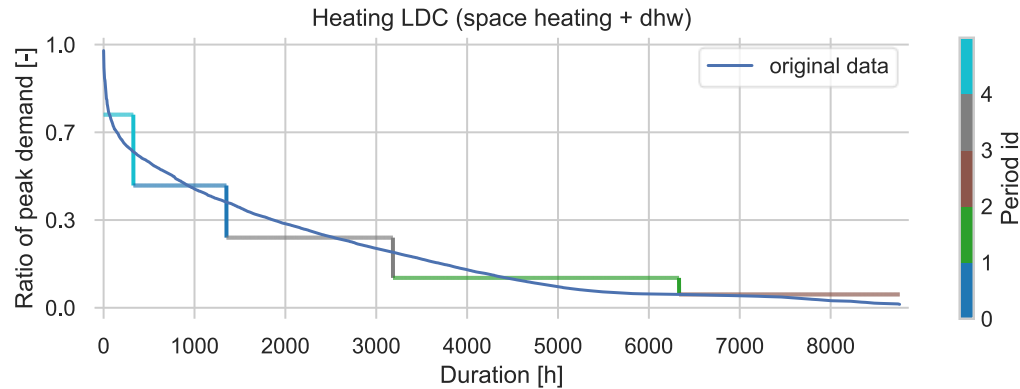

Figure 6.2 Discretization of a load duration curve (LDC) in 5 typical periods (time-steps) of various durations.

As pointed out by Kotzur et al. (2018), the difficulty with discretizing time series is that the system determines the level of detail required. For example, renewable energy systems require a higher resolution of the input time-series (solar radiation, wind, temperature, etc.) in order to correctly model transient effects. For conventional district energy design problems, as few as 10 time-steps can be sufficient to represent the full time series (Bahl, Kümpel, Seele, Lampe, & Bardow, 2017).

On the other hand, newer district energy technologies that are built on the notion of heat exchange between buildings cannot follow the same assumptions. By the temporal nature of the heat balance—consumer and prosumer signals—as well as the spatial nature of district-sharing networks—consumer dominated areas versus prosumer dominated areas—the optimization algorithms can no longer apply a single LDC discretization. To fully capture the spatial and temporal dynamics of the district-sharing network, problems must be defined using annual load profiles for every substation. This would result in a very large optimization problem difficult to tackle with currently available algorithms and computing power.

The solution is to use a temporal- and spatial-aggregation that captures the most out of the prosumer/consumer duality across the whole district while keeping the number of time durations small enough. The spatial energy demand aggregation is explained next, followed by the temporal energy demand aggregation.

6.3.2.1 Spatial Energy Demand Aggregation

To spatially aggregate building energy profiles, one can create a raster with a certain cell width and sum up or apply statistical indicators for all buildings within each cell; this is essentially how the thermal diversity index is calculated in 3.5.2. Another method is to aggregate geographically close buildings into clusters. Such a technique was used by Unternährer et al. (2017) to reduce the model complexity of a large-scale study by subdividing the urban context in smaller systems.

In the case of heat-sharing infrastructures, a method that respects the topology of the site is needed. As discussed in section 6.3.1, the closest topological structure that fits our requirements is the street network. Streets connect buildings together and can form the initial available paths between energy centers and their clients (i.e., buildings). For a complete topology, buildings are connected to the street segments, each street segment is connected to one another and together they connect to the thermal plant. This higher resolution topology effectively considers individual buildings as decision variables in the optimization problem. Consequently, the problem size can become quickly problematic. One solution is to lower the spatial resolution by aggregating the energy demand of buildings to the street segment that is closest to their centroid.

The identification of the closest edge to a point is an area of research in itself, but thanks to algorithms such as the *kd-tree*[16], a fast implementation could be prepared by the author of this dissertation and published as part of the OSMnx package (Boeing, 2017b). The novelty of this implementation is that the kd-tree algorithm processes a list of coordinates instead of calculating iteratively the Euclidian distance. Therefore, significant speed improvements are observed compared with iteratively identifying the closest point along a polyline. The general process of the algorithm is presented below for reference and the contribution is available on GitHub (Letellier-Duchesne, 2019) together with a speed benchmark comparing 3 methods (*kd-tree*, *balltree* and *iterative*).

---

[16] "The kd-tree is a binary tree, each of whose nodes represents an axis-aligned hyperrectangle. Each node specifies an axis and splits the set of points based on whether their coordinate along that axis is greater than or less than a particular value." (The SciPy community, 2019)

```
1   function getNearestEdges(Street Graph G = (V, E), X, Y, dist=10)

2       let X and Y be the set of coordinates for which to get the nearest edge in graph G

3       let N_e be the list of nearest edges for all pairs of x ∈ X and y ∈ Y coordinates

4       Let V_xy be the point coordinates matrix for created points along edges e ∈ E in G

5       for all edge e ∈ E in G:

6           create s, the evenly spaced points on edge e separated by length dist

7           assign the id of edge e to all created points

8           add x,y coordinates c ∈ ℝ² to V_xy for all created points

9       end for

10      build a k-d tree k for Euclidean nearest node search from V_xy

11      for all coordinates x ∈ X and y ∈ Y from sets X and Y:

12          set N_e(x, y) to the location returned by querying the k-d tree k(x, y)

13      end for

14      return N_e

15  end function
```

Algorithm 6.1 Closest edges for a list of point coordinates in a spatial graph.

6.3.2.2 Temporal Energy Demand Aggregation

Once the energy demand is spatially aggregated to each street segments, a temporal aggregation discretizes the load profiles in distinct periods. The ideal number of periods depends mostly on the type of energy system that is studied. As a general rule, around 10 typical periods of 24 hours (typical days) is found to provide enough accuracy in complex energy systems optimization while reaching significant solving durations (Kannengießer et al., 2019; Kotzur et al., 2018).

Because time-series aggregation smooths out extreme conditions, it is suggested to add an additional peak demand in the aggregation method as a heuristic. Some authors use an additional duration time step of 1h (Dorfner & Hamacher, 2014) while others use the day containing the peak demand as a typical period.

The method of time series aggregation applied to the building load profiles in this section is the one proposed by Kotzur et al. (2018) and publicly available as the python-based *time series aggregation module (TSAM)*. This tool performs a time series aggregation in 4 steps:

1. Preprocessing the timeseries: A number of periods and a period length (e.g., 1h, 24h, 186h) are chosen. A normalization of the time series is applied.

2. Aggregation algorithm: Four different aggregation algorithms can be applied to the group of time series: *averaging*, *k-means* clustering, *k-medoids* clustering and *hierarchical* clustering.

3. Additional extreme period: To avoid cutting off peak periods (e.g. peak heating and peak cooling) that are relevant in this district energy design context, additional periods can be specified.

4. Scaling back to original scale: The time series that were previously normalized in the first step are scaled back to their original scale.

An application of this method to our small example is done using a sample of buildings from the heat map of Chapter 5. The discretized annual time steps are shown in Figure 6.3. The purpose of this figure is to illustrate the resulting clustering process by which every hours of the time series is identified as belonging to a particular period (6 in this case). The period length is specified as 6 hours to represent the thermal mass of a district energy network.
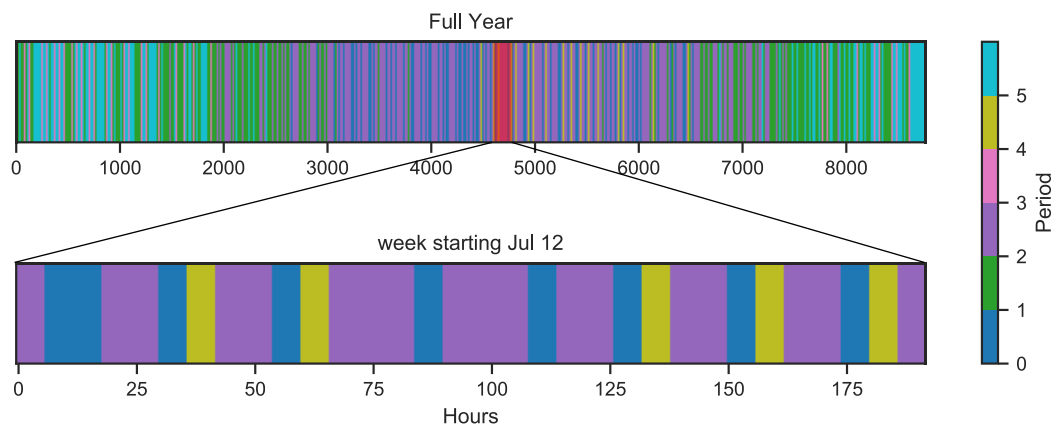
Figure 6.3 Example of a time series discretization using the k-means algorithm. The load profiles are discretized into 4+2 periods. The 2 extra periods preserve the period where the peak occurs. The top plot shows a full year while the bottom plot shows a single week sample. Each color represents one of 6 periods where the k-means algorithm determined a fit.

Once the heating and cooling profiles have been spatially and temporally aggregated, the optimization problem can be formulated.

6.4 Mathematical Formulation of the Optimization Problem

The model leverages the structure of the *dhmin* (seasonal) model presented in the thesis work of Johannes Dorfner (2016b, p. 89). Sets, parameters and equations were modified in a way to simulate heat-sharing networks. For clarity, the following mathematical description reproduces the original work and new additions are marked when necessary.

6.4.1 Sets

The mathematical representation of the model uses a graph structure of vertices and edges. Vertices are points corresponding to intersections or to endpoints. Edges are segments, such as streets, comprised of pairs of vertices. Let V be the set of vertices v_i and E be the set of edges e_{ij}. To allow flow to go in one or the other direction in an edge, E is considered to by symmetric where e_{ij} and e_{ji} are both elements of E. Sources vertices, such as thermal plants, are denoted V_0 and are a subset of V. In order to represent the temporality of the model, a set of discrete time steps T is introduced. These time steps represent different states of operation. Theoretically, 8760 time-steps would simulate the full operation of individual hours and produce an exact solution. In practice, the number of time steps can be reduced to less than 10 through aggregation or clustering, as described above.

6.4.2 Parameters

Parameters define the techno-economic properties of the model. They apply to edges and vertices as well as to the whole model. Vertices have a maximum capacity, denoted Q_i^{max}, representing the maximum power output given in kW. Since source vertices can operate as sources and sinks, the effective maximum capacity is $\pm Q_i^{max}$. Vertices that are not sources have this parameter set to 0.

Edges attributes are defined as the edge length, l_{ij} (m), the edge peak demand d_{ij} (kW) and the edge annual demand D_{ij} (kWh/a). Furthermore, to take into account existing pipes, which would not increase investment cost because they are already installed, edges have a binary parameter, ϵ_{ij}, that indicates the pre-existence of a pipe $(\epsilon_{ij} = 1)$. Finally, the maximum power flow capacity of a pipe is denoted C_{ij}^{max} (KW) and can be obtained from the maximum available pipe diameter.

Other parameters relate to the techno-economic properties of the network. For technical parameters the thermal losses in the pipes are represented by a fix and variable parameter, ν_{fix} and ν_{var}. The former represents the fixed thermal loss and depends on the pipe length (kW/m). The latter is the variable thermal loss and depends on both the pipe length and the power flow $((kW/m)/kW)$. Dimensionless parameters β and γ fix an undesirable effect of the aggregation of load profiles on edges that overestimate the heat demand by consumers. Indeed, aggregating load profiles based on coarse assumptions and uniform usage patterns results in overestimated peak loads, for example if all modeled office buildings use the same occupancy schedules. Moreover, we cannot assume all buildings along a street segment will connect to the network. Parameter β is the concurrence effect, which reduces the peak demand on a street and parameter γ is the connection quota which reduces the annual heat demand. The first parameter has the effect of reducing the investment costs while the other has the effect of reducing the heat revenues. If none of these effects is desired, they can simply be set to one. Additionally, a fixed plant investment cost term ($c\_heatfix$) was introduced to consider the power-dependant nature of thermal plant heat supply optimization (Frederiksen & Werner, 2013).

While *dhmin* uses a single pair of scaling factor s_t and duration w_t for each time-step, this work uses individual pairs for each edge as well as for heating and cooling demands—i.e., 2 pairs per edge $\times$ n time-steps. The original idea behind using a single pair per time step is that, in traditional district heating systems, the shape of the load duration curve is more or less the same for the whole network and the individual buildings. It is then acceptable to assume that the demand will change similarly across the whole network. On the other hand, in the case of a heat-sharing network, the load duration curve can be quite different in different parts of the network, depending if the thermal diversity is high or low. Having different scaling factors for each edge during a timestep $t \in T$ fixes this issue. A summary of the parameters is presented in Table 6-1.

Table 6-1 Model input parameters

Model component/Input parameter	Units	Symbol
Global Parameters		
Fixed pipe investment cost	\$/m	c_{fix}
Variable pipe investment cost	\$/kW/m	c_{var}
Operation & maintenance costs	\$/m	c_{om}
Retail price for heat	\$/kWh	c_{rev}^{heat}
Retail price for cold	\$/kWh	c_{rev}^{cold}
Annuity factor (years, interest)		α
Fixed thermal losses	kW/m	ν_{fix}
Variable thermal losses	(kW/m)/kW	ν_{var}
Concurrence effect	-	β
Edge-specific Parameters		
Pipe-exists already (1=yes)		ϵ_{ij}
Connection quota	-	λ_{ij}
Peak heating demand	kW	d_{ij}^{heat}
Peak cooling demand	kW	d_{ij}^{cold}
Maximum pipe capacity	kW	C_{ij}^{max}
Length	m	l_{ij}
Energy Source Parameter		
Fixed heating plant investment cost	\$/kW	$c_{heatfix}$
Fixed cooling plant investment cost	\$/kW	$c_{coolfix}$
Variable heating plant investment cost	\$/kWh	$c_{heatvar}$
Variable cooling plant investment cost	\$/kWh	$c_{coolvar}$
Source vertex capacity	kW	$\pm Q_i^{max}$
Time dependent		
Heating demand scaling factor	-	s_{ijt}^{heat}
Cooling demand scaling factor	-	s_{ijt}^{cool}
Duration (hours)	h	w_t
Source vertex availability (1=yes, 0=no)	-	y_i

6.4.3 Variables

The optimization algorithm asserts a series of variables that define the optimal solution. The primary variable is the decision to build or not a pipe. This binary decision variable is denoted as x_{ij}. For each time step, the decision to use a pipe is denoted by the variable y_{ij}. If its value is 1, then it is assumed a power flow π_{ijt}^{in} enters the pipe in the direction $i \rightarrow j$. It also implies the any demand on this edge is also satisfied. The power flow exiting the pipe is denoted π_{ijt}^{out} and is

reduced by the thermal losses and the edge heat demand but is increased by the edge cooling demand. Consequently, this model allows situations were $P_{ij}^{out} > P_{ij}^{in}$, which can translate into edges acting as energy sources (this is not the case in *dhmin*). The non-negative variable $\hbar_{it}$ represents the thermal power out of a source vertex while the negative variable c_{it} represents the thermal power into a source vertex.

Table 6-2 Model Variables

Model variables	Symbol
Total system cost (objective)	ζ
Binary decision variable: 1=build pipe	x_{ij}
Binary decision variable: 1=use pipe	y_{ijt}
Thermal power flow capacity for edge e_{ij}	$\bar{\pi}_{ij}$
Thermal power flow from v_i into edge e_{ij}	π_{ijt}^{in}
Thermal power flow out of edge e_{ij} into v_j	π_{ijt}^{out}
Heat generation power in source vertex v_i (positive)	$\hbar_{it}$
Heat extraction power in source vertex v_i (negative)	c_{it}

6.4.4 Equations

The model is defined using a set of equalities and inequalities (constraints) that bound the solution domain. The first equation is the cost function which acts as the objective function of the model. This cost function is formed by three elements: the network investment cost $\mathcal{N}$ (annualized investment), the heat generation (or extraction) cost $\mathcal{G}$, and the heat sold (revenues) $\mathcal{R}$. Together, they form the objective function which is equal to

$$\zeta = \mathcal{N} + \mathcal{G} - \mathcal{R} \tag{6.1}$$

The first element forms the network investment and operation & maintenance costs and is a combination of fixed and variable components. For clarity, these are represented by k_{ij}^{fix} and k_{ij}^{var} whose definitions are given below.

$$\mathcal{N} = \sum_{e_{ij} \in E} \left(k_{ij}^{fix} x_{ij} + k_{ij}^{var} \bar{\pi}_{ij} \right) \tag{6.2}$$

The second element of the cost function is the heat generation cost. In this model, the heat generation has an energy dependant component ($/kWh) and an extra demand dependant component ($/kW). This allows the model to account for more complex thermal plant cost functions and to properly model plant operation based on economic efficiency. For example, a thermal plant which typically satisfies the base load will have a high fixed cost but a low variable cost. On the other hand, a thermal plant that is brought online during peak hours will have a low fixed cost and a high variable cost.

$$\mathcal{G} = \sum_{\substack{v_i \in V \\ t \in T}} \left(k_i^{heatfix} \hbar_{it} + k_i^{heatvar} w_t \hbar_{it} - k_i^{coolfix} c_{it} - k_i^{coolvar} w_t c_{it} \right) \tag{6.3}$$

Finally, the last component is the heat revenues. This component is separated between revenues for selling heat and revenues for selling cold. The model assumes the demands are the ones that are "seen" by the network and are therefore already increased/reduced by the COP of the heat pumps. Whether the revenues should be associated to this demand or to the space heating/cooling demand directly is debatable. This model assumes two cost parameters that can be adjusted consequently.

$$\mathcal{R} = \sum_{\substack{e_{ij} \in E \\ t \in T}} \left(r_{ij}^{heat} x_{ij} s_{ijt}^{heat} w_t + r_{ij}^{cool} x_{ij} s_{ijt}^{cool} w_t \right) \tag{6.4}$$

The definition of the elements above are:

$\forall e_{ij} \in E$:
$$k_{ij}^{fix} = \left[c_{fix} l_{ij} \alpha (1 - \epsilon_{ij}) + c_{om} l_{ij} \right]/2 \tag{6.5}$$

$\forall e_{ij} \in E$:
$$k_{ij}^{var} = \left[c_{var} l_{ij} \alpha (1 - \epsilon_{ij}) \right]/2 \tag{6.6}$$

$\forall v_i \in V$:
$$k_i^{heatvar} = c_{heatvar}/\beta \tag{6.7}$$

$\forall v_i \in V$:
$$k_i^{coolvar} = c_{coolvar}/\beta \tag{6.8}$$

$\forall v_i \in V$:
$$k_i^{heatfix} = c_{heatfix} \alpha \tag{6.9}$$

$\forall v_i \in V$:
$$k_i^{coolfix} = c_{coolvar} \alpha \tag{6.10}$$

$$\forall e_{ij} \in E: \qquad\qquad r_{ij}^{heat} = c_{rev}^{heat} d_{ij}^{heat} \lambda_{ij}/2 \qquad\qquad (6.11)$$

$$\forall e_{ij} \in E: \qquad\qquad r_{ij}^{cold} = c_{rev}^{cold} d_{ij}^{cold} \lambda_{ij}/2 \qquad\qquad (6.12)$$
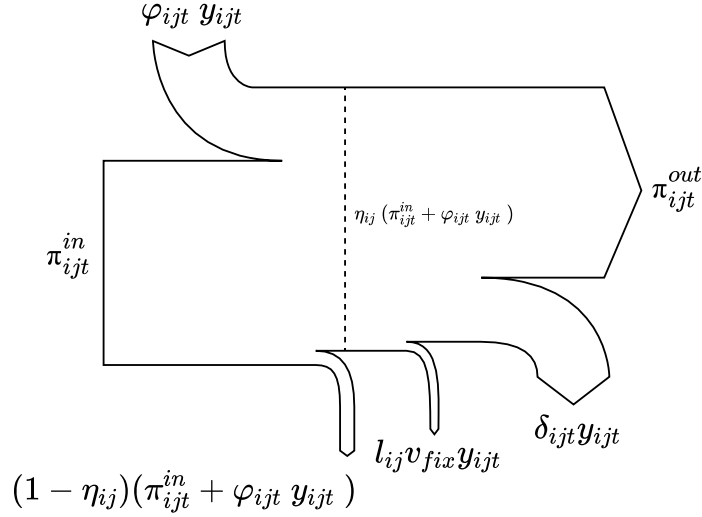
6.4.5 Constraints

Figure 6.4 Visual representation of the demand satisfaction equation (6.13)

The demand satisfaction equation represented graphically in Figure 6.4 above, is the main constraint of the network edges. It links the decision to use a pipe (y_{ijt}) with the satisfaction of heat and cold demand on an edge (d_{ij}^{heat} and d_{ij}^{cold}). This equation is formed by three derived components η_{ij}, δ_{ijt} and φ_{ijt}. The demand satisfaction equation is reduced to:

$$\forall e_{ij} \in E, t \in T : \qquad \eta_{ij}\left(\pi_{ijt}^{in} + \varphi_{ijt} y_{ijt}\right) = \pi_{ijt}^{out} + l_{ij} v_{fix} + \delta_{ijt} y_{ijt} \qquad (6.13)$$

The parameter η_{ij} represents the variable thermal losses that are proportional to the power flow into an edge e_{ij} including the power flow created by a cooling demand ($\varphi_{ijt} y_{ijt}$). A fixed thermal loss parameter is represented by $l_{ij} v_{fix} y_{ijt}$. The other two parameters, δ_{ijt} and φ_{ijt}, refer to the time-dependent edge demands, d_{ij}^{heat} and d_{ij}^{cold} respectively reduced by the connection quota and concurrence effect parameters. Their equations are:

$$\forall e_{ij} \in E : \qquad\qquad \eta_{ij} = 1 - l_{ij} v_{var} \qquad\qquad (6.14)$$

$$\forall e_{ij} \in E, t \in T: \qquad \delta_{ijt} = \beta\lambda d_{ij}^{heat} s_{ijt}^{heat} \qquad (6.15)$$

$$\forall e_{ij} \in E, t \in T: \qquad \varphi_{ijt} = \beta\lambda d_{ij}^{cold} s_{ijt}^{cold} \qquad (6.16)$$

The second constraint satisfies energy conservation in a vertex; in simple terms, everything that goes in must go out:

$$\forall v_{ij} \in V, t \in T: \qquad \sum_{n \in N_i} \left(\pi_{ijt}^{in} - \pi_{ijt}^{out}\right) = \hbar_{it} + c_{it} \qquad (6.17)$$

Various other constraints with respect to the pipe capacity, the unidirectionality of flow, the build capacity or the symmetry of the decision to build a pipe share the same assumptions as the traditional district heating model of developed by Dorfner (2016b). Readers are referred to this work for mathematical details of these constraints.

6.5 Example Model Results

Results of the mathematical optimization algorithm are illustrated in this section using a simple example of a fictitious neighbourhood. This example uses the same topological structure as Figure 6.1.

First, the data preparation is presented to lay down the assumptions of the model. Second, the aggregation of the thermal loads is described, and the global energy demand of the neighbourhood is illustrated. Third, the techno-economic context of the model is described and finally, the solution is presented and analyzed.

6.5.1 Edge Thermal Loads

First, building loads are assigned to a few segments of the street grid. This step corresponds to the spatial aggregation described in 6.3.2.1, but to simplify the process for the purpose of this example, let us assume that typical building load profiles are scaled such that the peak demand (kW) occurring on each edge corresponds to hand-picked arbitrary thermal load conditions. In a real scenario, the peak demand on each edge would correspond to the aggregated demand of all buildings belonging to an edge. Figure 6.5 illustrates the peak thermal demands for heating (red) and cooling (blue). For example, the buildings located next to the edge going from vertex 7 to

vertex 8 (henceforth referred to as edge 7–8) have a peak heating demand of 240 kW and a peak cooling demand of 20 kW. The figure also illustrates the location of three possible energy centre locations at vertices 0, 2, and 12 which all have a maximum capacity of 1 000 kW. The role of the energy centres is to supply the necessary power to meet the thermal demands along each edge.
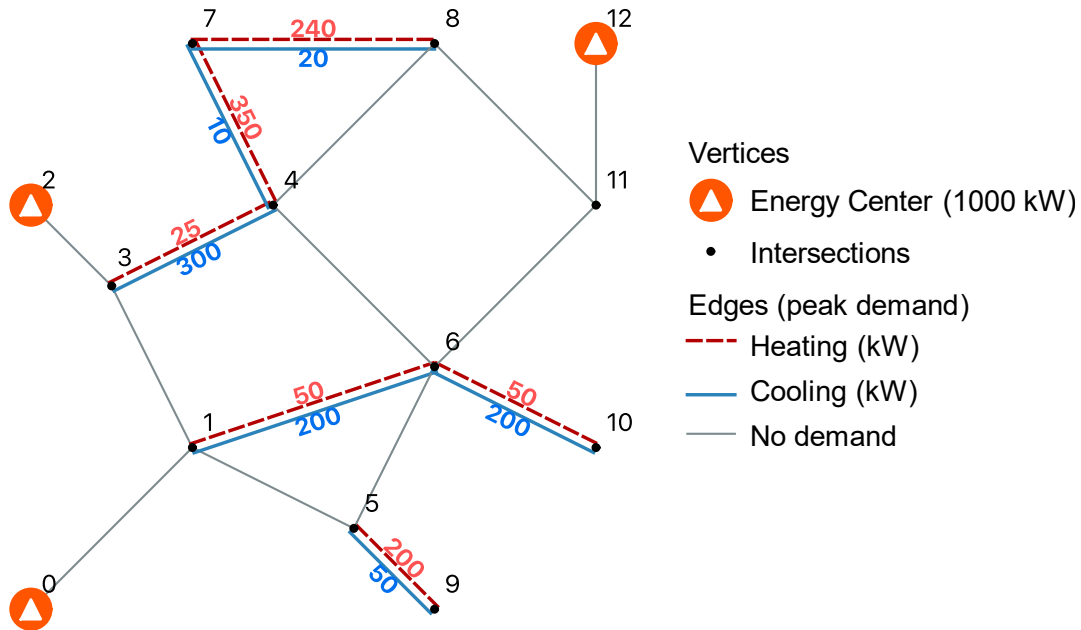

Figure 6.5 Thermal peak loads of a fictitious neighbourhood and locations of three possible energy centres.

An illustration of the dynamic heating profile of buildings aggregated to edge 7–8 is shown in Figure 6.6. This figure shows the hourly demands in slices of 24 hours and is well adapted to convey visually the effect of the aggregation algorithm that is applied in the next step.
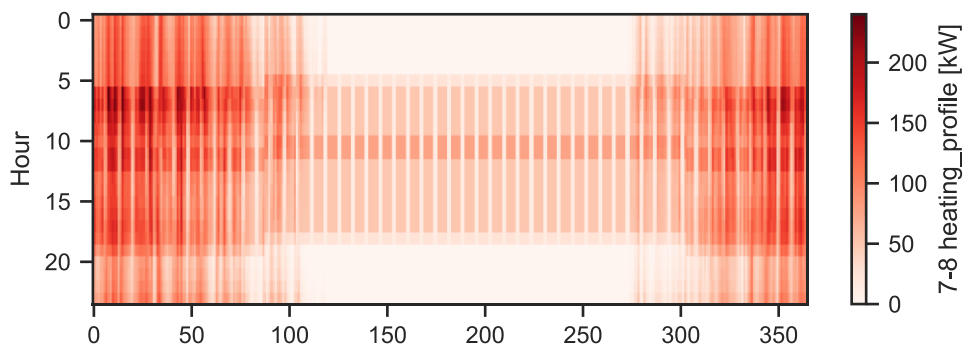

Figure 6.6 Initial heating demand profile of edge 7–8.

6.5.2 Load profile aggregation

The shape of the thermal loads such as the one occurring in edge 7–8 are weighted against the thermal loads of the other edges thanks to a time series aggregation (see section 6.3.2.2). This algorithm identifies patterns and attempts to group portions of the profiles into representative periods. It is possible to adjust the *period length* and the *number of periods*. For instance, aggregating all the loads of each edges into 6 periods of 6 hours has the following effect on the heating load profile of edge 7–8:
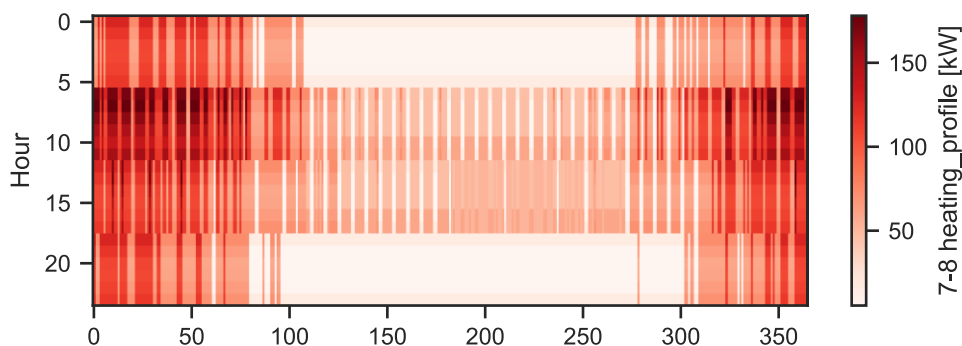

Figure 6.7 Effects of the aggregation algorithm on edge 7–8 (see Figure 6.6 for the original profile).

We can observe a clearer organization of the daily variations as well as a significant underestimation of the peak demand. On the other hand, the annual integrated quantity (497 134 kWh) is kept constant compared to the original profile. Figure 6.8 further illustrates the impact of the load profile clustering for edges 7–4 and 5–9. In the case of edge 7–4, the peak is properly portrayed because the overall neighbourhood peak occurs in that edge and has thus been chosen as a cluster centre in the aggregation algorithm. On the other hand, edge 5–9 experiences the same peak underestimation as in edge 7–8 (the peak of the original time series is 50 kW).
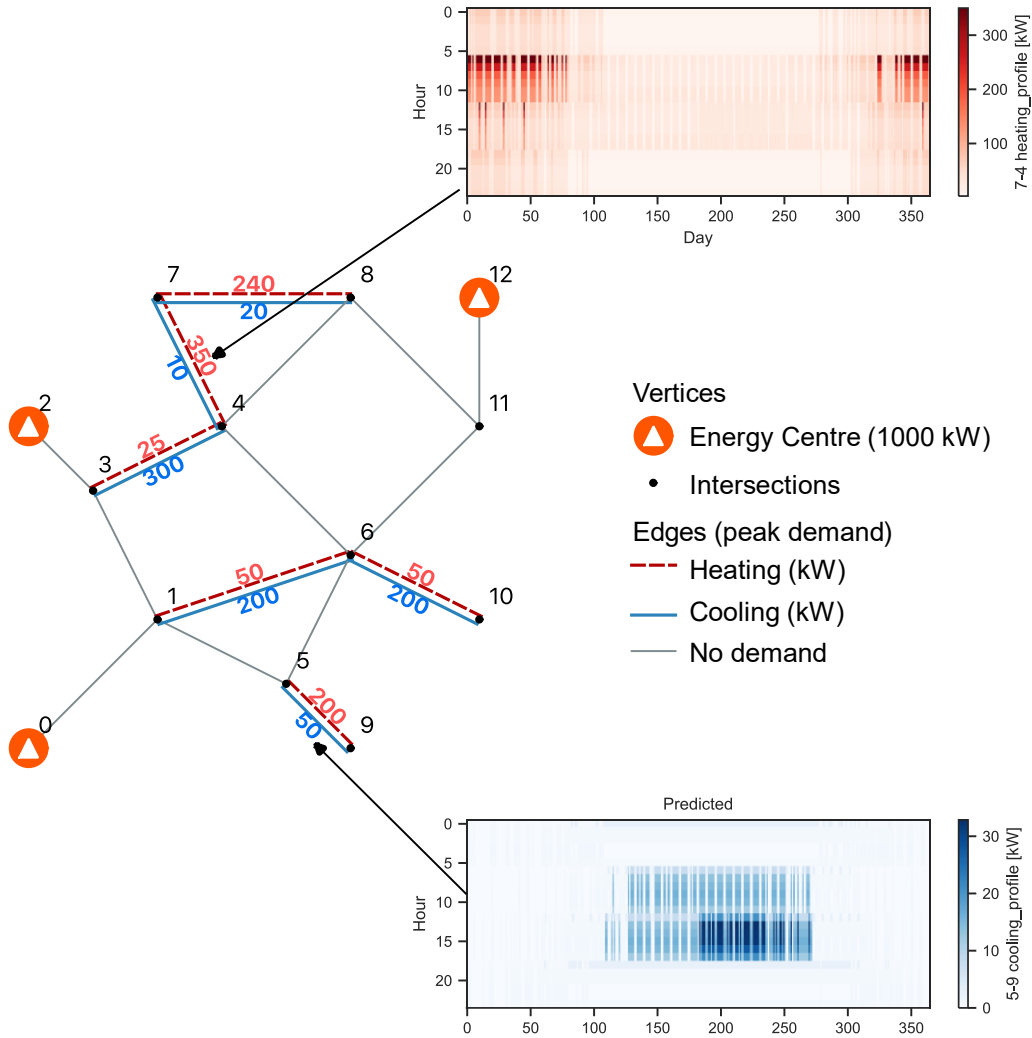
Figure 6.8 Data input of the network.

While the clustering algorithm can identify periods of peak demand, this period only occurs with respect to individual edges, which does not necessarily represent the combined peak of the whole network. Moreover, the mathematical optimization model can only model one discrete peak per period, which forces typical periods with a duration higher than 1 hour to be averaged, effectively creating a *step* discretization of the load duration curve. This effect is portrayed in the load duration curves shown in Figure 6.9. The load duration curves are the sorted hourly values of the combined demands. This figure more easily illustrates the corresponding period lengths between the various cooling and heating periods which allows the model to take into account the dynamic and concurrent nature of heating and cooling demands. Figure 6.9 shows the 6 steps that approximate the load duration curves as a result of the time aggregation. As illustrated in the figure, about

250 hours with a high cooling load and a low heating load were aggregated together and replaced with their average (period 4). Similarly, period 2 is shown to have 3000 hours of low heating and cooling loads (period 2).
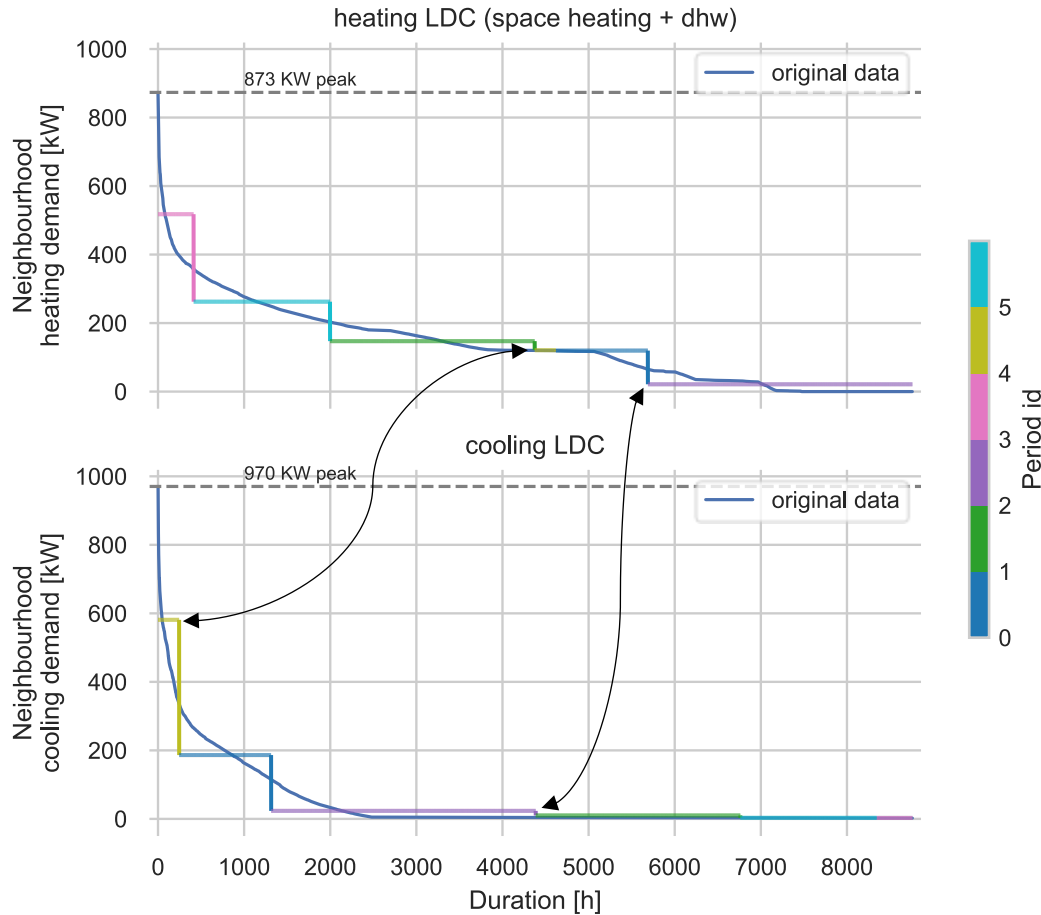
Figure 6.9 Heating (top) and cooling (bottom) load duration curves of total edge demands. The correspondence of period ids and time durations for 2 cases is highlighted.

6.5.3 Techno-Economic Optimization

The objective of the optimization algorithm is to maximize heat and cold revenues while minimizing generation and distribution costs. The best financial performance is achieved when the solver has found combinations of variables (see section 6.4.3) that respect the model constraints (see 6.4.5). For instance, the decisions to use a particular pipe, to use one or more thermal plants, to allow flow in a certain direction and the proportion of flow in an edge are weighted for each

period (symbols identified with a t in Table 6-2). The decision to build a pipe or the determination of the maximum capacity of a pipe, on the other hand, are evaluated globally.

All the aforementioned decisions are influenced by techno-economic parameters that can change the solution. For instance, higher heat prices could encourage reaching farther clients. In the current example, typical values of these parameters were taken from different sources in the literature to produce a consistent thermodynamic and economic set, which does not aim to represent a particular location or district energy market. An annuity of 40 years with an interest rate of 6% factors investment costs in annual payments. Table 6-3 summarizes these parameters.

Table 6-3 Summary of model parameters.

Input parameter	Units	Value
Global Parameters		
Fixed pipe investment cost	$/m	600
Variable pipe investment cost	$/kW/m	0.015
Operation & maintenance costs	$/m	5
Retail price for heat	$/kWh	0.07
Retail price for cold	$/kWh	0.05
Annuity factor (40 years, 6%)	-	0.0665
Fixed thermal losses	kW/m	0.02
Variable thermal losses	(kW/m)/kW	1.00E-07
Concurrence effect	-	1
Edge Parameters (for all edges)		
Connection quota	-	1
Maximum pipe capacity	kW	1 000

Three distinct cost characteristics can model the investment costs and the operation costs of thermal plants that could act as a *base load plant* (vertex 12), an *intermediate plant* (vertex 0) and a *peak load plant* (vertex 2). The energy source parameters are taken from Frederiksen & Werner (2013, p. 513). Table 6-4 summarizes these parameters.

Table 6-4 Summary of model parameters (continued).

		Vertex		
		2	0	12
Energy Source Parameter	Units	*peak*	*interm.*	*base*
Capacity (heating or cooling)	kW	1 000	1 000	1 000
Variable heating plant investment cost	$/kWh	0.072	0.036	0.018
Fixed heating plant investment cost	$/kW	10	46	154
Variable cooling plant investment cost	$/kWh	0.072	0.036	0.018
Fixed cooling plant investment cost	$/kW	10	46	154

6.5.4 Solution

With all the conditions detailed so far, the solver converges to a solution to the optimization problem. In this particular example, the Gurobi (Gurobi Optimization LLC, 2019) solver was used but other solvers such as the free GLPK solver could be used (see section 7.3.5 for more details on the specific tools used to solve this problem). A detailed illustration of the network operation is presented in Figure 6.10 on page 119. This figure shows the six operation periods described by the time aggregation step. These periods are identified with the same colour coding as in Figure 6.9 and are ordered according to the decreasing succession of periods of the heating LDC. Figure 6.10 shows the individual edge demands on the left side and the resulting edge power flow balance on the right side.

For example, the top two graphs correspond to period "T3" which experiences the network heating peak demand. Looking specifically at edge 7–8, a heating demand of 215.4 kW and a cooling demand of 4.4 kW are shown. This energy is supplied by the *base load plant* (vertex 12) which follows a path along edges identified by nodes 11, 6, 4 and 7. The heating demand of edge 4–7 (202.3 kW) and thermal losses along that edge (0.5 kW, not shown in the figure) are met by the incoming flow (414.4 kW). The remaining power flow (211.6 kW) meets the net demand on edge 7–8 (215.4 kW of heating minus 4.4 kW of cooling, i.e. 211 kW) and the thermal losses on that edge (0.6 kW, not shown in the figure). This results in zero power going to vertex 8, and thus completes the balance of this branch of the network at that particular period.

The cooling dominated operation of the network is a perfect example of the heat-sharing capabilities of 5GDHC networks. For period "T4," which experiences, overall, a cooling load of 564.3 kW, cooling demands are met by the capacity of the *intermediary* plant (vertex 0). In this case, edge 5–9 has nearly identical heating and cooling demands which results in little power flow coming from the rest of the network (numerical rounding hides the actual values). Edge 3–4, on the other hand, has a large cooling demand (362.8 kW) which is equivalent to a heating power flow that splits at vertex 4 to supply the heating demands of edges 4–7 and 7–8. The reminder of the power flow travels back to the thermal plant through vertices 6 and 1, picking up excess heat from edge 10-6 along the way.

The final solution suggests that only two of the three energy centres were needed, avoiding the costlier *peak thermal plant* (vertex 2). The solution also suggests that supplying every edge with a

heating or cooling demand is financially attractive. The capacities of both thermal plants are summarized in Table 6-5 for each period. A design of the thermal plants would choose moments of peak demand (emphasized in bold), resulting in a thermal plant capable of providing 660 kW of heating and 565 kW of cooling (after rounding).

Table 6-5 Plant sizing results.

	time-step	Cooling capacity (kW)						Heating capacity (kW)					
		t0	t1	t2	t3	t4	t5	t0	t1	t2	t3	t4	t5
vertex	0					**-564.3**		0.56		0.56			
	12	-71.88							190.0	1.72	**658.6**		353.2

The financial performance of the network is summarized in Table 6-6. For the particular set of economic parameters, the given network delivers a net benefit of about 80 k$.

Table 6-6 Financial performance.

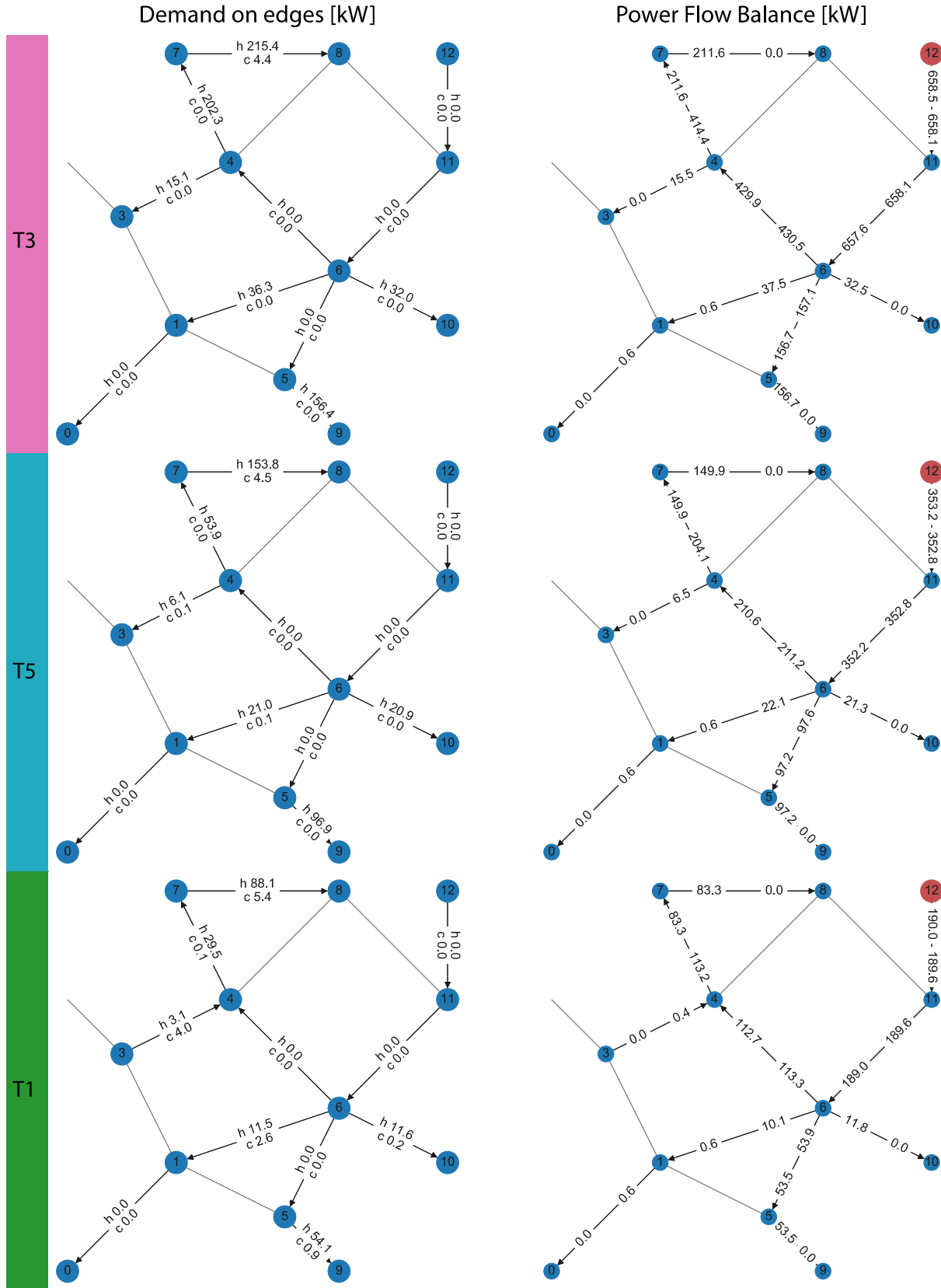| Name	Units	Value
Network Cost	$	12 136
Heat/Cold Production	$	44 443
Revenues	$	140 320
Balance	$	83 741

Figure 6.10 Detailed results of topology optimization. Rows represents periods identified in Figure 6.9 and ordered according to the heating LDC.
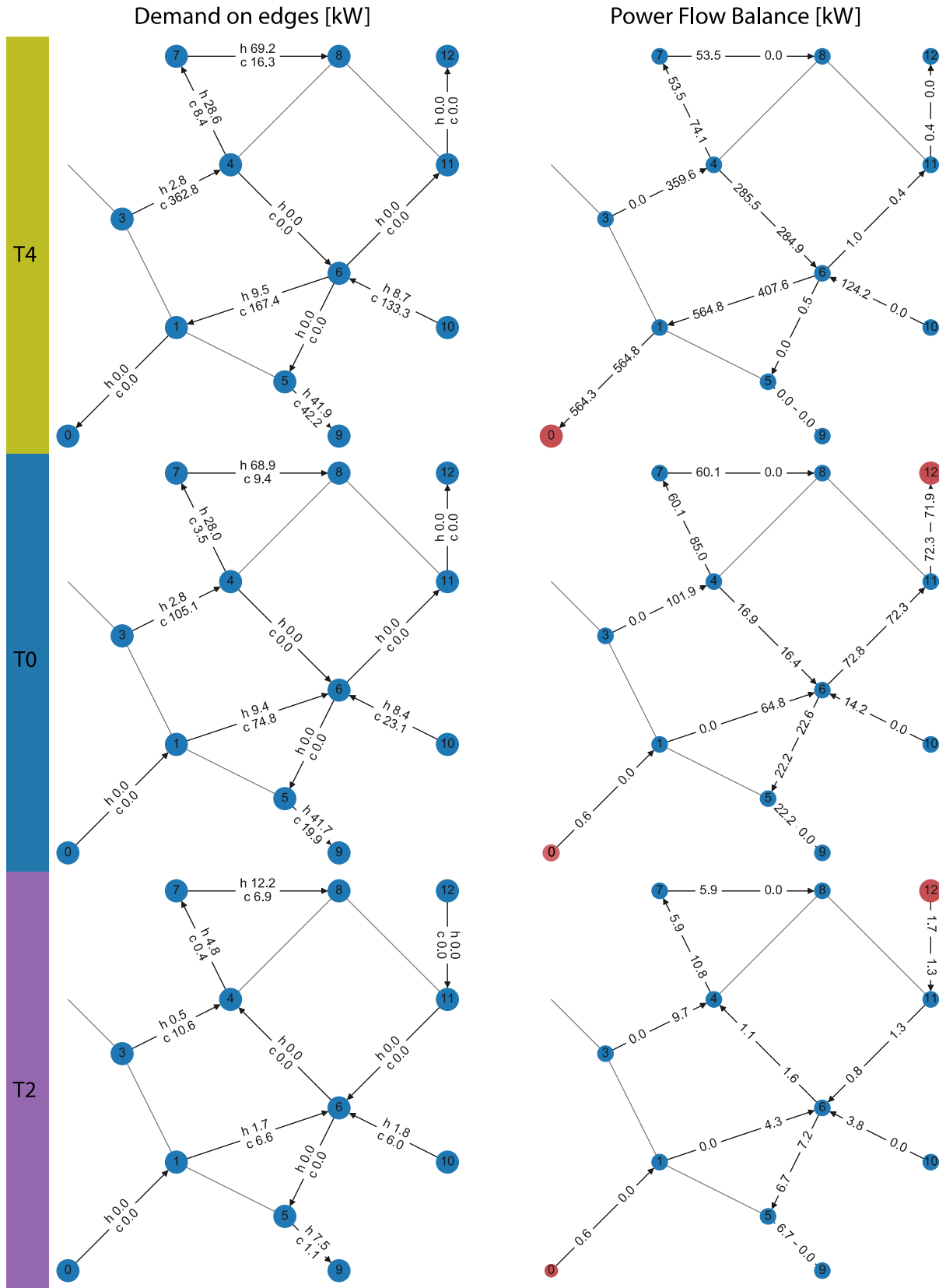
Figure 6.10 (Continued) Detailed results of topology optimization.

6.6 Discussion

The subject of this chapter is the culmination of all previous chapters which have prepared the methodological landscape necessary to design an optimized heat-sharing infrastructure. The core contribution of this chapter is a methodology that expands the capability of state-of-the-art optimization algorithms used for district heating and cooling networks: it allows bidirectional power flows that are inherent to heat-sharing networks, and to optimize the long term competitiveness of heat supply by balancing the total operating costs and the total investment costs of multiple heat supply units. The optimization weighs in the benefits of reaching farther clients that can have beneficial thermal demands to the overall performance (thermal and economic) of the network.

The model leverages different complexity reduction methods that are applied to the simulation of urban heat-sharing networks. For instance, simplifying the model formulation by avoiding nonlinearities avoids non-convexity of the problem, a necessity for fast convergence of problem solvers (Dorfner & Hamacher, 2014; Mehleri, Sarimveis, Markatos, & Papageorgiou, 2012). In addition, the spatial aggregation helps reduce the number of nodes (or buildings) in an energy system network as suggested in other related studies (Mancarella, 2014; Unternährer et al., 2017). This model considers both the temporal and the spatial aggregation of building loads, further decreasing the problem domain.

The proposed methodology shares with most other optimization algorithms the risk of over-simplifying the problem and finding a theoretically optimal solution which is inferior to other solutions in practice. In particular, the mathematical formulation presented above is capable of dealing with considerations on key temporal states such as the moment when the overall peak demand occurs, but this has not been implemented in the proposed algorithm. Comparisons with detailed simulations and measured data from 5GDHC networks could be performed to inform algorithm refinements.

CHAPTER 7   OPEN SOURCE SOFTWARE IMPLEMENTATION

This thesis hopes to contribute to the exploration of heat-sharing networks in innovative ways. A focus on tools produced different methodological frameworks in the hopes of providing a useful toolkit for other researchers and users alike. This chapter presents these tools from the angle of their main functionalities.

7.1 Introduction

Three tools accompany this thesis and are listed in Table 7-1.

Table 7-1 Summary of open source tools developed in this thesis.

	Tool	Description
1	*archetypal*	a Python package designed with the objective of helping building energy modelers and researchers maintain collections of building archetypes.
2	*district*	a Python package designed to model district energy networks in a GIS environment.
3	UMI Energy Supply Plugin	an UMI Plugin focused on the analysis of district energy supply scenarios. The economic and environmental performance of centralized energy production systems can be quickly assessed.

archetypal helps modellers analyze collections of building archetypes created with the EnergyPlus architecture. It offers three major capabilities:

1. Run, modify and analyze collections of EnergyPlus models in a persistent environment;

2. Convert EnergyPlus models to UMI Template File;

3. Convert EnergyPlus models to TRNSYS Models.

district, on the other hand, is focused on the analysis of district energy networks in a python-based GIS environment. The core element of *district* is the implementation of the algorithm detailed in Chapter 6. Moreover, *district* can leverage *archetypal* to create building energy profiles from building archetypes.

The *UMI Energy Supply Plugin* is a tool developed in collaboration with the Sustainable Design Lab at the Massachusetts Institute of Technology. The tool is a plugin for the UMI platform, which has been referred to in various occasions in this thesis. The tool leverages the shape modelling

platform of Rhino and the building energy modelling capabilities of UMI to analyse the impact of various supply energy scenarios.

The three tools are presented next.

7.2 *archetypal*: Methodology and Functionality

archetypal aims to make the collection and analysis of building archetypes simple and consistent. *archetypal* is a free, open-source Python package developed by this author that allows users to easily run collections of EnergyPlus models, to create summaries of parameters and to extract specific time series profiles. Users can also convert collections of models into archetype templates under a format known the UMI Template File. *archetypal* leverages Python's *eppy* [17] and *geomeppy* [18] packages to handle parsing and modifications of EnergyPlus files. It also takes advantage of *pandas*[19] and *matplotlib*[20] libraries for efficient and robust time series analytics and rich visualizations.

By the nature of the open source community, modifications and additions to the *eppy* package were suggested through the *pull request* system. Otherwise, additional functionalities that were deemed particular to the development of *archetypal* were developed for the package directly. For example, although *eppy* proposes a method to run an EnergyPlus model, a bespoke methodology was created in *archetypal* to handle the caching of results. This feature prevents EnergyPlus models to be rerun every time a new analysis is performed on the same unchanged model, when the model is no longer in memory.

The main features of *archetypal* are described next with some examples.

---

[17] https://pypi.org/project/eppy/

[18] https://pypi.org/project/geomeppy/

[19] https://pandas.pydata.org

[20] https://matplotlib.org

7.2.1 Run EnergyPlus Models

The main functionality of *archetypal* is to run an EnergyPlus file using the EnergyPlus executable in a Python environment. Assuming users have installed EnergyPlus, the *archetypal* `run_eplus` method will execute an IDF file using a defined weather file and various simulation parameters. Contrary to other open-source EnergyPlus tools, *archetypal* detects if the version of the IDF file is older than any EnergyPlus installations on the user's computer and proceeds with upgrading the file to the correct version. Another feature of the tool is that it simplifies the process of adding the necessary output commands to the IDF file. For example, if a user is interested in returning the Heat Exchanger Transfer Energy for a building, a specific output would need to be added to the IDF file prior to its simulation; in this case the "`HeatRejection:EnergyTransfer`" key. With archetypal, the user can specify additional inputs using the `prep_putputs` parameter. For simplification, a predefined list of useful outputs is automatically added to the IDF file when the parameter is simply set to `True`. An example of such a query that will upgrade the model, prepare the required outputs and run the simulation for the design day period is shown in Figure 7.1.

```python
from archetypal import run_eplus

file = "tests/input_data/regular/AdultEducationCenter.idf"
wf = "tests/input_data/CAN_PQ_Montreal.Intl.AP.716270_CWEC.epw"
result = run_eplus(
    file, wf, prep_outputs=True, design_day=True, expandobjects=True,
    verbose="q"
)
```

Figure 7.1 *archetypal* showcase: Run an EnergyPlus model and retrieve simulation results using a simple command.

Furthermore, *archetypal* introduces a caching method that handles simulation results. This is particularly useful for reproducible workflows such as the Jupyter Notebook programing

environment[21]. Reopening a closed notebook and running a cell containing a command such as the one presented in Figure 7.1 will use the cached simulation results instead of launching EnergyPlus again. This offers a drastic workflow speed gain especially when larger IDF files can take several minutes to complete. On the other hand, if the original IDF file is modified manually or if other input files needed by the model are updated, or if simulation parameters or modified, cached results will be ignored, and a new simulation will be executed. For convenience, the different cached simulations are kept in the file system along with a description of the simulation parameters and date & time of execution.
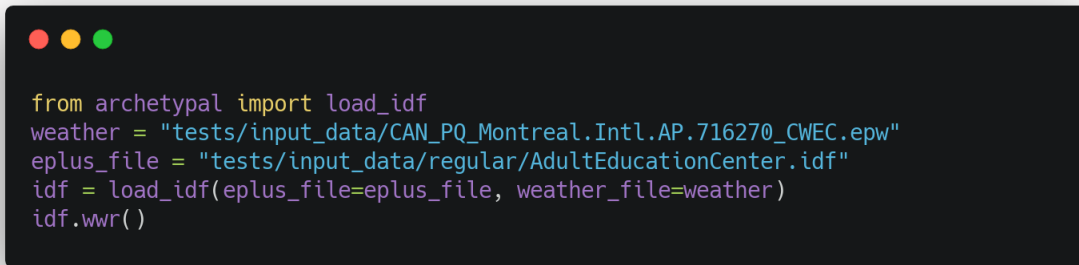
archetypal features an EnergyPlus *Exception* module, which detects when EnergyPlus fails to execute, and displays the EnergyPlus detailed error-log in the regular Python console. This way of handling model errors means that most coding errors can be caught in the programming environment instead of going back and forth between the simulation files and the code.

7.2.2 Analyse EnergyPlus Models

The process of maintaining archetype models can sometimes require simple model analytics without necessarily running the simulation. For instance, users can return a summary of the Window-to-Wall ratio of a model for each orientations of the building (Figure 7.2). They can also get a summary of the thermal properties of the envelope of the model (for the whole building, surface groups or for a particular surface).

---

[21] https://jupyter.org

```
from archetypal import load_idf
weather = "tests/input_data/CAN_PQ_Montreal.Intl.AP.716270_CWEC.epw"
eplus_file = "tests/input_data/regular/AdultEducationCenter.idf"
idf = load_idf(eplus_file=eplus_file, weather_file=weather)
idf.wwr()
```

Figure 7.2 *archetypal* showcase: Summary of the Window-to-Wall ratio. Various summaries can be returned from an EnergyPlus model in a similar fashion.

Moreover, *archetypal* exposes the EnergyPlus simulation results in a visual database format popular amongst python users: *Pandas DataFrames*. This database format offers a robust method to analyse and display EnergyPlus results in the Jupyter interactive environment.

7.2.3 Visualize Energy Profiles

Time series are particularly interesting to analyze in the context of building energy simulations. EnergyPlus has the advantage of centralizing all simulation time series through a database format known as *sqlite*[22]. *archetypal* lets users query this database to return specific time series and returns them in a `DataFrame` format. For convenience, useful time series such as the space heating, space cooling and domestic hot water profiles are accessible by default.

To analyse and visualize time series, archetypal makes use of the *pandas* library for the heavy lifting of time series data in combination with *pint*[23] for handling units and unit conversion. This allows users to easily aggregate and plot time series in the units of their choice. Feedback is provided when incompatible units are asked in order to limit human errors.

With *matplotlib*, time series can be visualized using many different plot styles: line plots, histogram plots, density plots or box and whisker plots, to name a few. A particularly useful plot type in the

---

[22] https://www.sqlite.org

[23] https://pint.readthedocs.io

case of annual time series is the Time Series Heat Map (TSHM), which will display the timeseries as a matrix with each value having a unique color. This type of plot is best for comparing observations of two different datasets.

Heat maps are slightly more complicated to setup, therefore *archetypal* provides a method that handles this process in a single command. One can specify the period length (e.g.: 24 hours), colormap as well as minimum and maximum values for the color normalization. For example, the space heating profile of the building presented previously is shown below (Figure 7.3).
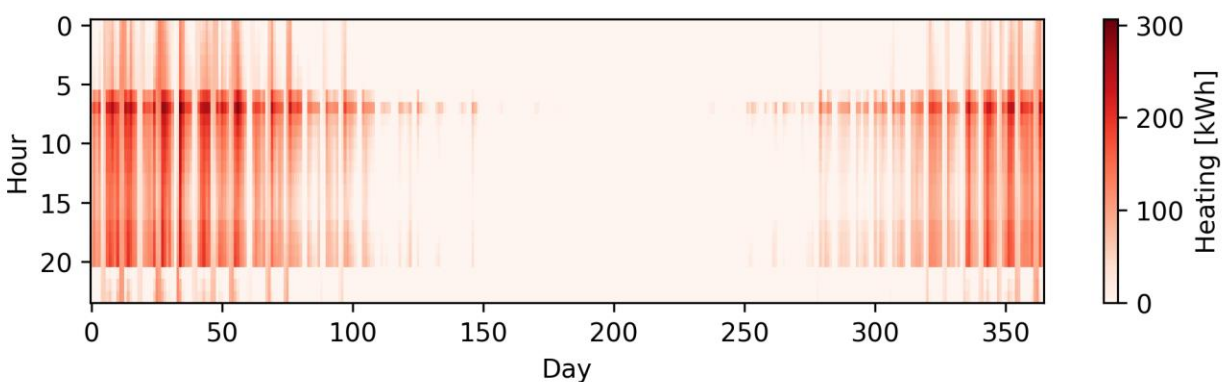

Figure 7.3 *archetypal* showcase: Visualizing time series from an EnergyPlus model as a time series heat map. Here a heat map is created by specifying the "plot_2d" method. The same image can be obtained by running the "test_plot_2d" unit test in the *archetypal* package.

Another useful visualization is the 3D plot of a timeseries (shown below). This plot type resembles the heat map presented above but with a third dimension. This type of visualization is best view in an interactive environment such as the Jupyter Notebook where it is possible to rotate and zoom the figure.
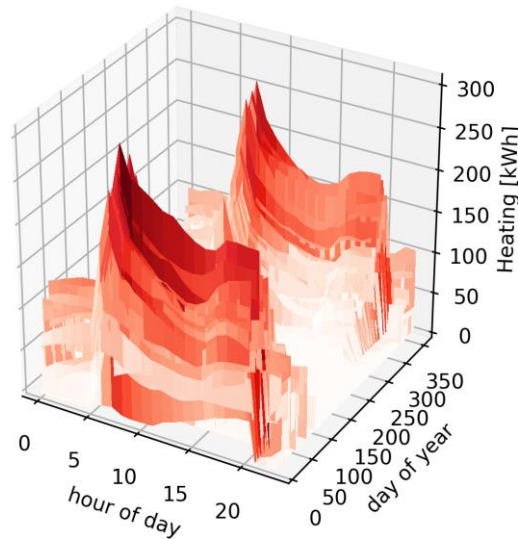
Figure 7.4 *archetypal* showcase: Visualizing time series in 3D form.

7.2.4 Create Archetype Templates

The UBEM method detailed in chapter 4 relies on so-called archetype templates. As a reminder, archetype templates differ from regular archetypes in their abstraction of any geometry. It is the role of the building massing model in combination with the *shoebox* method to recreate the geometry/physical model relationship between the model parameters specified by the template and the climatic conditions (solar incidence and temperature).

Therefore, another important contribution of *archetypal* is the automatic conversion of regular archetypes (EnergyPlus models) to archetype templates. *archetypal* lets users specify a list of EnergyPlus models to convert and outputs an UMI Template File (see Figure 7.5).

```
from archetypal import load_idf, BuildingTemplate, UmiTemplate

# load the model
weather = "tests/input_data/CAN_PQ_Montreal.Intl.AP.716270_CWEC.epw"
eplus_file = "tests/input_data/regular/AdultEducationCenter.idf"
idf = load_idf(eplus_file=eplus_file, weather_file=weather)

# create the building template
bld_template = BuildingTemplate.from_idf(idf, sql=idf.sql,
DataSource=idf.name)

# save the template to the UMI Template File format
file = UmiTemplate(name="my_umi_template", BuildingTemplates=
[bld_template]).to_json()
```

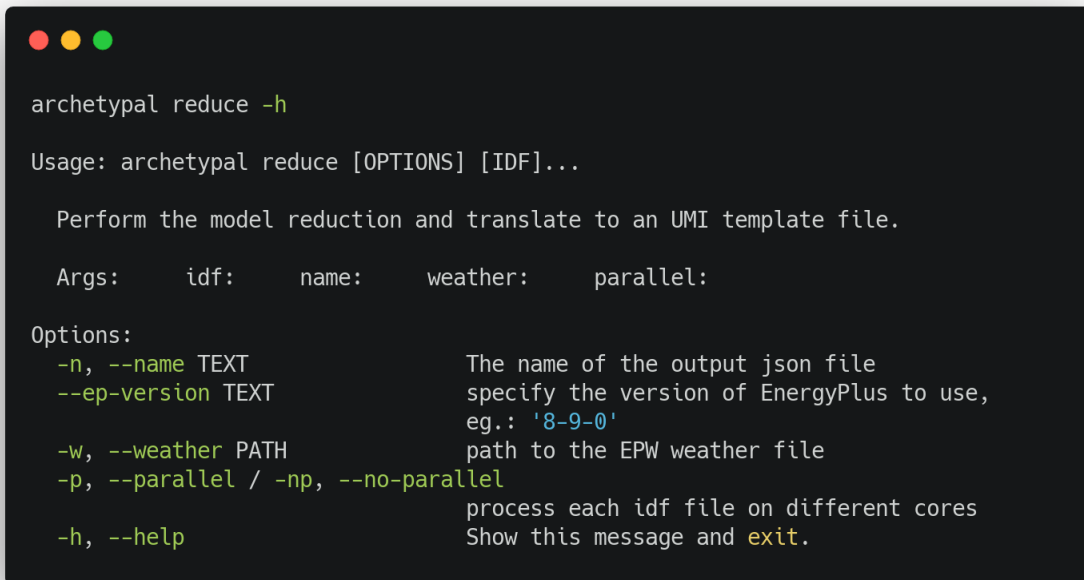Figure 7.5 *archetypal* showcase: Automatically create an archetype template from a regular EnergyPlus model.

If the different archetype templates share similar elements such as surface constructions or schedules, unnecessary duplications will be removed in an attempt to reduce the size and complexity of the template file.

7.2.5 Handle EnergyPlus Schedule Formats

This capability relates to the specific handling of EnergyPlus schedules as detailed in section 4.2.2.5 of the chapter on Automated Archetype Template Generation. EnergyPlus schedules can take various forms in the IDF file. The authors of EnergyPlus aimed at giving users different methods to input schedules of various complexity. For example, a constant schedule can be defined using less than 4 lines while a more complex schedule can be defined using a semantic logic that is more human readable. This presents a challenge especially when interoperability between models and tools is sought. For instance, the UMI Template File has data structure that resembles the original EnergyPlus Year-Week-Day format. This format uses 3 types of schedule definitions: 24h days form different weeks and lists of weeks form a whole year. To address this challenge, a utility was built into *archetypal* to convert any EnergyPlus schedule to the Year-Week-Day format.

7.2.6 Command Line Interface

archetypal features a command line interface to operate the building template creation methodology. This allows users to run *archetypal* directly from the command line, also known as the *Terminal* on MacOS computers or the *Command Prompt* on Windows computers (see Figure 7.6 below). This allows users to use archetypal in other scripting languages simply by invoking *archetypal* commands.


```
archetypal reduce -h

Usage: archetypal reduce [OPTIONS] [IDF]...

  Perform the model reduction and translate to an UMI template file.

  Args:    idf:    name:    weather:    parallel:

Options:
  -n, --name TEXT                 The name of the output json file
  --ep-version TEXT               specify the version of EnergyPlus to use,
                                  eg.: '8-9-0'
  -w, --weather PATH              path to the EPW weather file
  -p, --parallel / -np, --no-parallel
                                  process each idf file on different cores
  -h, --help                      Show this message and exit.
```

Figure 7.6 archetypal showcase: Excerpt of the Command Line Interface of *archetypal* shown here when a user inputs the "help" command.

7.3 *district:* Methodology and Functionality

District features various capabilities that aim to structure the data collection and analysis of heat-sharing networks in a Python-based coding environment: the tool implements methods to retrieve various sources of GIS building data and leverages rich visualization of categorical features and heat maps. Then, the tool structures the retrieval of topological street graphs to serve as the underlying grid on which the district energy network is built. Finally, *district* has built-in functions to analyze district energy networks, project and visualize networks, and quickly and consistently calculate various metrics (topological and energy measures).

7.3.1 Download Building Data

GIS data is collected at different scales. For urban energy studies, the data can amount to very large databases that can become quickly bloated and impractical to use. To speedup the retrieval of GIS data, *district* implements methods to download portions of complete building datasets that correspond to a certain geographical extent.

For example, retrieving data in a 1km radius using the following parameters:

```python
# We query the buffer (a polygon itself)
bbox = downtown_p.iloc[0].geometry.buffer(1000)  # 1km buffer

gdf = ds.dataportals.gis_server_request(cred, bbox, 'contains', 2950)
```

Figure 7.7 district showcase: Retrieve portions of datasets

yields a GeoDataFrame containing only features that are *contained* in the polygon.

7.3.2 Visualize Building Data and Heat Maps

district can visualize GIS data in specific projections. For the data retrieved in Figure 7.7, the following code produces a figure with categorical colors and the street grid in overprint:

```
fig, ax = ds.plot_map(
    gdf,
    column="code_utilisation",
    plot_graph=True,
    file_format="png",
    save=True,
    bgcolor=None,
    crs={"init": "epsg:2950"},
    annotate=False,
    legend=False,
    filename="1km2-downtown-mtl-wstreet",
)
```

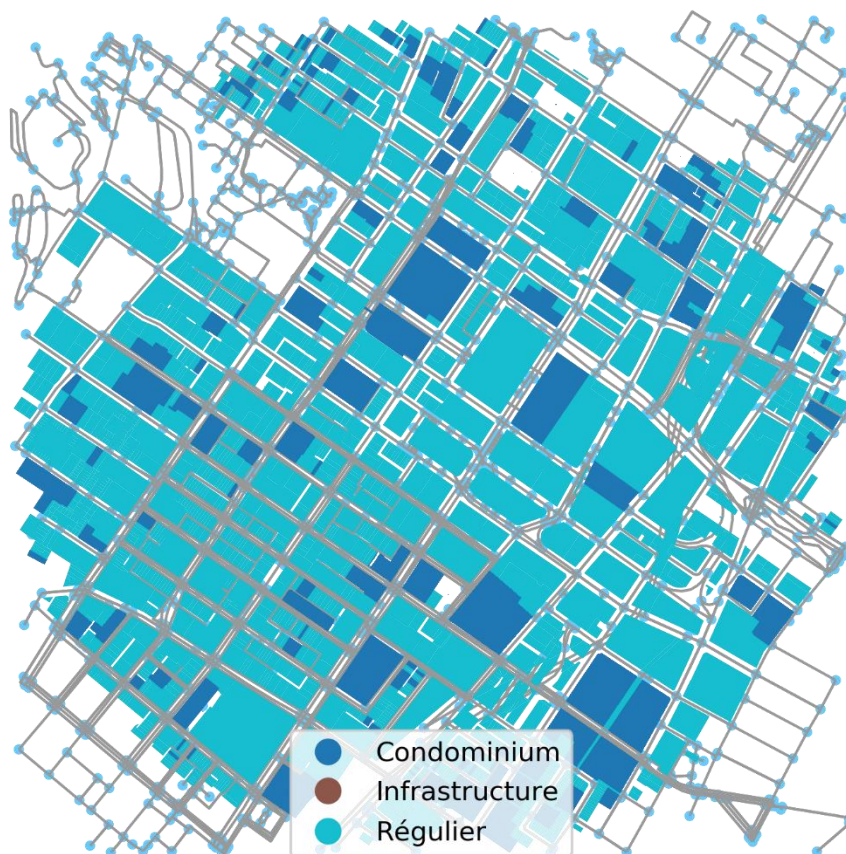Figure 7.8 district showcase: Visualize GIS data

Figure 7.9 Image produced from the code in Figure 7.8

7.3.3 Construct Networks

district simplifies the process of acquiring a street network and to prepare it for a district energy graph topology. The tool leverages the *OSMnx* package to handle the communication with the OSM server and to perform a first topological simplification. For instance, inconsistent nodes, extra points along a street segment where the street curves, etc. are removed while maintaining the full spatial geometry of the network. After the pre-process, the network may still contain loops and parallel edges which need to be removed before creating the mathematical model of a district energy network topology.

Given a topological street graph G recovered from OSM, a simple command returns the corrected graph:

```python
# Download street graph
G = ox.graph_from_bbox(
        north,
        south,
        east,
        west,
        simplify=False,
        truncate_by_edge=False,
        retain_all=False,
        network_type="bike",
        clean_periphery=True,
    )

# Correct topology
G = ds.clean_paralleledges_and_selfloops(G)
```

Figure 7.10 district showcase: correct topological errors

7.3.4 Create Network Topology Model

The creation of a topology optimization model such as the one presented in Chapter 6 is possible using a graph structure thanks to the available *from_graph* classmethod. Simply put, a complex optimization problem is setup with specific parameters:

```
# Given a network graph G, prepare a topological optimization model
prob = ds.HsminModel.from_graph(
    G,
    params,
    gen=5,
    source_label="u",
    target_label="v",
    noTypicalPeriods=4,
    hoursPerPeriod=6,
    addPeakMax=True,
    extremePeriodMethod="replace_cluster_center",
    use_availability=False,
)

prob.write("%s.lp" % prob.name, io_options={"symbolic_solver_labels": True})
```

Figure 7.11 district showcase: Create a topological optimization problem

7.3.5 Optimize the Topology

The topology optimization algorithm uses the *pyomo* to organise the mathematical problem formulation. The advantage of *pyomo* is that it can communicate with various solvers to solve the same mathematical problem; the same model formulation can be used by different solver languages. In this thesis, Gurobi and GLPK solvers have been successfully tested.

The optimization problem created in the code in Figure 7.11 is solved by running:

```
# an optimization model (prob) is solved
prob.solve(solver="gurobi", mip_gap=1e-4)
```

Figure 7.12 district showcase: Solving the optimization problem

7.3.6 Analyze and Visualize the Network

Once the optimization solver has converged on a solution, *district* accelerates the visualisation of the resulting solution. For instance, Figure 6.10 was generated with the following command:

```python
# func defines the metrics shown on each edges
func =
{
    "head": lambda d: "",
    "center": lambda d: "h {:,.1f}\nc {:,.1f}".format(d["heatpeak"],
d["coolpeak"]),
    "tail": lambda d: "",
}

for timestep in prob.timesteps:
    color_column = "peak"
    ds.plot_graph(
        solved_model.solution_graphs[timestep],
        color_column=None,
        cmap="Reds",
        colorbar=False,
        width_column=None,
        size_column=None,
        fig_title=None,
        edge_labels=func,
        dpi=100,
        save=True,
        filename=timestep + "_" + color_column + "_demand",
        file_format="pdf",
        font_size=10
    )
```

Figure 7.13 Visualizing the results of the topology optimization

Finally, various district energy network measures have been implemented in the package to quickly assess the performance of the solution. These metrics are summarized in Table 7-2:

Table 7-2 District energy network measures.

Measure	Definition
effective width	Information about the length of district heat pipes required to heat the buildings in the area
population density	Inhabitants per hectare within the service are of the network
specific heat demand	The area normalized heat demand (W/m^2)
specific heat use	The area normalized heat use (kWh/m^2)
total network length	The total length of the network (km)
network cost	The investment costs and operational/maintenance costs of buried pipes ($)
total heat sold	The revenues due to the sale of heat ($)
relative distribution heat loss	The annual heat loss compared to the annual heat input from the heat supply units (%)
heat generation cost	The costs of producing heat ($)
specific distribution capital cost	The total investment cost dived by the district heat sold per annum ($/GJ)
specific heat generation cost	The total heat generation cost dived by the district heat sold per annum ($/GJ)
specific heat revenue	The total heat revenues dived by the district heat sold per annum ($/GJ)
net profits	The balance of distribution costs, heat generation costs and heat revenues ($)
installed power	The combined maximum power capacity of the heat supply units (kW)
linear heat density	The district heat sold per annum divided by the trench length of the network (GJ/m)
effective width	The ratio between the land area and the route length of the network; a proxy for the techno-economic conditions in a particular district energy market (dimensionless)

7.4 UMI District Energy Plugin

Evaluating the suitability of certain energy supply technologies—e.g., combined heating and power, centralized heat pumps or wind power—is covered by this contribution known as the *Energy Supply Plugin* for UMI, a *Rhinoceros*-based software.

This tool was developed in collaboration with the Sustainable Design Lab at the Massachusetts Institute of Technology. The tool focuses on balancing demand and supply in district energy systems in an effort to understand the drivers of sustainability of various heat supply scenarios in different climate contexts (see Figure 7.14).

This analysis was the subject of a scientific publication (Letellier-Duchesne et al., 2018). The method presented in this paper is found to be a simple way of identifying the impact of a design decision on the performance of a neighborhood with a district heating system.
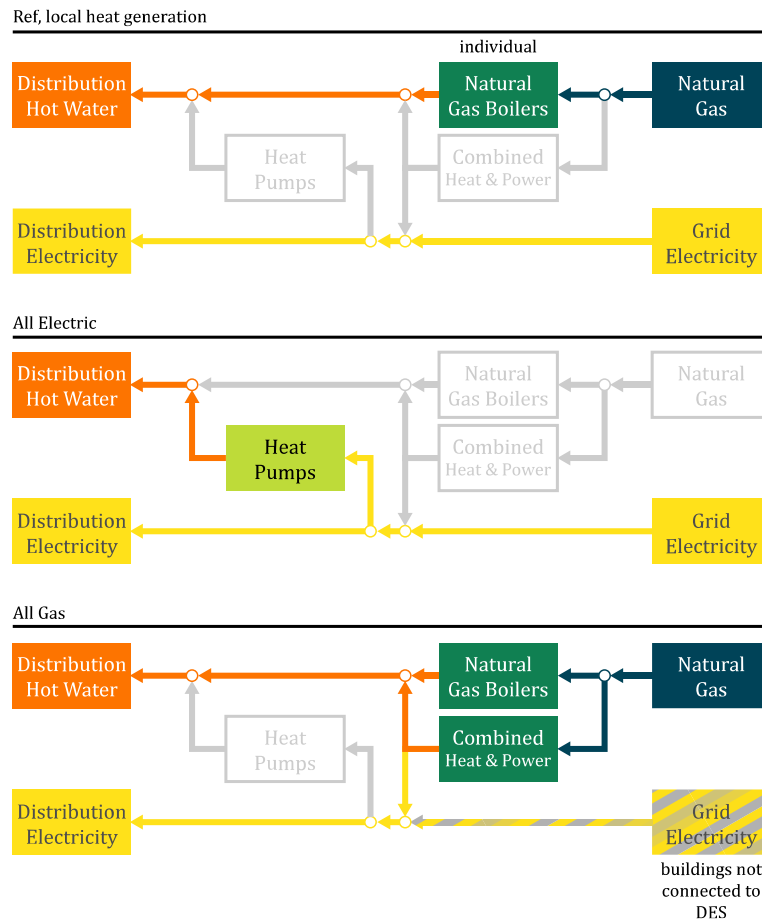
Figure 7.14 Three different energy supply scenarios that can be simulated using the energy supply plugin. source: (Letellier-Duchesne et al., 2018)

7.5 Discussion

In line with the motivation of this thesis, methodological contributions have been implemented in tools that contribute to the rapid expansion of the body of open source software.

The primary features of these tools have been exposed and detailed with examples of their use in the elaboration of the study presented in this thesis.

CHAPTER 8   CONCLUSIONS AND RECOMMENDATIONS

8.1 Synopsis of the Dissertation

The sustainable use of energy in cities is becoming one of the most important challenges of our time. With the increasing urbanization of the global population, existing energy systems are experiencing unprecedented strains. Nevertheless, solutions to this complex problem will have to compete with other solutions applied to the many areas of sustainability. Improving the flow of heating and cooling energy in cities by developing an integrated design toolkit for heat sharing networks is one promising solution proposed by this thesis.

Because building energy use is mostly a design problem, this thesis focused on the inherent links between architects and engineers and pushed the analysis further up to the urban planning level. This dissertation presented this interdisciplinary context in chapters 2 and 3. The second chapter introduced the inherent interconnections between urban planning, architecture and engineering and highlighted the importance of holistic design. These foundations laid the groundwork for the urban scale problem space of district energy networks presented in chapter 3. With the role that district energy systems need to play in sustainable cities clearly spelled out, the other chapters described the implementation of various methodologies and tools to enhance their design.

Chapter 4 tackled the quantification of building energy demand at the urban scale and suggested one method to accelerate the analyses of urban building energy modelling. Chapter 5 focused on a more local context by estimating the building energy demands of the city of Montréal, Québec. This new data not only enabled studies in chapter 3 but also provided the basis for the last contribution of this dissertation which focused on the topology optimization of a heat-sharing infrastructure elaborated in chapter 6.

Finally, chapter 7 presented the various tools that were developed to support the contributions of this thesis. Methodological contributions were embedded in these tools to help organize their implementation.

8.2 Summary of Key Contributions

Across six central chapters, this thesis makes various contributions to the literature. We review them here in order.

Chapter 2, although more focused on establishing the interdisciplinary actions enabled by the integrated design process, makes an argument for district energy networks as a catalyzer of the development of sustainable neighborhoods.

Consequently, chapter 3 proposes a data-driven analysis of the compatibility of buildings that would participate to a heat-sharing infrastructure. This chapter presents the theoretical aspects of thermal diversity and demonstrates its applicability in urban planning with a compelling example. A formal contribution in the form of an urban planning metric is presented as the *thermal diversity index* which builds on a *temporal* and a *spatial filter* that represent the effects of thermal storage and network extent for a given geographical context.

Chapter 4 focuses on the data preparation of urban building energy models and more specifically on the lack of building archetype templates. Its contribution is in the form of an algorithm that can convert automatically regular building archetypes to building archetype templates. These archetypes templates have the main advantage of enabling faster studies of urban building energy modeling, a necessary condition for large-scale adoption of UBEMs in urban development studies.

Chapter 5 prepares a dynamic heat map of the city of Montréal. Its main contribution is the methodological aspects of preparing the required building-related data in the presence of scarce and inconsistent data sources. The proposed methodology includes the use of virtual building footprints based on Airborne Laser Scanning (ALS) data (also known as LiDAR data) to estimate building footprint areas and building heights. The resulting heat map also contrasts with other example in the literature in the fact that it can model the dynamic energy profiles of buildings across the city and not just annual metrics.

Chapter 6 is enabled by the combined contributions of chapters 2 to 4. It introduces a heat sharing network topology optimization algorithm which finds optimal configurations of heat-sharing networks. This algorithm is specific to the operational context of fifth generation urban district heating and cooling system, which has been left unanswered until now.

Chapter 7 presents a toolkit assembling the methodological contributions of the former chapters into 3 open source tools: *archetypal*, a tool for researchers and practitioners to collect and analyse building archetypes. Submitted to Journal of Open Source Software (Letellier-Duchesne & Leroy, 2019); *district*: a tool for acquiring and preparing district energy network optimization and analysis.

In stage of manuscript preparation process; *UMI Energy Supply Plugin,* a tool integrated in UMI to analyse the impact of various supply energy scenarios.

8.3   Future Research

This thesis developed various methodological contributions to the analysis of the district scale dynamic energy demand. In all cases, the required energy was only analysed from the point of view of the energy sector and could benefit from a larger point of view inclusive of the life cycle assessment (LCA) of district energy. Although LCA is less popular than building energy simulation (BES) because it is not required by energy-rating systems such as LEED (Leoto & Lizarralde, 2019, p. 43), the inclusion of LCA into the development of district energy networks is a beneficial avenue.

This thesis introduced in chapter 4 a methodology for the automated approximation of complex multi-zone building energy models through *archetype templates*, which lack geometric attributes. Developing this contribution has uncovered certain areas of research which merit further exploration. First, a framework of modelling parameters structured around existing formats such as gbXML or CityGML (gbxml, 2019; Gröger, Kolbe, Nagel, & Häfele, 2012) could democratize earlier work on the standardization of building properties template files initiated by Cerezo Davila et al. (2014). This promising urban building energy modelling method enabled by *archetypal* should not only focus on the necessary data inputs needed by thermal models but also on the frameworks that allow various building energy simulation tools to communicate with each other. One such interoperability framework is the functional mock-up interface standard (FMI), which could create model-exchange formats between EnergyPlus models, for example, and archetype templates. Implementing this exchangeability would result in a more robust and enduring methodology. More concretely, enabling these frameworks would necessitate the creation of *functional mock-up units* that would include a description of the archetype template model that is understood by the *master* software, for example via DLLs.

This thesis has developed an urban scale dynamic heat map of building energy demands thanks to the availability of building archetypes. From the various represented groups of buildings, an obvious exclusion of industrial archetypes is observed. Characterizing typical industrial activities that are more common in cities such as the manufacturing sector should be implemented to improve

urban building energy models. Moreover, the current version of the dynamic heat map does not leverage the work on archetype templates that would allow using context-aware models.

The early work on empirical *effective width* analysis of regular district energy networks uncovered in chapter 3 paves the way for an analysis of effective width tied to the particular context of heat-sharing networks. There seems to be an increasing amount of fifth generation district heating and cooling systems as demonstrated by the extensive literature review of Buffa et al. (2019). An analysis of these existing systems could help establish accurate width correlations that could supplement the insights provided by the thermal diversity index.

REFERENCES

Allegrini, J., Orehounig, K., Mavromatidis, G., Ruesch, F., Dorer, V., & Evins, R. (2015). A review of modelling approaches and tools for the simulation of district-scale energy systems. *Renewable and Sustainable Energy Reviews*, *52*, 1391–1404. https://doi.org/10.1016/j.rser.2015.07.123

Antizar-Ladislao, B., Irvine, G., & Lamont, E. R. (2010). Energy from waste: Reuse of compost heat as a source of renewable energy. *International Journal of Chemical Engineering*, *2010*. https://doi.org/10.1155/2010/627930

Arasteh, D., Kohler, C., & Griffith, B. (2009). *Modeling windows in energy plus with simple performance indices (No. LBNL-2804E)*. (October). Retrieved from http://gaia.lbl.gov/btech/papers/2804.pdf

Aronsson, B., & Hellmer, S. (2011). *Existing legislative support assessments for DHC*. Retrieved from Ecoheat4eu website: http://www.diva-portal.org/smash/record.jsf?pid=diva2%3A505983&dswid=-6160

ASHRAE. (2013). ANSI/ASHRAE/IES Standard 90.1-2013 Energy Standard for Buildings Except Low-Rise Residential Buildings. In *ASHRAE Standard*.

Attia, S., Hensen, J. L. M., Beltrán, L., & De Herde, A. (2012). Selection criteria for building performance simulation tools: contrasting architects' and engineers' needs. *Journal of Building Performance Simulation*, *5*(3), 155–169. https://doi.org/10.1080/19401493.2010.549573

Averfalk, H., & Werner, S. (2018). Novel low temperature heat distribution technology. *Energy*, *145*, 526–539. https://doi.org/10.1016/J.ENERGY.2017.12.157

Bahl, B., Kümpel, A., Seele, H., Lampe, M., & Bardow, A. (2017). Time-series aggregation for synthesis problems by bounding error in the objective function. *Energy*, *135*, 900–912. https://doi.org/10.1016/J.ENERGY.2017.06.082

Barcelona Urban Ecology Agency. (2012). *Ecological Urbanism Certification - Urbanism Certification with Sustainability Criteria* (BCNecología (Agencia de Ecologia Urbana), Ed.). Retrieved from http://publicacionesoficiales.boe.es/detail.php?id=019516112-0001

Barcelona Urban Ecology Agency. (2018). *Charter for designing new urban developments and regenerating existing ones*. 1–63.

Bason, C. (2010). *Leading Public Sector Innovation: Co-Creating for a Better Society*. https://doi.org/10.1332/policypress/9781847426345.001.0001

Boeing, G. (2017a). Methods and Measures for Analyzing Complex Street Networks and Urban Form. *SSRN Electronic Journal*. https://doi.org/10.2139/ssrn.3012684

Boeing, G. (2017b). OSMnx: A Python package to work with graph-theoretic OpenStreetMap street networks. *The Journal of Open Source Software*, *2*(12), 215. https://doi.org/10.21105/joss.00215

Bradford, B., Richardson, M. E., Salter, S., Cutler, D., Uhlig, A. D., Hethley, J., … Herbert, Y. (2015). *Plan4DE Literature Review*.

Brange, L., Englund, J., & Lauenburg, P. (2016). Prosumers in district heating networks - A Swedish case study. *Applied Energy*, *164*, 492–500. https://doi.org/10.1016/j.apenergy.2015.12.020

Brounen, D., Kok, N., & Quigley, J. M. (2013). Energy literacy, awareness, and conservation behavior of residential households. *Energy Economics*, *38*, 42–50. https://doi.org/10.1016/j.eneco.2013.02.008

Buffa, S., Cozzini, M., D'Antoni, M., Baratieri, M., & Fedrizzi, R. (2019). 5th generation district heating and cooling systems: A review of existing cases in Europe. *Renewable and Sustainable Energy Reviews*, *104*(December 2018), 504–522. https://doi.org/10.1016/j.rser.2018.12.059

Bünning, F., Wetter, M., Fuchs, M., & Müller, D. (2018). Bidirectional low temperature district energy systems with agent-based control: Performance comparison and operation optimization. *Applied Energy*, *209*(July 2017), 502–515. https://doi.org/10.1016/j.apenergy.2017.10.072

C40 Reinventing Cities. (2019). De la Commune Service Yard | Reinventing Cities. Retrieved October 31, 2019, from https://www.c40reinventingcities.org/en/sites/de-la-commune-service-yard-1309.html

CanmetENERGY. (2019). *Building Technology Assessment Platform (BTAP)*. Retrieved from https://github.com/canmet-energy/btap

Centre for Sustainable Energy. (2019). London Heat Map. Retrieved November 4, 2019, from https://maps.london.gov.uk/heatmap

Cerema. (2014). Carte nationale de chaleur – France. Retrieved November 4, 2019, from http://reseaux-chaleur.cerema.fr/carte-nationale-de-chaleur-france

Cerezo, C., Sokol, J., AlKhaled, S., Reinhart, C., Al-Mumin, A., & Hajiah, A. (2017). Comparison of four building archetype characterization methods in urban building energy modeling (UBEM): A residential case study in Kuwait City. *Energy and Buildings*, *154*, 321–334. https://doi.org/10.1016/j.enbuild.2017.08.029

Cerezo, C., Sokol, J., Reinhart, C., & Al-mumin, A. (2015). Three Methods for Characterizing Building Archetypes in Urban Energy Simulation. A Case Study in Kuwait City. *Proceedings of BS2015: 14th Conference of International Building Performance Simulation Association, Hyderabad, India, Dec. 7-9*, 2873–2880. Hyderabad, India: International Building Performance Simulation Association.

Cerezo Davila, C., Dogan, T., & Reinhart, C. (2014). Towards standardized building properties template files for early design energy model generation. *2014 ASHRAE/IBPSA-USA Building Simulation Conference, Atlanta, GA, Sep 10-12*, 25–32. Retrieved from http://web.mit.edu/SustainableDesignLab/publications/TemplateEditor_SimBuild2014.pdf

Cerezo Davila, C., Reinhart, C., & Bemis, J. L. (2016). Modeling Boston: A workflow for the efficient generation and maintenance of urban building energy models from existing geospatial datasets. *Energy*, *117*, 237–250. https://doi.org/10.1016/j.energy.2016.10.057

Chen, Y., Hong, T., & Piette, M. A. (2017). Automatic generation and simulation of urban building energy models based on city datasets for city-scale building retrofit analysis. *Applied Energy*, *205*(April), 323–335. https://doi.org/10.1016/j.apenergy.2017.07.128

Chun, B., & Guldmann, J. (2012). Two- and Three-Dimensional Urban Core Determinants of the Urban Heat Island: A Statistical Approach. *Journal of Environmental Science and Engineering B*, *1*(3), 363–378. https://doi.org/10.17265/2162-5263/2012.03.010

Cirule, D., Pakere, I., & Blumberga, D. (2016). Legislative Framework for Sustainable

Development of the 4th Generation District Heating System. *Energy Procedia*, *95*, 344–350. https://doi.org/10.1016/j.egypro.2016.09.020

CTBUH. (2015a). *Calculating the Height of a Tall Building Where Only the Number of Stories Is Known,*. *9*, 1–3. Retrieved from www.ctbuh.org

CTBUH. (2015b). *Calculating the height of a tall building where only the number of stories is known*. Chicago, IL: Council on Tall Buildings and Urban Habitat.

Czechowski, D., Hauck, T., & Hausladen, G. (2014). *Revising Green Infrastructure: Concepts Between Nature and Design*. CRC Press.

Davis, D. (2011). The MacLeamy curve. Retrieved October 15, 2019, from https://www.danieldavis.com/macleamy/

Davis, D. (2013). *Modelled on Software Engineering: Flexible Parametric Models in the Practice of Architecture*. RMIT University.

Delmas, M. A., Fischlein, M., & Asensio, O. I. (2013). Information strategies and energy conservation behavior: A meta-analysis of experimental studies from 1975 to 2012. *Energy Policy*, *61*, 729–739. https://doi.org/https://doi.org/10.1016/j.enpol.2013.05.109

Dogan, T. (2015). *Procedures for Automated Building Energy Model Production for Urban and Early Design. Thesis: Ph. D. in Architecture: Building Technology* (Massachusetts Institute of Technology). Retrieved from http://hdl.handle.net/1721.1/101500

Dogan, T., & Reinhart, C. (2017). Shoeboxer: An algorithm for abstracted rapid multi-zone urban building energy model generation and simulation. *Energy and Buildings*, *140*, 140–153. https://doi.org/10.1016/j.enbuild.2017.01.030

Dong, B., Yan, D., Li, Z., Jin, Y., Feng, X., & Fontenot, H. (2018). Modeling occupancy and behavior for better building design and operation—A critical review. *Building Simulation*, *11*(5), 899–921. https://doi.org/10.1007/s12273-018-0452-x

Dorfner, J. (2011). GIS-based mapping tool of urban energy demand for room heating and hot water. *Mechanical and Building Industry Days*, (October), 13–14.

Dorfner, J. (2016a). dhmin. Retrieved October 5, 2017, from https://github.com/tum-ens/dhmin

Dorfner, J. (2016b). *Open Source Modelling and Optimisation of Energy Infrastructure at Urban*

Scale. Technical University of Munich.

Dorfner, J., & Hamacher, T. (2014). Large-Scale District Heating Network Optimization. *IEEE Transactions on Smart Grid*, *5*(4), 1884–1891. https://doi.org/10.1109/TSG.2013.2295856

Dorfner, J., Krystallas, P., Durst, M., & Massier, T. (2017). District cooling network optimization with redundancy constraints in Singapore. *Future Cities and Environment*, *3*(1), 1. https://doi.org/10.1186/s40984-016-0024-0

Duffie, J. A., & Beckman, W. A. (2013). *Solar engineering of thermal processes*. John Wiley & Sons, Incorporated.

Erhan, H., Woodbury, R., & Salmasi, N. H. (2009). *Visual sensitivity analysis of parametric design models: Improving agility in design*. Retrieved from http://summit.sfu.ca/item/585

ESRI. (2016). How Filter works—Help | ArcGIS for Desktop. Retrieved October 22, 2019, from http://desktop.arcgis.com/en/arcmap/10.3/tools/spatial-analyst-toolbox/how-filter-works.htm

ETH Zurich. (2012). Anergy grid for enhanced energy efficiency of campus buildings. *ISCN Conference*.

European Commission. (2015). *Fifth generation, Low temperature, high EXergY district heating and cooling NETworkS*. Retrieved from https://cordis.europa.eu/project/rcn/194622_en.html

Fernald, F. A. (1891, May). Ice-Making and Machine Refrigeration. *Popular Science Monthly*, *Vol. 39*.

Fischer, E. E. (2000). The Federal Transportation Livability Initiative - Building Livable Communities for The 21st Century. *Public Roads*, *63*(6). Retrieved from https://www.fhwa.dot.gov/publications/publicroads/00mayjun/liability.cfm

Frayssinet, L., Merlier, L., Kuznik, F., Hubert, J. L., Milliez, M., & Roux, J. J. (2018). Modeling the heating and cooling energy demand of urban buildings at city scale. *Renewable and Sustainable Energy Reviews*, *81*(March 2017), 2318–2327. https://doi.org/10.1016/j.rser.2017.06.040

Frederiksen, S., & Werner, S. (2013). *District Heating and Cooling* (First Edit). Lund: Studentlitteratur AB.

gbxml. (2019). The Green Building XML open schema. Retrieved November 6, 2019, from

http://www.gbxml.org

Gillet, N., Flato, G., Zhang, X., Derksen, C., Bonsal, B., Greenan, B., … Gilbert, D. (2019). *Canada's Changing Climate Report; Government of Canada*. Retrieved from http://www.changingclimate.ca/CCCR2019

Godschalk, D. R. (2004). Land Use Planning Challenges: Coping with Conflicts in Visions of Sustainable Development and Livable Communities. *Journal of the American Planning Association*, *70*(1), 5–13. https://doi.org/10.1080/01944360408976334

Gough, M. Z. (2015). Reconciling Livability and Sustainability: Conceptual and Practical Implications for Planning. *Journal of Planning Education and Research*, *35*(2), 145–160. https://doi.org/10.1177/0739456X15570320

Gröger, G., Kolbe, T. H., Nagel, C., & Häfele, K.-H. (2012). OpenGIS City Geography Markup Language (CityGML) Encoding Standard, Version 2.0.0. *OGC Document No. 12-019*, 344. Retrieved from https://portal.opengeospatial.org/files/?artifact_id=47842

Gurobi Optimization LLC. (2019). *Gurobi Optimizer Reference Manual*. Retrieved from http://www.gurobi.com

Gustafsson, A., & Gyllenswärd, M. (2005). The Power-Aware Cord: Energy Awareness through Ambient Information Display. *CHI '05 Extended Abstracts on Human Factors in Computing Systems - CHI '05*, 1423–1426. https://doi.org/10.1145/1056808.1056932

Hart, J., & Lindquist, E. (n.d.). *Whistler Athletes Village District Energy Sharing System*.

Hay, G. J., Kyle, C., Hemachandran, B., Chen, G., Rahman, M. M., Fung, T. S., & Arvai, J. L. (2011). Geospatial technologies to improve urban energy efficiency. *Remote Sensing*, *3*(7), 1380–1405. https://doi.org/10.3390/rs3071380

Heat Network Partnership for Scotland. (2017). *District Heating Strategy Factsheet: Planning Heat Network Infrastructure*. Retrieved from http://www.districtheatingscotland.com/wp-content/uploads/2017/10/Module-5-Infrastructure.pdf

Henchoz, S., Chatelan, P., Maréchal, F., & Favrat, D. (2016). Key energy and technological aspects of three innovative concepts of district energy networks. *Energy*. https://doi.org/10.1016/j.energy.2016.05.065

Henchoz, S., Weber, C., Maréchal, F., & Favrat, D. (2015). Performance and profitability perspectives of a CO2 based district energy network in Geneva's City Centre. *Energy*. https://doi.org/10.1016/j.energy.2015.03.079

Hong, T., Chen, Y., Lee, S. H., & Piette, M. A. (2016). CityBES : A Web-based Platform to Support City-Scale Building Energy Efficiency. *Urban Computing*, (August), 9.

Hosey, L. (2007, April). The Good, The Bad ... - Where is the design in sustainable design? *Architect Magazine*. Retrieved from https://www.architectmagazine.com/technology/the-good-the-bad_o

Hosseini, S., Barker, K., & Ramirez-Marquez, J. E. (2016). A review of definitions and measures of system resilience. *Reliability Engineering and System Safety*, *145*, 47–61. https://doi.org/10.1016/j.ress.2015.08.006

Howard, B., Parshall, L., Thompson, J., Hammer, S., Dickinson, J., & Modi, V. (2012). Spatial distribution of urban building energy consumption by end use. *Energy and Buildings*, *45*, 141–151. https://doi.org/10.1016/j.enbuild.2011.10.061

Intergovernmental Panel on Climate Change. (2014). Climate Change 2014 Mitigation of Climate Change. In *Intergovernmental Panel on Climate Change*. https://doi.org/10.1017/CBO9781107415416

IPCC. (2014). *Climate Change 2014: Synthesis Report. Contribution of Working Groups I, II and III to the Fifth Assessment Report of the Intergovernmental Panel on Climate Change [Core Writing Team, R.K. Pachauri and L.A. Meyer (eds.)]*. https://doi.org/10.1021/om00044a023

Kannengießer, T., Hoffmann, M., Kotzur, L., Stenzel, P., Markewitz, P., Schuetz, F., … Robinius, M. (2019). *Reducing Computational Load for Mixed Integer Linear Programming : An Example for a District and an Island Energy System*. (May), 9–20. https://doi.org/10.20944/preprints201905.0116.v1

Kavgic, M., Mavrogianni, A., Mumovic, D., Summerfield, A., Stevanovic, Z., & Djurovic-Petrovic, M. (2010). A review of bottom-up building stock models for energy consumption in the residential sector. *Building and Environment*, *45*(7), 1683–1697. https://doi.org/10.1016/j.buildenv.2010.01.021

Köppl, A., & Schleicher, S. P. (2018). What will make energy systems sustainable? *Sustainability*

(Switzerland), *10*(7). https://doi.org/10.3390/su10072537

Kotzur, L., Markewitz, P., Robinius, M., & Stolten, D. (2018). Impact of different time series aggregation methods on optimal energy system design. *Renewable Energy*, *117*, 474–487. https://doi.org/10.1016/J.RENENE.2017.10.017

Kruis, N., Lyons, P., & Wong, J. (2017). *RP-1588: Representative Layer-by-Layer Descriptions For Fenestration Systems With Specified Bulk Properties Such as U-Factor and SHGC*.

Kurtz, A. J. (2016). *1 Page at a Time*. Penguin Publishing Group.

Landgren, M., Skovmand Jakobsen, S., Wohlenberg, B., & Jensen, L. M. B. (2019). Integrated design processes–a mapping of guidelines with Danish conventional 'silo' design practice as the reference point. *Architectural Engineering and Design Management*, *15*(4), 233–248. https://doi.org/10.1080/17452007.2018.1552113

Leoto, R., & Lizarralde, G. (2019). Challenges in evaluating strategies for reducing a building's environmental impact through Integrated Design. *Building and Environment*, *155*, 34–46. https://doi.org/10.1016/j.buildenv.2019.03.041

Leroy, L., Letellier-Duchesne, S., & Kummert, M. (2019). Using Model Calibration to Improve Urban Modeling. *Building Simulation 2019*.

Letellier-Duchesne, S. (2019). Enable finding nearest edges from list of coordinates. Retrieved from GitHub: OSMnx, Pull Request #234 website: https://github.com/gboeing/osmnx/pull/234

Letellier-Duchesne, S., & Leroy, L. (2019). archetypal: A Python package for collecting, simulating, converting and analyzing building archetypes. *Journal of Open Source Software*, *4*(42), 1833. https://doi.org/10.21105/joss.01833

Letellier-Duchesne, S., Nagpal, S., Kummert, M., & Reinhart, C. (2018). Balancing demand and supply: Linking neighborhood-level building load calculations with detailed district energy network analysis models. *Energy*, *150*(September), 913–925. https://doi.org/10.1016/j.energy.2018.02.138

Lim, H., & Zhai, Z. J. (2017). Review on stochastic modeling methods for building stock energy prediction. *Building Simulation*, *10*(5), 607–624. https://doi.org/10.1007/s12273-017-0383-y

Lindquist, E., & Vaughan, W. T. (2010). *Patent No. WO2010145040-A1*. Retrieved from https://apps.webofknowledge.com/full_record.do?product=DIIDW&search_mode=GeneralS earch&qid=2&SID=6Bj1ncnhHQLA78Z8Zdo&page=1&doc=2

Ling, C., Hamilton, J., & Thomas, K. (2006). What makes a city liveable? Retrieved January 7, 2020, from Community Research Connections website: https://crcresearch.org/case-studies/case-studies-sustainable-infrastructure/land-use-planning/what-makes-a-city-liveable

Lund, H., Werner, S., Wiltshire, R., Svendsen, S., Thorsen, J. E., Hvelplund, F., & Mathiesen, B. V. (2014). 4th Generation District Heating (4GDH): Integrating smart thermal grids into future sustainable energy systems. *Energy*, *68*, 1–11. https://doi.org/10.1016/j.energy.2014.02.089

Lund, R., Østergaard, D. S., Yang, X., & Mathiesen, B. V. (2017). Comparison of Low-temperature District Heating Concepts in a Long-Term Energy System Perspective. *International Journal of Sustainable Energy Planning and Management*, *12*(0). https://doi.org/10.5278/ijsepm.2017.17.x

Lund, R., & Persson, U. (2016). Mapping of potential heat sources for heat pumps for district heating in Denmark. *Energy*, *110*, 129–138. https://doi.org/10.1016/j.energy.2015.12.127

MacLeamy, P. (2004). MacLeamy curve. *Collaboration, Integrated Information, and the Project Lifecycle in Building Design and Construction and Operation (WP-1202)*.

Mairs, J. (2017, March). Bjarke Ingels launches "silo-shattering" BIG Engineering department. *Dezeen*. Retrieved from https://www.dezeen.com/2017/03/09/bjarke-ingels-big-engineering-department-architecture-news/

Mancarella, P. (2014). MES (multi-energy systems): An overview of concepts and evaluation models. *Energy*, *65*, 1–17. https://doi.org/10.1016/J.ENERGY.2013.10.041

Mehleri, E. D., Sarimveis, H., Markatos, N. C., & Papageorgiou, L. G. (2012). A mathematical programming approach for optimal design of distributed energy systems at the neighbourhood level. *Energy*, *44*(1), 96–104. https://doi.org/10.1016/J.ENERGY.2012.02.009

Mendon, V., & Taylor, Z. T. (2014). Development of residential prototype building models and analysis system for large-scale energy efficiency studies using energyplus. *2014*

ASHRAE/IBPSA-USA Building Simulation Conference, 457–464.

Microsoft. (2019a). Computer generated building footprints for Canada. Retrieved October 1, 2019, from https://github.com/Microsoft/CanadianBuildingFootprints

Microsoft. (2019b). Computer generated building footprints for the United States. Retrieved October 1, 2019, from https://github.com/microsoft/USBuildingFootprints

Modelica Association. (2019). Modelica.

Möller, B., & Nielsen, S. (2014). High resolution heat atlases for demand and supply mapping. *International Journal of Sustainable Energy Planning and Management*, *1*, 41–58. Retrieved from dx.doi.org/10.5278/ijsepm.2014.1.4

Müller, D., Teichmann, J., Streblow, R., Fuchs, M., Remmen, P., & Lauster, M. (2016). Workflow automation for combined modeling of buildings and district energy systems. *Energy*, *117*, 478–484. https://doi.org/10.1016/j.energy.2016.04.023

National Renewable Energy Laboratory. (2019a). EnergyPlus. Retrieved November 10, 2019, from https://energyplus.net

National Renewable Energy Laboratory. (2019b). URBANopt Advanced Analytics Platform. Retrieved November 4, 2019, from https://www.nrel.gov/buildings/urbanopt.html

Natural Resources Canada. (2019). Comprehensive Energy Use Database. Retrieved November 1, 2019, from http://oee.nrcan.gc.ca/corporate/statistics/neud/dpa/menus/trends/comprehensive_tables/list.cfm

New, J., Adams, M., Im, P., Yang, H. L., Hambrick, J., Copeland, W., … Ingraham, J. A. (2018). Automatic Building Energy Model Creation (AutoBEM) for Urban-Scale Energy Modeling and Assessment of Value Propositions for Electric Utilities. *Proceedings of the International Conference on Energy Engineering and Smart Grids (ESG)*.

Nick Douglas. (2017). An Artist Explains What "Great Artists Steal" Really Means. Retrieved May 12, 2019, from https://lifehacker.com/an-artist-explains-what-great-artists-steal-really-me-1818808264

Novitski, B. J. (2009, October). In-house engineers make sustainable design work better.

Architectural Record.

NREL. (2011). *U.S. Department of Energy Commercial Reference Building Models of the National Building Stock* (No. TP-5500-46861). Retrieved from National Renewable Energy Laboratory website: http://digitalscholarship.unlv.edu/renew_pubs/44

NREL. (2019). *Preparing for a City-Scale Building Energy Upgrade Analysis: A Case Study for New York City*. Retrieved from https://www.nrel.gov/news/program/2019/building-stock-analysis-case-study-for-new-york-city.html

Oliver, A. (2018). *Lessons learned from eco-district pilot projects: the importance of stakeholder relations*. Université de Montréal.

Olsen, C., & Namara, S. Mac. (2014). *Collaborations in Architecture and Engineering*. https://doi.org/10.4324/9781315777047

Ommen, T., Thorsen, J. E., Markussen, W. B., & Elmegaard, B. (2017). Performance of ultra low temperature district heating systems with utility plant and booster heat pumps. *Energy*, *137*, 544–555. https://doi.org/10.1016/j.energy.2017.05.165

Ontario Regulation. *Reporting of Energy Consumption and Water Use*. , (2019).

openmod. (2018). Open Models - wiki.openmod-initiative.org. Retrieved October 4, 2019, from https://wiki.openmod-initiative.org/wiki/Open_Models

Overbey, D. (2016, April 4). Performance Modeling Tools for Any Designer. *Building Enclosure Online*. Retrieved from http://www.buildingenclosureonline.com/articles/85754-performance-modeling-tools-for-any-designer?v=preview

Pacific Northwest National Laboratory. (2018). *Unique Building Identification*. Retrieved from https://buildingid.pnnl.gov/

Page, J., Robinson, D., & Scartezzini, J.-L. (2007). Stochastic Simulation of Occupant Presence and Behaviour in Buildings. *Building Simulation 2007*. Retrieved from http://infoscience.epfl.ch/record/113867

Pattijn, I. P., & Baumans, A. (2017). Fifth-generation thermal grids and heat pumps: A pilot project in Leuven, Belgium. *HPT Magazine*, *35*(2), 53–57.

Pearl, D. S., & Oliver, A. (2015). The role of 'early-phase mining' in reframing net-positive

development. *Building Research & Information*, *43*(1), 34–48. https://doi.org/10.1080/09613218.2014.939511

Pellegrini, M., & Bianchini, A. (2018). The Innovative Concept of Cold District Heating Networks: A Literature Review. *Energies*, *11*(1), 236. https://doi.org/10.3390/en11010236

Perry, R., & Ren, T. (2013, November). 2013 ASHRAE Technology Award Case Study: Sewage Plant Heats Village. *ASHRAE Journal*, 40–46.

Persson, U., Möller, B., & Werner, S. (2014). Heat Roadmap Europe: Identifying strategic heat synergy regions. *Energy Policy*. https://doi.org/10.1016/j.enpol.2014.07.015

Persson, Urban, & Werner, S. (2010). Effective Width: The Relative Demand for District Heating Pipes Length in City Areas. *12th International Symposium on District Heating and Cooling*, 129–131. Tallinn, Estonia.

Persson, Urban, & Werner, S. (2011). Heat distribution and the future competitiveness of district heating. *Applied Energy*, *88*(3), 568–576. https://doi.org/10.1016/j.apenergy.2010.09.020

Phetteplace, G. (2013). *District Cooling*. Atlanta, GA: W. Stephen Comstock.

Philip, S., Tran, T., Youngson, E. A., & Bull, J. (2004). *Eppy*. Retrieved from https://github.com/santoshphilip/eppy

Pöyry Management Consulting Oy. (2016). *Two-way district heating business models*. Helsinki: The Energy Industry Association; Sitra.

QUEST Canada. (2012). *Building Smart Energy Communities: Implementing Integrated Community Energy Solutions*. QUEST Canada.

Rager, J., Rebeix, D., Maréchal, F., Cherix, G., & Capezzali, M. (2013). MEU: An urban energy management tool for communities and multi-energy utilities Strategic energy planning under uncertainty View project. *CISBAT 2013, Cleantech for Smart Cities and Buildings – From Nano to Urban Scale*, (September). https://doi.org/10.13140/2.1.2716.9921

Rakha, T., Rose, C. M., & Reinhart, C. (2014). A framework for modeling occupancy schedules and local trips based on activity based surveys. *2014 ASHRAE/IBPSA-USA Building Simulation Conference*, 433–440. Retrieved from http://www.scopus.com/inward/record.url?eid=2-s2.0-84938903923&partnerID=tZOtx3y1

Ramallo-González, A. P., Vellei, M., Brown, M., & Coley, D. A. (2015). Remote facade surveying of windows characteristics. *Energy Procedia*, *78*(0), 925–930. https://doi.org/10.1016/j.egypro.2015.11.020

Re4 Montréal. (2019). *Pour des quartiers durables: Les réseaux urbains d'énergie au cœur d'une stratégie holistique pour Montréal*. Montréal, QC.

Reinhart, C., & Cerezo Davila, C. (2016). Urban building energy modeling – A review of a nascent field. *Building and Environment*, *97*, 196–202. https://doi.org/10.1016/j.buildenv.2015.12.001

Reinhart, C., Dogan, T., Jakubiec, J. A., Rakha, T., & Sang, A. (2013). Umi - an Urban Simulation Environment for Building Energy Use , Daylighting and Walkability. *Proceedings of BS2013: 13th Conference of International Building Performance Simulation Association*, 476–483.

Roberts, T. (2013). Energy Modeling Early and Often. *Environmental Building News*, *22*(3), 1, 8–15.

Salat, S., Bourdic, L., & Nowacki, C. (2010). Assessing Urban Complexity. *International Journal of Sustainable Building Technology and Urban Development*, *1*(2), 160–167. https://doi.org/10.5390/SUSB.2010.1.2.160

Saroglou, T., Meir, I. A., Theodosiou, T., & Givoni, B. (2017). Towards energy efficient skyscrapers. *Energy and Buildings*, *149*(November), 437–449. https://doi.org/10.1016/j.enbuild.2017.05.057

Schluck, T., Kräuchi, P., & Sulzer, M. (2015). Non-linear thermal networks - How can a meshed network improve energy efficiency? *CISBAT 2015 Lausanne*, 779–785. https://doi.org/10.5075/epfl-cisbat2015-779-784

Schmidt, D., Kallert, A., Blesl, M., Svendsen, S., Li, H., Nord, N., & Sipilä, K. (2017). Low Temperature District Heating for Future Energy Systems. *Energy Procedia*, *116*, 26–38. https://doi.org/10.1016/j.egypro.2017.05.052

Schmidt, D., Kallert, A., Orozaliev, J., Best, I., Vajen, K., Reul, O., … Gerhold, P. (2017). Development of an Innovative Low Temperature Heat Supply Concept for a New Housing Area. *Energy Procedia*, *116*, 39–47. https://doi.org/10.1016/j.egypro.2017.05.053

Scottish Government. (2018). Scotland Heat Mapping. Retrieved November 4, 2019, from http://heatmap.scotland.gov.uk/

Senatsverwaltung für Wirtschaft Energie und Betriebe. (2019). Energieatlas Berlin. Retrieved November 4, 2019, from https://energieatlas.berlin.de/

Smith, L. B. (2013, November). Viewpoint: How BIM is Crushing the Art from Architecture and How to Stop It. *Archintosh*. Retrieved from https://architosh.com/2013/11/viewpoint-how-bim-is-crushing-the-art-of-architecture/comment-page-1/

Sokol, J., Cerezo Davila, C., & Reinhart, C. (2017). Validation of a Bayesian-based method for defining residential archetypes in urban building energy models. *Energy and Buildings*, *134*, 11–24. https://doi.org/10.1016/j.enbuild.2016.10.050

Sustainability Solutions Group. (2016). *IEA DHC Annex XI: Plan4DE Final Report*. International Energy Agency Energy Technology Initiative on District Heating and Cooling including Combined Heat and Power (IEA DHC).

Swan, L. G., & Ugursal, V. I. (2009). Modeling of end-use energy consumption in the residential sector: A review of modeling techniques. *Renewable and Sustainable Energy Reviews*, *13*(8), 1819–1835. https://doi.org/10.1016/j.rser.2008.09.033

TABULA Project Team. (2012). *Typology Approach for Building Stock Energy Assessment: Main Results of the TABULA project*. Retrieved from Institut Wohnen und Umwelt GmbH website: https://ec.europa.eu/energy/intelligent/projects/sites/iee-projects/files/projects/documents/tabula_final_report_en.pdf

The SciPy community. (2019). scipy.spatial.KDTree. Retrieved from SciPy website: https://docs.scipy.org/doc/scipy/reference/generated/scipy.spatial.KDTree.html#scipy.spatial.KDTree

Tozzi, P., & Jo, J. H. (2017). A comparative analysis of renewable energy simulation tools: Performance simulation model vs. system optimization. *Renewable and Sustainable Energy Reviews*, *80*(February), 390–398. https://doi.org/10.1016/j.rser.2017.05.153

Transition Énergétique Québec. (2019). Facteurs d'émission et de conversion. Retrieved from https://transitionenergetique.gouv.qc.ca/fileadmin/medias/pdf/FacteursEmission.pdf

Tsilingiris, P. T. (2004). On the thermal time constant of structural walls. *Applied Thermal Engineering*, *24*(5–6), 743–757. https://doi.org/10.1016/j.applthermaleng.2003.10.015

UNEP. (2015). *District Energy in Cities: Unlocking the Potential of Energy Efficiency and Renewable Energy*. Retrieved from United Nations Environment Program website: http://www.unep.org/energy/portals/50177/DES_District_Energy_Report_full_02_d.pdf

Union of BC Municipalities. *Resolutions to be Considered at the 2014 UBCM Convention*. , (2014).

United Nations Department of Economic and Social Affairs Population Division. (2019). *World Urbanization Prospects: The 2018 Revision (ST/ESA/SER.A/420)*. New York: United Nations.

Unternährer, J., Moret, S., Joost, S., & Maréchal, F. (2017). Spatial clustering for district heating integration in urban energy systems: Application to geothermal energy. *Applied Energy*, *190*, 749–763. https://doi.org/10.1016/j.apenergy.2016.12.136

US Department of Energy. (2010). EnergyPlus Engineering Reference: The Reference to EnergyPlus Calculations. *US Department of Energy*, pp. 1–847. https://doi.org/citeulike-article-id:10579266

US DOE - Building Technology Office. (2018). Commercial Prototype Building Models.

Van Vliet, O., Brouwer, A. S., Kuramochi, T., Van Den Broek, M., & Faaij, A. (2011). Energy use, cost and CO2 emissions of electric cars. *Journal of Power Sources*, *196*(4), 2298–2310. https://doi.org/10.1016/j.jpowsour.2010.09.119

Vesterlund, M., Toffolo, A., & Dahl, J. (2016). Simulation and analysis of a meshed district heating network. *Energy Conversion and Management*, *122*, 63–73. https://doi.org/10.1016/j.enconman.2016.05.060

Vetterli, N., & Sulzer, M. (2015). Dynamic Analysis of the Low-Temperature District Network " Suurstoffi " Through Monitoring. *Cisbat 2015*, (October), 517–522. https://doi.org/10.5075/epfl-cisbat2015-517-522

Ville de Montréal. (2011). Montréal en statistiques - Utilités publiques. Retrieved November 3, 2019, from

http://ville.montreal.qc.ca/portal/page?_pageid=6897,67889708&_dad=portal&_schema=P
ORTAL

Ville de Montréal. (2019). *Inventaire 2015 des émissions de gas à effet de serre de la collectivité montréalaise*. Retrieved from ville.montreal.qc.ca/ pls/portal/docs/page/enviro_fr/media/documents/VDM_ InventaireCollectiviteGES_2015.PDF

von Rhein, J., Henze, G. P., Long, N., & Fu, Y. (2019). Development of a topology analysis tool for fifth-generation district heating and cooling networks. *Energy Conversion and Management*, *196*, 705–716. https://doi.org/10.1016/j.enconman.2019.05.066

Vraa Nielsen, M. (2012). *Integrated energy design of the building envelope*. Retrieved from http://issuu.com/martinvraa/docs/intergrated_energy_design_of_the_building_envelope

Weber, C., & Favrat, D. (2010). Conventional and advanced CO2 based district energy systems. *Energy*. https://doi.org/10.1016/j.energy.2010.08.008

Werner, S. (2017). International review of district heating and cooling. *Energy*, pp. 617–631. https://doi.org/10.1016/j.energy.2017.04.045

Whitmore, J., & Pineau, P.-O. (2018). *État de l'énergie au Québec*. Retrieved from http://energie.hec.ca/wp-content/uploads/2017/12/EEQ2018_WEB-FINAL.pdf

Wilke, U., Haldi, F., Scartezzini, J. L., & Robinson, D. (2013). A bottom-up stochastic model to predict building occupants' time-dependent activities. *Building and Environment*, *60*, 254–264. https://doi.org/10.1016/j.buildenv.2012.10.021

Yan, W. Y., Shaker, A., & El-Ashmawy, N. (2015). Urban land cover classification using airborne LiDAR data: A review. *Remote Sensing of Environment*, *158*, 295–310. https://doi.org/10.1016/j.rse.2014.11.001

Yu, B., Liu, H., Wu, J., Hu, Y., & Zhang, L. (2010). Automated derivation of urban building density information using airborne LiDAR data and object-based method. *Landscape and Urban Planning*, *98*(3–4), 210–219. https://doi.org/10.1016/j.landurbplan.2010.08.004

Zarin Pass, R., Wetter, M., & Piette, M. A. (2018). A thermodynamic analysis of a novel bidirectional district heating and cooling network. *Energy*, *144*, 20–30.

https://doi.org/10.1016/j.energy.2017.11.122

Zhu, P., Yan, D., Sun, H., An, J., & Huang, Y. (2019). Building Blocks Energy Estimation
(BBEE): A method for building energy estimation on district level. *Energy and Buildings*,
185, 137–147. https://doi.org/10.1016/j.enbuild.2018.12.031

APPENDIX A   SUPPORTING DATA

Virtual Building Footprints Supplemental Data

Table A-1 Difference between hand drawn building footprints and VBFs.

Borough	Number of Footprints	BF Area {m²}	VBF Area {m²}	Relative difference
Ahuntsic	14081	2,597,150	3,347,866	0.29
Bordeaux-Cartierville	7247	1,587,983	2,169,329	0.37
Centre-Sud	4654	1,163,987	1,462,741	0.26
Côte-des-Neiges	8416	2,367,453	2,963,672	0.25
Faubourg Saint-Laurent	1389	712,749	952,398	0.34
Hochelaga-Maisonneuve	5988	1,603,030	1,863,574	0.16
Le Plateau-Mont-Royal	14347	2,660,467	3,203,335	0.20
Mercier-Est	8435	1,103,343	1,504,674	0.36
Mercier-Ouest	7260	2,114,166	2,552,868	0.21
Notre-Dame-de-Grâce	10683	1,735,582	2,330,230	0.34
Parc-Extension	3187	495,512	627,157	0.27
Peter McGill	2125	1,122,715	1,375,129	0.22
Petite-Bourgogne	1004	450,359	508,530	0.13
Petite-Patrie	8488	1,560,867	1,871,516	0.20
Pointe Saint-Charles	2166	663,209	793,656	0.20
Pointe-aux-Trembles	11163	1,893,482	2,668,395	0.41
Rivière-des-Prairies	11763	2,180,385	3,357,128	0.54
Rosemont	12303	1,980,502	2,700,999	0.36
Rosemont-La Petite-Patrie	20791	3,541,369	4,572,515	0.29
Saint-Henri	1959	653,426	780,621	0.19
Saint-Michel	8632	1,552,143	2,015,603	0.30
Vieux-Montréal	567	557,224	862,294	0.55
Ville-Émard/Côte Saint-Paul	5868	997,887	1,168,755	0.17
Villeray	9392	1,522,372	1,889,436	0.24

APPENDIX B   MODEL COMPLEXITY REDUCTION

Software availability

The archetype template generation tool detailed in chapter 4 has been integrated in *archetypal,* an open source python package, available on the GitHub repository[24]. Accompanying documentation is hosted on a website[25]. Readers are referred to this online documentation for more details on the data structure and the model assumptions.

Detailed model assumptions

Table B-2 Model assumptions of the complexity reduction algorithm presented in section 4.2

Parameter	Description	Parameter values	Algorithm Assumption
Cooling COP	Performance factor of the cooling system	Float greater than 0	The annual COP of the cooling system is calculated for the whole building as the ratio of input energy and the energy removed in the zone by the HVAC system.
Cooling Limit Type	Limits the capacity of the cooling equipment for this zone	*LimitFlowRate, LimitCapacity, LimitFlowRateAndCapacity* or *NoLimit*	Uses the *UserDesignLoads* from the *ZoneSized* report. See *MaxCoolFlow* and *MaxCoolingCapacity*
Cooling Set Point	The temperature above which the zone cooling is turned on	Float	Uses the average value of the cooling schedule
Cooling Schedule	The availability schedule for space cooling in this zone. If the value is 0, cooling is not available, and cooling is not supplied to the zone.	A yearly schedule with values between 0 and 1	The zone thermostat setpoint is converted to an availability schedule, where 0 means the system is unavailable and any other value means the system can supply cooling to the zone
Economizer Type	Specifies if there is an outdoor air economizer.	*NoEconomizer, DifferentialDryBulb*, or *DifferentialEnthalpy*	Same assumption for the entire building. Economizer Type values that are not supported by UMI default to *DifferentialEnthalpy*

---

[24] https://github.com/samuelduchesne/archetypal

[25] https://archetypal.readthedocs.io/en/latest/

Parameter	Description	Parameter values	Algorithm Assumption
Heat Recovery Type	Heat recovery parameters for this zone	*None*, *Sensible*, or *Enthalpy*	Defaults to *Enthalpy* if any of the Economizer Type are detected
Heat Recovery Efficiency Latent	The latent heat recovery effectiveness, where effectiveness is defined as the change in supply humidity ratio divided by the difference in entering supply and relief air humidity ratios	Float between 0 and 1	- If the HeatExchanger is an AirToAir FlatPlate, HeatRecoveryEfficiencyLatent = HeatRecoveryEfficiencySensible (= 0.05) - If the HeatExchanger is an AirToAir SensibleAndLatent, HeatRecoveryEfficiencyLatent = Latent Effectiveness at 100% Heating Air Flow - If the HeatExchanger is a Desiccant BalancedFlow, the default value is used (=0.65).
Heat Recovery Efficiency Sensible	The sensible heat recovery effectiveness, where effectiveness is defined as the change in supply temperature divided by the difference in entering supply and relief air temperatures	Float between 0 and 1	- If the HeatExchanger is an AirToAir FlatPlate, HeatRecoveryEfficiencySensible $= \frac{T_{supply} - T_{inlet}}{T_{secondary_{inlet}} - T_{supply}}$ - If the HeatExchanger is an AirToAir SensibleAndLatent, HeatRecoveryEfficiencySensible = Sensible Effectiveness at 100% Heating Air Flow - If the HeatExchanger is a Desiccant BalancedFlow, default value for the efficiency (=0.70)
Heating COP	Performance factor of the heating system	Float greater than 0	The annual COP of the heating system is calculated for the whole building as the ratio of input energy and the energy supplied to the zone by the HVAC system.
Heating Limit Type	Limits the capacity of the heating equipment for this zone	*LimitFlowRate*, *LimitCapacity*, *LimitFlowRateAndCapacity* or *NoLimit*	Set to *LimitFlowRateAndCapacity* if the capacity can be calculated from the *ZoneSizes* report; *NoLimit* otherwise.
Heating Set Point	The temperature below which the zone heating is turned on	Float	Uses the average value of the heating schedule
Heating Schedule	The availability schedule for space heating in this zone. If the value is 0, heating is not available, and heat is not supplied to the zone	A yearly schedule	The zone thermostat setpoint is converted to an availability schedule, where 0 means the system is unavailable and any other value means the system can supply heating to the zone
Is Cooling On	Whether or not cooling is available	0 or 1	If cooling schedule, set to 1, else 0
Is Heating On	Whether or not heating is available	0 or 1	If heating schedule, set to 1, else 0

Parameter	Description	Parameter values	Algorithm Assumption
Is Mechanical Ventilation On	Whether or not mechanical ventilation is available	0 or 1	If mechanical ventilation controller, set to 1, else 0
Minimum Fresh Air per Area	The design outdoor air volume flow rate per square meter of floor area (units are m3/s-m2).	Float	Set to *OutdoorAirFlowperZoneFloorArea*
Minimum Fresh Air per Person	The design outdoor air volume flow per person for this zone in cubic meters per second per person.	Float, default is 0.00944 (20 cfm per person)	Set to *OutdoorAirFlowperPerson*
Mechanical Ventilation Schedule	The availability schedule of the mechanical ventilation. If the value is 0, the mechanical ventilation is not available and air flow is not requested.	A yearly schedule	Set to the schedule of the Controller:MechanicalVentilation object